CLUSTERING ACTIVITY AND SOMATO-DENDRITIC RELEASE IN RAT SUPRAOPTIC NUCLEUS NEURONS

by

Ariane Gagnon

Integrated Program in Neuroscience

McGill University, Montréal, Québec

March 2016

A thesis submitted to

The Faculty of Graduate Studies and Research,

McGill University,

In partial fulfillment of the requirements for the degree of

Doctor of Philosophy.

TABLE OF CONTENTS

Abstract…… i
Résumé…… ii
Acknowledgements…… iii
Publications arising from this work…… v
Contributions and originality…… vi
Abbreviations and symbols…… viii

I: INTRODUCTION

1.1. Magnocellular neurosecretory cells
1.1.1. Role in survival: an evolutionary perspective …… p.1
1.1.2. In animals: a behavioral and social perspective…… p.1
1.1.3. In humans: a behavioral and social perspective…… p.3
1.1.4. Oxytocin cells…… p.4
1.1.4.1 Structure, synthesis and release…… p.4
1.1.4.2. Role in parturition and lactation…… p.5
1.1.4.3. Role in rodent natriuresis…… p.7
1.1.5. Vasopressin cells…… p.8
1.1.5.1. Structure, synthesis and release…… p.8
1.1.5.2. Role in osmoregulation…… p.9
1.1.5.2a. Defining the concept of osmoregulation: from central to peripheral osmoreceptors…… p.9
1.1.5.2b. Vasopressin cells act as mechanical transducers …… p.12
1.1.5.2c. Activation of V2 receptors and water reabsorption from the kidneys…. p.14
1.2. OVLT synaptic inputs onto MNC…… p.15
1.2.1. Glutamatergic inputs…… p.15
1.3. Pattern and frequency of electrical activity displayed by MNC…… p.16
1.3.1. Phasic activity in VP cells…… p.17
1.3.2. Clustering activity in OT and VP cells…… p.18
1.3.3. MNC electrical activity is correlated to hormone output …… p.20
1.3.4. *Hypothesis one*…… p.23
1.4. Modulation of MNC electrical activity…… p.23
1.4.1. Depolarizing neuropeptides: angiotensin II and neurotensin…… p.24
1.4.2. Calcium-activated potassium channels…… p.26

1.4.2.1 Large-conductance calcium-activated potassium channels..... p.26
1.4.2.2. Small-conductance calcium-activated potassium channels..... p.27
1.4.3. Neurotensin and the after hyperpolarizing potential..... p.28
1.4.4. *Hypothesis two*..... p.29
1.5. Somato-dendritic release..... p.29
1.5.1. First evidence about somato-dendritic release..... p.30
1.5.2. Depolarization-induced suppression of excitatory and inhibitory transmission..... p.31
1.5.3. Dendro-dendritic synapses..... p.32
1.5.4. Role of somato-dendritic release during early development..... p.34
1.5.5. Somato-dendritic release in adult MNC: a general perspective..... p.35
1.5.5.1. Intanuclear somato-dendritic release from oxytocin cells..... p.37
1.5.5.2. Intanuclear somato-dendritic release from vasopressin cells..... p.38
1.5.6. Somato-dendritic release of messengers inhibits presynaptic excitatory neurotransmitter release..... p.40
1.5.6.1. Somato-dendritic release of messengers from OT cells inhibits excitatory transmission..... p.40
1.5.6.2. Somato-dendritic release of messengers from VP cells inhibits excitatory transmission..... p.42
1.5.7. *Hypothesis three*..... p.44
1.5.8. *Hypothesis four* p.45
1.6. Role of calcium in somato-dendritic release..... p.46
1.6.1. Basal calcium and priming..... p.46
1.6.2. Voltage-gated calcium channels..... p.48
1.6.3. Vesicle fusion machinery..... p.50
1.6.4. Action potential broadening and calcium entry..... p.51
1.6.5. Calbindin, calretinin and calcium buffering..... p.53
1.6.6. *Hypothesis five*..... p.54
1.7. Summary..... p.55

II: METHODS

2.1. Animals..... p.60
2.1.1. Transgenic rats expressing enhanced green fluorescent protein..... p.60
2.1.2. Transgenic rats expressing monomeric red fluorescent protein 1..... p.61
2.2. Solutions..... p.61
2.3. Experimental tissue preparations..... p.62

2.3.1. Superfused hypothalamic explants preparations..... p.62
2.3.2. Acute angled hypothalamic sections..... p.62
2.4. Electrophysiological recordings..... p.63
2.4.1. Extracellular recordings..... p.63
2.4.2. Intracellular recordings..... p.63
2.4.2.1. Current clamp..... p.63
2.4.2.2. Voltage clamp..... p.64
2.5. Tissue and single cell PCR..... p.65
2.6. Two-photon calcium imaging..... p.66
2.7. Pharmacology..... p.68
2.8. Data and statistical analysis..... p .69

III: MODULATION OF SPIKE CLUSTERING BY NMDA RECEPTORS AND NEUROTENSIN IN RAT SUPRAOPTIC NUCLEUS NEURONS

3.1. Overview..... p.73
3.2. Results..... p.74
3.2.1. Stimulation of the OVLT induces spike clustering in MNC..... p.74
3.2.2. Variations in membrane potential modulate clustering activity..... p.75
3.2.3. Inhibition of SK channels modulates clustered firing..... p.76
3.2.4. Neurotensin receptor activation modulates NMDA receptor-dependent clustering activity..... p.76
3.2.5. Neurotensin does not directly inhibit SK channels..... p.78
3.3. Discussion..... p.80
3.3.1. Stimulation of the OVLT elicits clustering activity via endogenous glutamate release..... p.80
3.3.2. SK channel activity and neurotensin receptor activation both modulate clustered firing..... p.81
3.3.3. Neurotensin receptor activation does not directly inhibit SK channels in SON slices..... p.83

IV: SOMATO-DENDRITIC RELEASE IS REGULATED IN A SPIKE- AND FREQUENCY-DEPENDENT MANNER TO IBHIBIT GLUTAMATERGIC NEUROTRANSMISSION

4.1. Overview..... p.89
4.2. Results..... p.91
4.2.1. Frequency-dependent inhibition of glutamatergic transmission via somato-dendritic release..... p.91
4.2.2. Pattern-dependent inhibition of glutamate release via somato-dendritic release..... p.93
4.2.3. Locus of inhibition involved in the suppression of glutamate release..... p.93
4.2.4. Discovering the identity of retrograde messengers released from OT and VP neurons..... p.95

4.3. Discussion..... p.97
4.3.1. Somato-dendritic release inhibits glutamatergic transmission in a frequency- and pattern- dependent manner..... p.97
4.3.2. Presynaptic locus of inhibition for OT and VP neurons..... p.99
4.3.3. Activity-dependent retrograde EPSC inhibition in oxytocin neurons..... p.101
4.3.4. Activity-dependent retrograde EPSC inhibition in vasopressin neurons..... p.102

V: IMPACT OF CALCIUM AND SPIKE BROADENING IN SOMATO-DENDRITIC RELEASE

5.1. Overview..... p.111
5.2. Results..... p.112
5.2.1. Presynaptic inhibition of glutamate release is dependent on postsynaptic calcium..... p.112
5.2.2. Per spike intra-dendritic calcium influx is correlated to somatic action potential broadening..... p.113
5.3. Discussion..... p.114
5.3.1. Frequency-dependent rise in intra-dendritic calcium is differentially regulated in OT and VP neurons..... p.114
5.3.2. Role of calcium in the frequency-dependent inhibition of excitatory transmission..... p.116
5.3.3. Frequency-dependent action potential broadening is correlated to a proportional rise in intra-dendritic calcium..... p.116

VI: GENERAL DISCUSSION

6.1. Overview..... p.121
6.2. Differential short-term facilitation in OT and VP neurons at the onset of OVLT electrical Stimulation..... p.122
6.3. Role of NMDA receptors in somato-dendritic release..... p.125
6.4. What is the point of inhibiting presynaptic neurotransmitter release?..... p.127
6.5. Overview of the NMDA-induced clustering model..... p.130
6.6. Overview of the somato-dendritic release model for OT and VP neurons..... p.131
6.7. Concluding remarks..... p.133

VII: REFERENCES..... p.138

VIII: APPENDICES..... p.151

This work is dedicated to

Gabriel, Gilles, Maryse, Roxanne and Anna

You all played a major role in my life.

ABSTRACT

Magnocellular neurosecretory cell (MNC) somata are located in the paraventricular and supraoptic nuclei of the hypothalamus. Following the arrival of an action potential at the synaptic terminal, these neurons release the hormones oxytocin (OT) vasopressin (VP) in the bloodstream, in a frequency-dependent manner. Previous *in vivo* studies have reported the emergence of a short rhythmic oscillation in MNC of water deprived rats, referred to as clustering activity. We show herein that this clustered firing can be induced *in situ* via endogenous glutamate release following the electrical stimulation of the organum vasculosum laminae terminalis. Additionally, we show that this clustering activity depends on NMDA receptor activation and that this rhythmic firing is modulated via the depolarizing effect of neurotensin and SK3 channel activity. It was also previously demonstrated that postsynaptic spiking eliciting somato-dendritic release of retrograde messengers suppresses excitatory neurotransmission. However, how a clustered firing as well as different spike frequencies contribute to this presynaptic inhibition is not known. Here we demonstrate for the first time, using a constant number of action potentials, that a clustering activity is more effective at inhibiting excitatory transmission than a tonic firing, in VP neurons. We also show the presence of a frequency-dependent inhibition of glutamate release that is correlated to a higher intra-dendritic calcium influx per spike at higher frequencies of discharge.

RÉSUMÉ

Les somata des cellules magnocellulaires neurosécrétoires (CMN) sont localisés dans les noyaux paraventriculaires et supraoptiques de l'hypothalamus. Suivant l'arrivée d'un potentiel d'action aux terminaisons synaptiques, ces neurones relâchent les hormones ocytocine (OT) et vasopressine (VP) dans la circulation sanguine en fonction de la fréquence de décharge. Des études *in vivo* ont reporté l'émergence d'une courte oscillation rythmique dans les CMN de rats privés d'eau, appelé activité de *clustering*. Nous démontrons que cette activité de *clustering* peut être induite *in situ* via un relâchement synaptique endogène de glutamate suivant la stimulation électrique de l'organum vasculosum laminae terminalis. De plus, nous démontrons que cette activité rythmique dépend de l'activation des récepteurs NMDA et est modulée via l'effet dépolarisant de la neurotensin ainsi que par l'activité des canaux SK3. Il a aussi été précédemment démontré que l'activité de décharge post synaptique induit un relâchement somato-dendritique de messagers rétrogrades qui supprime la transmission excitatrice. Cependant, de quelle façon une activité de *clustering* ainsi que différentes fréquences de décharge post synaptique contribuent à cette inhibition pré synaptique est encore inconnue à ce jour. Ici, nous démontrons pour la première fois, en utilisant un nombre de potentiels d'action constant, qu'une activité de *clustering* dans les cellules VP est plus efficace pour inhiber la transmission excitatrice qu'une décharge tonique. Nous démontrons aussi que l'inhibition du relâchement de glutamate est proportionnelle à la fréquence de décharge post synaptique qui est corrélée à l'augmentation de calcium intra-dendritique et ce, par potentiel d'action.

ACKNOWLEDGEMENTS

When starting my doctoral studies in 2010, I knew very little about science. Freshly graduated with a bachelor's degree in Psychology, I knew more about theories of the mind than how a neuron behaves or fires action potentials. However, I was more ready than ever to learn about new neuroscience concepts and more precisely, from an electrophysiological perspective.

Following my participation in the rotation program (September 2010-June 2011), I started to work on my PhD project with my supervisor Charles Bourque. I am grateful that I had the chance to work with such a great mind, since my supervisor gave me a solid project and was considerate for including my personal interests in my research. I would also like to thank my committee members, Keith Murai and David Stellwagen, for their insightful input and guidance during my project. Through my daily interactions with former and present lab members, I have gown a lot as a person. I would like to thank Jessica Sudbury (from whom I based the organization of my thesis, considering her excellent work), Katrina Choe, Cristian Zaelzer, Éric Trudel, Jerneja Stare, Masha Prager-Khoutorsky , Claire Gizowski, Pierre Yves Laroche and Shidasp Siami. From the CRN, I would like to thank Yvonne Gardner and my friends Sejal Davla, Sarah Konefal and Marie Franquin.

I have a very special place for my two best friends, Roxanne LeBlanc and Anna Bumagin, who have been there for me, through the good and the bad. I cannot count the number of times that Roxanne took her time to listen to my concerns and provided me with support and insightful advice. Moreover, having Anna work in the lab for three summers in a row has been a lot of fun and I can only keep good memories of her short passage in the field of neuroscience!

My mother, Maryse Tourigny, from whom I got my organizational skills and my father, Gilles Gagnon, who pushed me towards intellectual discussions and introduced me to great authors from an early age, have been exerting a strong influence on the person that I am today. I would also like to thank my brothers Gabriel, Vincent and Julien and my grandparents: Jules Gagnon, Lucille Lacroix and Fleur-Ange Martel, who were always proud of me and very supportive of everything I do. Finally, I am grateful that I have spent good moments with Camille Bouthillier, whom I know through Grands Frères Grandes Soeurs de Montréal, since 2011.

PUBLICATIONS ARISING FROM THIS WORK

Published:

Gagnon A, Walsh M, Okuda T, Choe KY, Zaeler C and Bourque CW (2014). Modulation of spike clustering by NMDA receptors and neurotensin in rat supraoptic nucleus neurons. Journal of Physiology, 592 (19): 4177-4186.

Manuscripts in preparation:

Gagnon A, Sjöström J and Bourque CW (2016). Activity-dependent retrograde inhibition of excitatory transmission in rat supraoptic nucleus neurons.

Gagnon A and CW Bourque (2016). Role of clustered firing and NMDA receptors in the suppression of excitatory transmission in OT and VP neurons.

Abstracts:

Gagnon A, Walsh M, Okuda T, Choe KY, Zaeler C and Bourque CW (2012). Modulation of NMDA receptor-dependent burst firing by Neurotensin in rat supraoptic nucleus neurons. Society for Neuroscience annual meeting, New Orleans, United States.

Gagnon A, Walsh M, Okuda T, Choe KY, Zaeler C and Bourque CW (2012). Neurotensin inhibits rhythmic burst firing in rat magnocellular neurosecretory cells. Proceedings of the 7th International conference for neurons and brain disease. Montreal, Canada.

CONTRIBUTION AND ORIGINALITY

The results presented in this thesis have been reported previously at scientific conferences in abstract form (data from *Chapter III*) or during oral presentations (data from *Chapter III, IV and V*). The content of *Chapter III* was used to publish an article in the *Journal of Physiology*, in 2014. *Chapter IV and V* are in preparation for publications. I performed all experiments described herein, with the exception of Figure 3.2.1.A,C,D and E (*Chapter III*) for which Mike Walsh collaborated with me to collect more data. Additionally, in *Chapter III*, Cristian Zaelzer performed a RT-PCR for Figure 3.2.4.A and Katrina Choe collected some data for figure 3.2.4.G. Moreover, Jesper Sjöström created a software in Igor Pro for the spike width analysis, in *Chapter V* (Fig. 5.2.3.B-D).

Chapter I, *Introduction*, provides a review of the scientific literature that led to the formulation of all hypotheses presented in this thesis. Section 1.1 summarizes the literature pertaining to the structure, synthesis and release of OT and VP peptides during specific physiological contexts. Section 1.2 summarizes the literature pertaining to OVLT excitatory inputs onto SON neurons. Section 1.3 summarizes the literature pertaining to the effect that different patterns and frequencies of electrical activities exert on hormone release from the neurohypophysis. Section 1.4 summarizes the literature that directly pertains to the modulation of MNC electrical activity via depolarizing peptides and intrinsic mechanism regulating spike accommodation. Section 1.5 summarizes the literature pertaining to somato-dendritic release in MNC and how release from this neuronal area inhibits excitatory transmission. Section 1.6 summarizes the literature that pertains to the role of calcium in somato-dendritic release. Finally, Section 1.7 summarizes the hypotheses that will be investigated in this thesis.

Chapter II, *Methods*, describes the methodology applied for all the experiments reported in this thesis to investigate *Hypothesis one* (section 1.3.4), *Hypothesis two* (section 1.4.4), *Hypothesis three* (section

1.5.7), *Hypothesis four* (section 1.5.8) and *Hypothesis five* (section 1.6.6). The contribution of this chapter includes the protocols and analysis procedures that were applied for quantitatively determining the impact of different parameters in clustering activity as well as in the suppression of excitatory transmission via somato-dendritic release of retrograde messengers.

Chapter III, *Modulation of spike clustering by NMDA receptors and neurotensin in rat supraoptic nucleus neurons*, describes how clustered firing is triggered *in situ* and which parameters modulate this rhythmic oscillation, thus providing a new model of clustering activity.

Chapter IV, *Somato-dendritic release is regulated in a spike- and frequency-dependent manner to inhibit glutamatergic neurotransmission*, deepens the understanding on how somato-dendritic release inhibits glutamate release by providing a new role for the pattern as well as the frequency of postsynaptic firing in this inhibitory response, for both cell types.

Chapter V, *Impact of calcium and spike broadening in somato-dendritic release*, describes a novel mechanism by which a frequency-dependent action potential broadening leads to a proportional rise in intra-dendritic calcium influx per spike, thus providing a graded inhibition of excitatory afferents, which is proportional to the firing frequency of OT and VP neurons.

Chapter VI, *General Discussion*, provides supplementary results acquired during my PhD project which further help in the comprehension of the results presented herein. Moreover, this chapter provides an integrative perspective on the relevance of my research within its physiological context and proposes new models that bring an original contribution to previous scientific concepts.

ABBREVIATIONS AND SYMBOLS

~	Approximately
<	Less than
>	Greater than
%	Percent
μm	Micrometre
μM	Micromolar
4AP	4-aminopyridine
ACSF	Artificial cerebrospinal fluid
AEA	Anandamide
AG	Agonist
2-AG	2-Arachidonoylglycerol
AHP	After hyperpolarizing potential
Ang II	Angiotensin II
APV	2R-Amino-5-phosphonopentanoic acid
AQP	Aquaporin
AV3V	Anteroventral third ventricle
BK channels	Big/large conductance Ca^{2+}-activated K^{+} channels
Ca^{2+}	Calcium
CB1	Cannabinoid type-1 receptor
Cd^{2+}	Cadmium
C_m	Membrane capacitance
CPM	Cluster per minute
DAG	Diacylglycerol
DAGL	Diacylglycerol lipase
DAP	Depolarizing after potential
DNQX	6,7-Dinitroquinoxaline-2,3(1H,4H)-dione
DSE/I	Depolarization-induced suppression of excitatory/ inhibitory transmission
DYN	Dynorphin
EC	Endocannabinoid
ECF	Extracellular fluid
eEPSC	Evoked excitatory postsynaptic current
e.g.	For example
EM	Electron microscopy
EPSC	Excitatory postsynaptic current
EPSP	Excitatory postsynaptic potential
GABA	Gamma-aminobutyric acid

Gd^{3+}	Gadolinium
GPCR	G-protein coupled receptor
HAP	Hyperpolarizing after potential
Hz	Hertz
i.e.	In other words
I_{NAP}	Sodium persistent current
i.p.	Intraperitonal
IPSC	Inhibitory postsynaptic current
IPSP	Inhibitory postsynaptic potential
ISI	Interspike interval
i.v.	Intraventricular
I/V	Current voltage
K^+	Potassium
Kg	Kilogram
KHz	Kilohertz
κ-opioid	Kappa-opioid
Kyn	Kynurenic acid
LDCV	Large dense core vesicle
MC	Manning compound
mEPSC	Miniature EPSC
Mg^{2+}	Magnesium
Min	Minute
mL	Milliliter
mm	Millimeter
mM	Millimolar
MNC	Magnocellular neurosecretory cells
MnPo	Median preoptic nucleus
mOsm	Milliosmole
ms	Millisecond
mV	Millivolt
nA	Nanoampere
Na^+	Sodium
NaCl	Sodium chloride
NMDA	N-methyl-D-aspartate
Nor-BNI	nor-binaltorphimine
NT	Neurotensin
NTS	Neurotensin receptor
OT	Oxytocin
OVLT	Organum vasculosum laminae terminalis

pA	Picoamps
pg	Picogram
POA	Preoptic area
PPR	Paired pulse ratio
Pr	Probability of release
pS	Picosiemens
PVN	Paraventricular nucleus
Q	Charge transfer
RT-PCR	Reverse transcriptase polymerase chain reaction
s/sec	Second
SCN	Suprachiasmatic nucleus
sEPSC	spontaneous excitatory postsynaptic current
SfO	Subfornical organ
SIC	Stretch-inactivated cation
sIPSC	Spontaneous inhibitory postsynaptic current
SK channels	Small conductance Ca^{2+}-activated K^{+} channels
SNARE	Soluble NSF attachment protein receptor
SON	Supraoptic nucleus
TEA	Tetraethylammonium
TG	Thapsigargin
THL	Tetrahydrolipstatin
TRPV	Transient receptor potential vanilloid
Trpv1$^{-/-}$	TRPV1 gene knockout mice
TRPV1dn	N-terminal truncated variant of TRPV1
TTX	Tetrodotoxin
VGCC	Voltage gated calcium channel
Vm	Membrane voltage
VP	Vasopressin (antidiuretic hormone)
WT	Wild-type
Δ	Variation
τ	Time constant
Ω	Ohm

I : INTRODUCTION

1.1. Magnocellular neurosecretory cells

1.1.1. Role in survival: an evolutionary perspective

What have in common these physiological phenomena in humans: giving birth, regulating the amount of water excreted in the urine, or breastfeeding a baby? As a simple answer, these three phenomena are mainly under the control of magnocellular neurosecretory cells (MNC), a group of vasopressin (VP) and oxytocin (OT) neurons located in the supraoptic nucleus (SON) and the paraventricular nucleus (PVN) of the hypothalamus. Multiple players, from the peripheral as well as the central nervous system, are involved in the activation of MNC, which release their respective hormone (i.e. VP and OT) from the posterior pituitary into the blood circulation in response to physiological demands. Additionally, OT, VP and other messengers are released from the soma and dendrites of MNC. However, how these messengers are released from the somato-dendritic compartment of these neurons has not yet been fully elucidated. Therefore, this aspect will be further addressed as well as how retrograde messengers inhibit presynaptic neurotransmitter release.

1.1.2. In animals: a behavioral and social perspective

In basal vertebrates, including fish and amphibians, MNC are located in the preoptic nucleus (Garlov, 2005). Interestingly, during times of high peptidergic demand such as seasonal changes for frogs and migration for fish, neurogenesis is observed in this region to compensate for the neuronal loss associated with a higher neurosecretory activity (Polenov and Chetverukhin, 1993; Knobloch and Grinevich, 2014). In advanced vertebrates including birds, reptiles and mammals, MNC are located both in the SON and the PVN (Knobloch and Grinevich, 2014) (Figure 1.1.2). OT and VP have been shown to

play a major role in reproduction as well as pro-social related behaviors (Bosch and Neumann, 2012). For example vasotocyn (a VP homologue), when applied to the preoptic area of the anterior hypothalamus of plainfin midshipman fish, modulates social vocalization during courtship situation and promotes the defense of the nest and eggs in males that already display parental behaviors (Goodson et al., 2003). In the teleost fish Lythrypnus dalli, when a dominant male is removed from the social group, the dominant female will change sex to male, and this change is associated with a marked loss of isotocin immunoreactivity (i.e. a OT homologue) in the preoptic area (Black et al., 2004). Even if this sex change from female to male is related to a decrease in the number of isotocin neurons, no direct conclusion can be drawn from this correlation. However, it is worth mentioning that administration of an OT antagonist in midshipman fish females led to a significant increase in the number of bursts recorded (i.e. a parameter linked to male vocalizations in order to protect the eggs and the nest), suggesting a direct link between peptidergic function and sexual behavior. (Goodson and Bass, 2000).

Fear-related responses are also important in the conservation of species. It was observed that OT released on the central amygdala is capable of changing the microcircuit activity and amygdala-dependent behavior related to conditioned fear responses in rats (Knobloch et al., 2012). More specifically, blue light activation of channel rhodopsin-2-expressing axons was shown to trigger OT release *in vitro*, and the same stimulation *in vivo* caused a decrease of freezing response behaviors in fear-conditioned rats.

Interestingly, the monogamous behavior of prairie voles has been linked to the distribution and activation OT and VP receptors. Concerning the spatial distribution of these receptors, the prairie vole, which forms a lasting bond, presents a higher density of OT receptors in the medial prefrontal cortex, the nucleus accumbens and the lateral amygdala compared to non-monogamous montane and meadow voles (Insel and Shapiro, 1992). Pair bonding mechanisms are also correlated to VP type 1a (V1a) receptor distribution since their expression was shown to be higher in the ventral pallidum of prairie

voles compared to non-monogamous montane voles (Young and Wang, 2004). In regard to the functional role of these receptors, it was demonstrated that blocking V1a receptors in the ventral pallidum prevents partner preference formation in males after mating (Lim and Young, 2004), but only when the antagonist is injected before the partner preference has been made (Donaldson et al., 2010). In other words, blocking V1a receptors prior to cohabitation or before partner preference has been established prevents pair bonding, whereas a blockade of these receptor once the preference is integrated does not interfere with their monogamous behavior.

1.1.3. In humans: a behavioral and social perspective

In humans, analyzing VP and OT concentration by collecting blood plasma samples is a potent tool to understand the contribution of these respective neurons in different physiological states, since centrally synthesized peptides are released in the blood circulation. The examples mentioned below will highlight the relationship between levels of peripheral neurohypophyseal hormones and human behaviors, notably in the context of emotions, prosocial behavior and mental illness.

A pioneer study performed on males has reported that intranasal administration of OT increased trusting behavior during a simulated game where they had to take calculated risks when interacting with other people, showing the importance of OT in human trust (Kosfeld et al., 2005). It was also shown that intranasal OT administration in men led to fewer errors in identifying facial emotional expressions using the Reading the Mind in the Eyes Test (RMET), a test used to identify emotional states when evaluating pictures (Domes et al., 2007). Concerning intimate relationships, it was observed that plasma OT is significantly higher in new lovers compared to singles (Schneiderman et al., 2012). Interestingly, salivary OT levels in humans were found to be positively correlated with bonding to parents while inversely correlated to psychological distress, such as depressive symptoms (Gordon et al., 2008). Interestingly, variations observed in the human V1a receptor gene (*AVPR1A*) have been correlated

to pair bonding satisfaction in males. Indeed, the variant RS3 334 is associated with a lower bonding quality with their partner (i.e. characterized by lower scores on the partner bonding scale), therefore increasing the likelihood of reporting marital problems (Walum et al., 2008).

Neurohypophyseal peptides have also been shown to play a role in mental health. Indeed, it was observed that blood VP levels are lower in children with autistic spectrum disorder when performing the Theory of Mind test (i.e. an evaluation of social behaviors) in comparison to normal children (Carson et al., 2015). Moreover, schizophrenic patients display lower plasma OT levels compared to healthy control subjects and a trend is also observed for VP (Jobst et al., 2014), since schizophrenic patients show a lower amount of this peptide (p=.052). This study also revealed that OT levels were correlated with familial history because schizophrenic children that were orphan or raised by only one parent displayed significantly lower OT plasma levels compared to children that were growing up with both parents.

1.1.4. Oxytocin cells

1.1.4.1. Structure, synthesis and release of oxytocin

The OT gene contains 3 exons (exon I: OT and OT-associated neurophysin; exon II: central part of neurophysin; exon III: final section of neurophysin) which are transcribed into mRNA template and then translated into the OT prepropeptide molecule by ribosomes in the rough endoplasmic reticulum (RER). Subsequent processing within the RER includes removal of the signal sequence (i.e. giving rise to a propeptide structure) and formation of disulfide bonds (–S–S–) between the cysteine residues. The OT propeptide molecules then enter the Golgi apparatus to be packaged into secretory granules. Neurophysin, the carrier protein of OT, plays a role against proteolytic degradation and increases the peptide half-life when attached to its peptide in the extracellular space. Indeed, OT may remain attached to neurophysin on immediate release from the axon terminal, but once the peptide-neurophysin complex is dissociated, the free hormone attaches to its receptor (McEwen, 2004). The final OT peptide

contains 9 amino acids with only two different residues at positions 3 and 8 (lle and Leu) compared to VP (Acher and Chauvet, 1988). In dogs, Intracisternal injection of radioactive tyrosine has been used to estimate intra-axonal peptidergic transport rate, and the results have shown that neurohypophyseal peptides migrate from the hypothalamus to the axon terminal at a rate of about 2 mm/hour (Jones and Pickering, 1972), so considering that rat MNC are 3-5 mm in length (Randle et al., 1986b), it would take an hour for newly synthesized peptides to reach the axon terminal (Yao et al., 2011). It was found that neurohypophyseal peptides migrate along microtubules since colchicine treatment (i.e. an inhibitor of microtubule polymerization) prevents peptide transport, especially from the RER to the Golgi apparatus (Alonso, 1988). Several studies have shown that electrical stimulation of the posterior pituitary leads to OT and VP neurosecretory granule fusion with the plasma membrane and exocytosis, following calcium entry at the axonal terminal (Cazalis et al., 1985; Bicknell, 1988). Secretion of neurosecretory hormones is tightly coupled to the electrical activity of MNC and this aspect will be further elaborated in section 1.3.

1.1.4.2. Role in parturition and lactation

During the last few hours of pregnancy, oxytocin receptors are at high concentrations in the uterus, and thus establish a positive-feedback loop with the hypothalamic oxytocinergic system (Russell et al., 2003). During parturition, high levels of OT are secreted from the posterior pituitary, which in turn lead to prostaglandin production that triggers uterine contractions (Higuchi et al., 1986). More precisely, this feedback loop is seen when uterine contractions, triggered by prostaglandins, excite OT cells, which in turn release the OT peptide that triggers further prostaglandin production and further uterine contraction (Leng and Russell, 1999).

Importantly, blocking OT secretion or its signaling in rats impairs the process of parturition (Antonijevic et al., 1995), while electrical stimulation of the posterior pituitary induces uterine

contractions (Boer et al., 1975). A pioneer study using extracellular recordings in PVN neurons of awake (i.e. non-anaesthetized) rat has shown that the neuronal electrical activity starts to increase about 15 minutes prior to the first contraction (i.e. rising from 0.2 Hz to 3 Hz) (Summerlee, 1981). Moreover, uterine contractions were followed by a burst of high frequency of discharge (around 10-32 Hz; 6-14 s.) and a more pronounced burst was observed about less than 30 seconds before delivery (peak rate of 32-80 Hz; 5-12 s.). In humans, synthetic oxytocin is used to induce or accelerate labor and oxytocin antagonist has been shown to be effective in women for delaying pre-term labor (Coomarasamy et al., 2002).

The study performed by Summerlee (1981) using extracellular recording in PVN neurons was the first to correlate the activity of OT cells observed during parturition to the emergence of a burst of electrical activity found during lactation, within the same neuron. Indeed, this group found that some of the neurons that had previously shown an increase in electrical activity during parturition did show a burst of electrical discharge about 10 seconds before the arrival of the milk ejection reflex (i.e. a burst lasting around 6-8 s.). A previous study performed on antidromically identified PVN neurons (Figure 1.1.4.2) of anesthetized rats (Wakerley and Lincoln, 1973) has shown that 58% of the recorded cells displayed a burst of activity lasting 2-4 seconds with a peak of frequency between 24-80 Hz, followed by a pause (7-56 s.) right before the milk ejection reflex.

Using the same experimental approach in the SON, it was then shown that OT neurons within this nucleus display a similar phenotype of electrical activity during lactation (Lincoln and Wakerley, 1974). More precisely, several important findings were highlighted in this study. First, the milk ejection reflex, triggered via suckling from the pups, could also be induced by intraventricular (i.v.) injection of synthetic oxytocin or electrical stimulation of the neurohypophysis (50 pulses per s.). Second, SON neurons were divided into phasic cells (i.e. a type of electrical activity characteristic of VP cells, further described in section 1.3.1) and non-phasic cells, the latter category being linked to the behavior of OT

cells. Third, the non-phasic cells (i.e. about 43% of SON neurons) responsive to suckling displayed a dramatic acceleration of their firing rate 13 seconds before the milk ejection reflex with a mean peak frequency of 39 Hz and a mean duration of 2.2 seconds, followed by a period of inhibition (i.e. about 4-40 seconds with a high variability in the silent duration). Importantly, the peak of the firing rate was obtained within the first 5 to 10 spikes of the train.

A particular characteristic of OT neurons is that the initiation of lactation bursts during suckling of the pups is synchronized among this cell type. The evidence supporting this notion was first shown by Lincoln and Wakerley who reported that two non-phasic cells responsive to suckling showed a synchronicity in the onset of their response (Lincoln and Wakerley, 1974). Using paired extracellular recordings, it was later demonstrated that OT bursts are synchronized during lactation when recording from two different neurons within the SON, and a synchronicity was also found among cells located in this nucleus and within the PVN (Belin et al., 1984).

1.1.4.3. Role in rodent natriuresis

It was shown that both OT and VP cells increase their firing rate following intraperitonal (i.p.) injection of NaCl in rats, whereas injection of isotonic NaCl had no effect (Brimble and Dyball, 1977). Indeed, OT cells will reach a mean firing rate of about 7 Hz, with a similar value for VP cells, suggesting that both cell types display osmosensitive properties. Importantly, it was observed that rats receiving a subcutaneous dose of OT, via a mini-pump, increase their natriuresis (i.e. the excretion of sodium in urine) in a dose-dependent response (Verbalis et al., 1991). More precisely, rats were fed with a sodium deficient diet, a protocol used to optimize the detection of changes in urinary sodium excretion to avoid the large amount of natriuresis related to a normal chow (i.e. sodium rich) diet provided in laboratories (Stricker, 1981). The results showed that OT treatment increased natriuresis, while injection of OT antagonist prevented this effect. Another study has shown that NaCl infusion in rat femoral artery

resulted in an increased natriuresis consequently to the rise in endogenous OT, whereas the addition of OT antagonist delayed to onset and the magnitude of natriuresis compared to control rats. More precisely, the natriuretic response in rats receiving the OT antagonist was delayed by 30 minutes compared to the control group and the amplitude was attenuated by 60% (Huang et al., 1995).

Despite the link observed between high systemic sodium level and enhanced endogenous OT level in rats, so far no data support the evidence that this correlation is present in humans. Indeed, infusion of NaCl in male humans does not lead to an increase in plasma OT despite a substantial increase in natriuresis (Andersen et al., 1998) and intravenous injection of OT did not alter the natriuretic response in these subjects (Rasmussen et al., 2004). These findings suggest that OT participates in the natriuretic response in rats, whereas it does not appear to be the case in humans.

1.1.5. Vasopressin cells

1.1.5.1. Structure, synthesis and release of vasopressin

The VP gene contains 3 exons (exon I: tripeptide signal, VP nonapeptide and N-terminal part of neurophysin; exon II: central part of neurophysin; exon III: final section of neurophysin and a glycoprotein extension). The same steps described in section 1.1.4.1 for the formation of OT also apply for the generation of a VP peptide, with the exception of a 39 amino acid glycopeptide sequence, called copeptin, added at the C-terminal segment of this peptide (Bolignano et al., 2014) . Like OT, when the signal sequence is removed and gives rise to the propeptide structure in the RER, the newly formed propeptide VP then enters the Golgi apparatus to be packaged into secretory granules (McEwen, 2004). The VP molecule contains 9 amino acids (Cys-Tyr-Phe-Gln-Asn-Cys-Pro-Arg-Gly) and 2 amino acids, Phe and Arg are distinct from OT (Acher and Chauvet, 1988). A lot of articles, when referring to VP, frequently use the term *arginine-vasopressin* (AVP) because of the presence of an arginine residue at position 8, and to make a distinction with other mammals that possess a lysine residue at the same

position. More precisely, the term *lysine- vasopressin* (LVP) is employed for mammals such as pigs, hippopotamus, warthogs and some marsupials (Acher and Chauvet, 1995). VP is commonly referred to as the anti-diuretic hormone because its binding to V2 receptors on the kidneys promotes water reabsorption and prevents diuresis (Pearce et al., 2015) (see section 1.1.5.2c). Similarly to OT release, upon the arrival of an action potential at the nerve terminal, calcium entry triggers fusion of VP secretory granules with the plasma membrane and diffusion of VP molecules into the extracellular space (Bicknell, 1988).

1.1.5.2. Role in osmoregulation

1.1.5.2a. Defining the concept of osmoregulation: from central to peripheral osmoreceptors

Osmolality can be defined as a quantitative measure of the total solute concentration in a solution expressed in moles per kilogram of a solution, and mammals generally adopt appropriate behaviors to maintain their plasma osmolality near to a set-point of ~300 mOsm kg^{-1} (Bourque, 2008). Water intake is critical to body homeostasis and is involved in digestion, the absorption and transport of nutrients, elimination of body toxins, thermoregulatory processes and reproduction among many other functions (Kleiner, 1999). Dehydration occurs when body fluid losses are not properly compensated, which leads to a total weight loss of 1% or greater (Kristal-Boneh et al., 1988). In the case of dehydration, the extracellular fluid (ECF) osmolality will be above the osmotic set-point and mammals will therefore try to correct this value, mainly by drinking water, following the sensation of thirst. Now that a definition about the concept of osmoregulation has been formulated, the aim of the present section will be to briefly describe the role of central as well as peripheral structures involved in osmoregulatory processes.

Several brain regions are activated when dehydration occurs. A study using Fos-immunoreactivity (i.e. a technique used to see the expression of the protein C-Fos, which is produced during neuronal activation (Morgan et al., 1987)) in 48 hours water-deprived rats has shown that several

forebrain structures are activated at this stage of dehydration, including the median preoptic nucleus (MnPO), the organum vasculosum laminae terminalis (OVLT), the SON and the PVN, with only a small and sparse activation in the subfornical organ (SfO) (McKinley et al., 1994). The OVLT, an osmosentitive region located in the anteroventral third ventricle (AV3V), has been shown to play a role in drinking behavior, natriuresis and VP release. Indeed, destruction of OVLT neurons resulted in an attenuation of drinking behavior following intravenous administration of NaCl in dogs, and this ablation also abolished the positive relationship between plasma osmolality and VP release (Thrasher et al., 1982). In humans, destruction of osmoresponsive cells in the OVLT leads to a chronic state of hypernatremia (i.e. an abnormally high extracellular fluid (ECF) sodium concentration) with a deficit in VP secretion, a condition called adipsic hypernatremia (Baylis and Thompson, 1988). Several studies have shown that OVLT neurons display osmosensitive properties. Indeed, hypertonic solutions were shown to increase the firing rate of OVLT neurons, whereas hypotonic solutions had the opposite effect (Sayer et al., 1984; Vivas et al., 1990). Interestingly, the linear relationship found between plasma osmolality and the firing rate of OVLT neurons is abolished in knock-out mice for the transient receptor potential vanilloid type-1 (TRPV1) gene (Ciura and Bourque, 2006), suggesting that these channels are of critical importance for the osmosensitive properties of OVLT neurons.

The SON and the PVN are key structures for the mediation of osmoregulatory processes. Both of these nuclei enclose MNC somata that extend their axon into the posterior pituitary to release VP (as well as OT, see section 1.1.4.1) into the bloodstream upon the arrival of an action potential. A pioneer experiment performed by Verney has revealed that intra-carotid infusion of NaCl in dogs promotes anti-diuresis, while ablation of the posterior pituitary leads to an increase in the total quantity of urine collected, indicating that neurohypophyseal hormones play a role in diuresis (Verney, 1947). In another experiment (Arnauld and du Pont, 1982), rhesus monkeys were water deprived for 2-6 days and then allowed to drink water for a short period of time (i.e. about 5 minutes). Right away following drinking,

two observations were made. First, upon drinking, a decrease of plasma VP was immediately seen before plasma osmolality values were corrected. Second, extracellular recordings in the SON showed that the firing activity of phasic VP neurons was significantly reduced following drinking. The findings above support the involvement of SON cells in osmoregulatory functions and the idea that receptors on the periphery can inhibit MNC and VP release before plasma osmolality is corrected. The intrinsic ability of SON cells to detect changes in ECF osmolality and to transduce this information into a change in their electrical activity will be extensively described in section 1.1.5.2b.

Because SON neurons play a major role in osmoregulatory processes, it is important to consider how their electrical activity is influenced by neurons in other brain structures that synapse onto these cells. The OVLT is of critical importance in the regulation of SON cell activity. Studies using retrograde tracer labeling (McKinley et al., 1994) and electrophysiology (Yang et al., 1994) have shown that OVLT neurons send glutamatergic and GABAergic inputs onto SON neurons and hence, exert a control on the electrical activity of MNC. Considering the significant contribution of OVLT neurons in MNC excitability, a section investigating the role of OVLT inputs onto MNC will be addressed in section 1.2.

Verney was the first person to introduce the idea of osmoreceptors, which he designated as sensory elements that allow osmotic stimuli to be transmuted into electrical signals (Verney, 1947). Peripheral osmoreceptors have been shown to play an important role in osmoregulation. For example, splanchnic receptors located in the small intestine display osmosensitive properties because gastric infusion of hypertonic solution was found to increase plasma VP (Choi-Kwon and Baertschi, 1991) . This study also proposed that the information coming from the splanchnic zone travels by splanchnic nerves to reach the central nervous system because VP release was attenuated by 61% when a lesion was performed on these nerves, while no effect was found in vagotomized rats. It was also observed that peripheral osmoreceptors are localized in the rat liver. Indeed, the electrical activity of the hepatic vagus nerve increases following the application of a hypertonic solution to the liver, via the portal vein, while

other groups of fibers from the liver increase their firing rate following the application of a hypotonic solution (Adachi et al., 1976). After 24 hours of water and food deprivation, it was found for the vagotomized group, compared to the control group, that their urine was less concentrated and an increase in diuresis was also observed (i.e. VP secretion deficit), suggesting that this nerve has its importance to relay osmotic information to the central nervous system. Although peripheral osmoreceptors associated with the gut and liver contribute to the osmotic control of VP release, a large amount of data indicates that central osmoreceptors are also critical for this function. Therefore, the next section will describe the advances that have been made to understand the role as well as the identity of central osmoreceptors within the SON.

1.1.5.2b. Vasopressin cells act as mechanical transducers

An important feature of MNC is that they display mechanosensitive properties. Indeed, applying suction via a patch pipette, in order to decrease the cell volume, leads to an enhanced firing rate, whereas inflating the cell decreases firing activity (Oliet and Bourque, 1993). Recordings from isolated MNC have shown that application of hypertonic solutions increase the cell conductance, while hypotonic solutions decrease this conductance. More specifically, an inward current triggered by increases in external fluid osmolality is mediated via the opening of non-selective cationic channels (Bourque, 1989). Importantly, changes in cell volume, rather than the osmolality of a solution itself, are responsible for the observed changes in the electrical conductance of MNC. Indeed, the increase in cation conductance following the application of a hypertonic solution is prevented when MNC are inflated with positive pressure via a patch pipette, whereas a decrease in cell conductance, subsequent to the application of a hypotonic solution, is prevented by cell shrinking (Zhang et al., 2007). The increase in membrane conductance following cell shrinking appears to be mediated by the activation of stretch inactivated cation (SIC) channels because the presence gadolinium (Gd^{3+}) in the pipette, a blocker of mechano-sensitive channels, decreases the magnitude of this effect by reducing the mean opening time of these

channels in isolated cells (i.e. 50% reduction of the mean opening time for 30 μM Gd^{3+}) and external solutions containing Gd^{3+} decrease macroscopic current responses after osmotic stimulation (Bourque and Oliet, 1997). Interestingly, changes in cell volume were shown to depend on the folding or unfolding of existing membrane (i.e. membrane reserves) rather than insertion of new material to the plasma membrane (Zhang and Bourque, 2003). On the contrary, hippocampal neurons, used as a control in this study, displayed proportional changes in total surface membrane area as cell volume was changed by osmotic stimulation.

A question that arises from these findings is *what is the molecular identity of these SIC channels that transduce changes in cell volume (i.e. swelling or shrinking) into changes in the electrical activity of MNC*? Several evidences suggest that a variant of the N-terminal part of the TRPV1 receptor is involved in the transduction mechanism of MNC in mice (Sharif Naeini et al., 2006). First, the message encoding the N-terminal end of Trpv1 (i.e. exons 2–6) was not detected in the SON, using reverse transcription polymerase chain reaction (RT-PCR), while the N-terminal end was found in dorsal root ganglia, indicating that a N-terminal variant of TRPV1 might be present in SON cells. Second, application of a hypertonic solution on acutely isolated VP cells in mice lacking the TRPV1 gene ($TRPV1^{-/-}$) showed a decrease in cell volume, but no increase in cell conductance was observed in comparison to control mice. Third, the increase in membrane conductance following a hyperosmotic challenge was prevented in wild-type cells when treated with ruthenium red (i.e. a non-specific TRP channel blocker). Lastly, the linear relationship between serum VP and plasma osmolality is attenuated in $TRPV1^{-/-}$ mice, indicating that for osmolality concentration above the osmotic set-point, VP release is not secreted in a sufficient amount to correct plasma osmolality.

Recently, the molecular identity of the channel responsible for the increase in MNC electrical conductance during a hypertonic challenge or an increase in body temperature was discovered (Zaelzer et al., 2015). Indeed, using RT-PCR, it was shown that isolated SON and OVLT neurons contain a

transcript for the N-terminal truncated variant of TRPV1, referred as *TRPV1dn,* whereas the full TRPV1 transcript was not found in these neurons. Importantly, this study has shown that cell-induced shrinking as well as bath application of a hypertonic solution on cultured hypothalamic neurons from TRPV1$^{-/-}$ mice, transfected with *TRPV1dn,* resulted in an increased firing rate and an enhanced resting membrane potential compared to untransfected or TRPV1 transfected neurons. Moreover, HEK293 cells transfected with either rat *TRPV1dn* or mouse *TRPV1dn* showed an increase in inward current following a hyperosmotic challenge, while HEK293 cells transfected with TRPV1 did not display this response.

Other important players are involved in the mechanical gating of MNC. In response to suction, MNC treated with Cyt-D (i.e. a drug that depolymerize F-actin) displayed a smaller inward current, whereas cells treated with JSK (i.e. a dug that promotes actin polymerization) showed a larger inward current compared to control cells (Zhang et al., 2007), suggesting that actin filaments play a role in regulating the volume of MNC. Moreover, it was shown recently that microtubules interact with the C-terminal part of TRPV1, providing a pushing force that leads to the channel activation during cell shrinking and thus, enhances the electrical activity of MNC (Prager-Khoutorsky et al., 2014).

1.1.5.2c. Activation of V2 receptors and water reabsorption from the kidneys

V2 receptors are expressed in the kidney, more specifically in the basolateral membrane of epithelial cells of the renal distal collecting tubules (van Lieburg et al., 1995). These receptors are part of the 7-transmembrane domain G-protein coupled receptor (GPCR) family and VP binding activates the Gs subunit (Stockand, 2010) which is coupled to adenylate cyclase and cAMP activity (Orloff and Handler, 1962). A pioneer experiment has shown that VP application on renal papilla will promote the translocation of endosomes in close proximity of the luminal membrane of the collecting tubules. These endosomes contain vesicles that enclose *water channels,* called *aquaporin 2* (AQP2) (Deen et al., 1994) that will be inserted on the apical membrane of the collecting tubules to enable water diffusion into the

cell, down to a favorable osmotic gradient (Verkman et al., 1988). More specifically, because the renal medulla (i.e. the inside of the kidney) is kept hypertonic, the insertion of water channels will promote water reabsorption in the kidney (van Lieburg et al., 1995).

In other words, during hypertonic conditions, VP is released from the posterior pituitary and binds to V2 receptors to activate a cAMP cascade that leads to the insertion of AQP2 at the apical membrane of the collecting duct. Water then enters the cell and exits into the interstitium via AQP3 and AQP4, located in the basolateral membrane, to reintegrate the bloodstream, leading to a more concentrated urine (Pearce et al., 2015).

1.2. OVLT synaptic inputs onto MNC

The aim of previous sections was mainly to describe how SON cells operate as an intrinsic unit: how their peptides are synthesized, what are their characteristic roles and firing patterns according to their cell type and how they transduce osmotic information into an electrical output. The following section will investigate how the electrical activity of MNC is modulated via glutamatergic inputs, and a particular emphasis will be given to OVLT afferents, knowing that these cells also display osmosensitive properties as elaborated in section 1.1.5.2a.

1.2.1. Glutamatergic inputs

A study using autoradiographic retrograde labeling has shown that glutamatergic inputs onto MNC originate from different regions such as the OVLT, the SfO, the MNPO, the suprachiasmatic nucleus (SCN), the amygdala complex and the bed nucleus of the stria terminalis (Csaki et al., 2002). The first *in vivo* evidence that osmotic stimulation of the OVLT impacts the electrical activity of MNC was provided about 30 years ago (Honda et al., 1987). This group found that injection of NaCl in the AV3V, a region enclosing the OVLT, leads to an enhancement of MNC firing rate. Later on, an effort was made to

characterize the nature of the electrical connection between the OVLT and the SON. The electrophysiological evidence that glutamatergic and GABAergic inputs synapse onto MNC, and presumably originate from the OVLT, was provided about 20 years ago (Yang et al., 1994). In this study, electrical stimulation of the OVLT resulted in the apparition of inhibitory post synaptic potentials (IPSP) in 89% of the cells recorded, while the remaining cells displayed excitatory post synaptic potentials (EPSP). In most neurons showing an IPSP, application of biccuculine (i.e. a $GABA_A$ receptor antagonist) revealed the presence of an EPSP. Importantly, the fast EPSP was shown to be mediated by the activation of AMPA and kainate receptors, whereas the slow EPSP was shown to depend on N-methyl-D-aspartate (NMDA) receptor activation since CNQX (i.e. a AMPA/kainate receptor antagonist) prevented the fast response and D,L-2-amino-5-phosphonovalerate (i.e. APV; a NMDA receptor antagonist) blocked the slow component. Another study has shown that application of a hypertonic solution over the OVLT leads to an increase in the firing rate of MNC, whereas application of hypotonic solutions decreases MNC firing rate (Richard and Bourque, 1995). Moreover, this study provided the evidence that the degree of osmotic stimulation over the OVLT is correlated to the increase of spontaneous EPSP (sEPSP) frequency observed in MNC. Interestingly, no change was observed for the frequency of sIPSP when the OVLT was osmotically challenged, suggesting that the increased excitability of MNC following OVLT osmotic stimulation is attributable to glutamatergic afferents activity rather than a suppression of GABAergic activity.

1.3. Pattern and frequency of electrical activity displayed by MNC

As discussed earlier (in section 1.1.4.1 and 1.1.5.1), upon the arrival of an action potential at the nerve terminal, calcium enters the neurohypophysis, which triggers OT and VP release into the blood circulation by their respective neurons. Considering that a direct link exists between the electrical activity of MNC and their hormonal output, the following sections will investigate two types of electrical activity that were shown to maximize VP release from the neurohypophisis. These two types of electrical firing,

which are *phasic* and *clustering activity*, will be discussed as well as the mechanisms that lead to their formation.

1.3.1. Phasic activity in VP cells

Early *in vivo* studies using extracellular recordings in rats have been of critical importance to describe the characteristics of phasic activity in VP cells (Poulain and Wakerley, 1982). Electrophysiologically, phasic activity can be defined as the grouping of action potentials that forms bursts lasting in average between 4 and 100 seconds with a mean intra-burst frequency of 3 to 15 Hz. Each burst is separated by silent intervals of comparable duration (4-200 seconds with a mode of 5-25 seconds). Moreover, these bursts begin with a higher frequency of discharge for the first 1-2 seconds to then reach a plateau of firing activity (Poulain and Wakerley, 1982). *In vivo* experiments have shown that a transition from a slow irregular activity to a fast continuous firing, that ultimately leads to a phasic firing, can be observed during hemorrhage (Wakerley et al., 1975) or when a hypertonic solution is injected in rats (Brimble and Dyball, 1977). It appears that the summation of depolarizing after potentials (DAP) following each action potential promotes burst initiation by forming a plateau potential, thereby increasing the likelihood of additional spikes and DAP, resulting in a prolonged burst duration (Andrew and Dudek, 1983).

Phasic activity is thought to emerge from intrinsic mechanisms as well as network activity. Indeed, it was shown that injecting positive current in a phasic cell increases burst length as well as intra-burst frequency (Andrew and Dudek, 1983). Moreover, this study demonstrated that tetrodotoxin (TTX) application, which blocks synaptic transmission, does not affect the plateau potential in phasic cells, suggesting that intrinsic mechanisms are involved in this type of firing activity. On the other hand, synaptic potentials are also essential in the generation of a burst since their presence is required to elicit

action potentials, which in turn will lead to the DAP that sum into a plateau potential (Bourque et al., 1998).

A mechanism was proposed to explain burst cessation during phasic activity. Specifically, dynorphin (DYN), an opioid peptide copackaged within VP-containing neurosecretory vesicles (Whitnall et al., 1983), has been shown to be critical in this process. *In vivo*, extracellular single unit recordings have shown that nor-binaltorphimine (nor-BNI; a κ-opioid receptor antagonist) administration (via a U-shaped microdialysis probe placed over the SON) decreased the probability of burst termination (Brown et al., 2006), while administration of the κ-opioid receptor agonist U50-,488H reduced VP cells activity and decreased the proportion of phasic cells from 26% to 3% (Brown et al., 1998). Data acquired from recordings in hypothalamic explants have led to the conclusion that activity-dependent somato-dendritic release of DYN terminates phasic burst by inhibiting the DAP amplitude in MNC, therefore decreasing the probability to observe a subsequent spike and reducing the plateau potential amplitude (Brown and Bourque, 2004). This study has also shown that the DAP inhibition caused by conditioning spike trains is blocked by nor-BNI or when neurovesicle stores are depleted by α-latrotoxin.

1.3.2. Clustering activity in OT and VP cells

It is interesting to note that within longer phasic bursts, induced via i.p. injection of hypertonic saline or hemorrhage, a second form of periodicity is observed whereby shorter clusters (2-4 s. on, 2-4 s. off) begin to appear (Poulain and Wakerley, 1982). Statistical analysis of interspike intervals (ISI) from *in vivo* data in dehydrated rats (i.e. 0-24 hours) has shown the emergence of clustering activity in both OT and VP cells, with a higher incidence for VP cells, during the stationary phase of a phasic burst (Poulain et al., 1988). Pharmacologically, NMDA receptor activation appears to be effective in eliciting the initiation and the formation of clustering activity. Intracellular recordings in explants have demonstrated that bath application of NMDA induced clustered firing (0.5-1 s. ISI; 1-3 s. intercluster interval), whereas activation

of the non-NMDA AMPA and kainate receptors do not lead to cluster formation (Hu and Bourque, 1992). Moreover, this study has shown that glutamate application triggers clustering activity, which remains in the presence of CNQX, but is abolished upon APV application. Importantly, this study has shown that depolarization induced by positive current injection cannot alone trigger clustering activity, but once initiated by bath application of NMDA, the cluster length is strongly affected by voltage variation due to the magnesium (Mg^{2+}) block of NMDA receptors, since Mg^{2+}-free solutions suppress clustering activity. Moreover, calcium-free solution or cells filled with an internal solution containing BAPTA caused a suppression of clustering activity. Lastly, exogenous bath application of apamin (i.e. a blocker of small conductance Ca^{2+}- activated K^{+} channels; SK channels) also abolished clustering activity, leading to a tonic firing. Arising from this work, a model was created by Hu and Bourque (1992) in an attempt to explain the underlying mechanism involved in the initiation and the regeneration of this NMDA-induced clustering activity (see figure 1.3.2).

Other mechanisms have been shown to be capable of inducing the emergence of clustered firing in SON neurons. Indeed, in cells displaying phasic activity and DAP (i.e. putative VP cells), decreasing extracellular calcium concentration (1.2 mM – 0 mM) led to repetitive oscillations considered as clusters, arising from a sodium persistent current (I_{NAP}) which is enhanced in the presence of low extracellular Ca^{2+} concentration (Li and Hatton, 1996). More specifically, replacing ~80% of external Na^{+} by choline or lithium strongly prevented clustering induced in free-Ca^{2+} ACSF. Similarly, clustering induced by low calcium solution was prevented when cells were filled with BAPTA. This form of clustering activity, found in MNC, was also observed in neurons from the dorsal principal sensory trigeminal nucleus, during mastication (Brocard et al., 2006). It appears that astrocytes act as a Ca^{2+} buffer to lower extracellular Ca^{2+} concentration (i.e. by releasing the Ca^{2+} binding protein S100β) and thus, are a key component in the generation of clustering activity in the trigeminal nucleus by enhancing I_{NAP} current, upon NMDA receptor activation (Morquette et al., 2015). Whether astrocytes play a role in cluster formation in SON

neurons remained to be determined. Interestingly, it was observed that bath application of norepinephrine on hypothalamic explants depolarizes MNC and induces clustering activity via activation of α1-adrenergic receptors (Randle et al., 1986a). Indeed, *in vitro* data showed that isoproterenol administration, an α-adrenergic receptors blocker, suppresses clustered firing (Randle et al., 1984). Therefore there are many possible mechanisms that could support clustered firing in MNC during hypertonicity *in vivo*. In the next section, we will explore how changes in the firing pattern of SON neurons modulate neurosecretion.

1.3.3. MNC electrical activity is correlated to hormone output

In the 70s and the 80s, important questions arose from the observation that distinct types of electrical activity were recorded extracellularly during specific physiological contexts, such as phasic firing during dehydration and short high-frequency bursts during lactation. Some questions were; *does the emergence of phasic firing seen during dehydration or hemorrhage lead to a higher amount of VP secretion from the posterior pituitary? And do the typical lactation bursts recorded in female rats, during suckling by the pups, result in a higher output of OT from the neurohypophysis?* To answer such questions, several groups used an *in vitro* preparation containing the rat isolated neurohypophysis, and the idea was to stimulate this region electrically and see how changes in stimulation parameters (i.e. frequency, pattern of stimulation, pauses) would affect hormone release, quantified by radioimmunoassay.

One of the first studies using this technique showed that there is a positive relationship between the frequency of stimulation and OT release from the posterior pituitary, which becomes less effective when exceeding 35 Hz (Dreifuss et al., 1971). Moreover, this study led to the conclusion that a basal action potential-independent release occurred at rest, since an OT output was seen in the presence of TTX. However, stimulating the neural lobe in the presence of TTX greatly decreased the amount of OT

released compared to the control condition (i.e. no drug). The latter finding reinforced the idea that action potentials must invade the axon terminal to trigger a substantial amount of hormone release (i.e. a higher level than basal release). Concerning VP secretion from the neurohypophysis, a linear relationship was observed between the firing frequency and the hormone output, up to ~15 Hz (Bicknell, 1988). Interestingly, the mean firing rate recorded during phasic activity is also close to 15 Hz (Poulain and Wakerley, 1982), indicating that reaching higher frequencies of discharge might be ineffective at maximizing the release of this peptide *in vivo*.

Because pauses are observed between bursts of activity, the effect of this parameter on hormone release was also studied. It was observed that stimulating the neural lobe with templates derived from *in vivo* recordings of either continuous or a phasic activity lead to different amount of VP release, despite the fact that the mean frequency (i.e. 6 Hz) and the ISI were the same in both conditions (Bicknell and Leng, 1981). Indeed, a phasic pattern of activity led to significantly more VP release compared to a continuous stimulation, indicating that pauses between bursts are essential for optimizing hormone release. Confirming this idea, it was shown that bursts delivered such as seen in VP cells (phasic bursts) or OT cells (lactation burst) elicit more exocytosis of their respective peptide when pauses are introduced in the sequence of stimulation (Cazalis et al., 1985). Long stimulations with the absence of pauses appear to more negatively affect VP secretion than OT secretion. More precisely, a phenomenon called *fatigue* is observed within the first seconds of continuous neurohypophysis stimulation (i.e. at 13 Hz) in terminals of VP cells where exocytosis of this peptide drastically decreases over 72 seconds, while the OT output remains constant (Bicknell et al., 1984). Stimulating the neural lobe during long periods (i.e. ~20 minutes) and allowing only short pauses (i.e. 30 s. to 2 min) effectively reversed the *fatigue* phenomenon. However, introducing longer pauses (i.e. 20 minutes) between period of stimulation led to a better recovery and hence, a higher VP output within the following burst.

Importantly, the ISI within a burst seems to play an important role because a "regular" burst with a constant ISI elicits less VP release compared to a "real" burst where ISI are shorter at the beginning of the train and mimic the ISI pattern observed in a burst *in vivo* (Cazalis et al., 1985). Indeed, the amount of VP released was found to be higher during the first 9 seconds of a burst compared to the contribution of subsequent spikes in a 27 second burst. Lastly, this study also showed that "real" bursts as well as pauses between these bursts trigger more calcium uptake at the nerve terminal compared to the case where "regular" bursts or no pauses were given. How calcium uptake is modulated by such parameters is important because release from the neurohypophysis is tightly coupled to calcium influx (Bicknell, 1988), and this aspect will be further discussed in section 1.6.

So far, only one study has investigated the role of clustering activity on hormone output (Cazalis et al., 1985). In this study, the posterior pituitary was stimulated, in the first case, with a clustering activity and in the second case, with a continuous firing and both stimulations contained the same number of pulses and displayed the same mean frequency (i.e. 4 Hz). In the clustering condition, 4 pulses were given at the beginning of every second (i.e. 60 ms ISI) with a silent pause of 920 ms between clusters. The result indicates that a clustering conditioning elicits significantly more VP release from the neurohypophysis compared to the tonic stimulation. As mentioned above, it was shown that phasic activity seen in VP-containing neurons, and lactation bursts observed in OT-containing neurons, are two potent firing patterns in eliciting release from the neurohypophysis. However, despite the promising role of clustering activity in enhancing peptide release, little attention has been given to this rhythmic oscillation in MNC. Therefore, one of the aims of this thesis is to further address how clustering activity is generated *in vitro* (i.e. from a network perspective) and which parameters contribute to the shaping of this rhythmic firing.

1.3.4. Hypothesis one

As described in section 1.3.2, the appearance of clustering activity was reported *in vivo* within segments of electrical activity in OT and VP cells under different experimental conditions that are known for enhancing hormone release from the neurohypophysis, such as dehydration, hemorrhage and injection of hypertonic saline. However, very little is known about the mechanisms that lead to the emergence of this rhythmic firing. As discussed in section 1.2.1, the OVLT sends glutamatergic afferents onto MNC to modulate their firing activity, but if these excitatory connections are involved in the emergence of clustered firing is not known. Given the fact that pharmacological activation of NMDA receptors *in vitro* leads to the formation of clustering activity (see section 1.3.2), the first hypothesis formulated in my doctoral project is that *electrical stimulation of the OVLT will evoke endogenous glutamate release onto MNC and subsequently, the activation of NMDA receptors will lead to the emergence of clustering activity*.

1.4. Modulation of MNC electrical activity

Because we saw in section 1.3.3 that the electrical activity of MNC is directly linked to their hormone output, it is also of critical importance to understand how the firing activity of these cells can be modulated. As discussed in section 1.2, glutamatergic and GABAergic inputs exert an impact on the electrical activity of MNC. Additionally, locally released neuropeptides also exert an impact on the firing rate of SON neurons and these cells display some intrinsic mechanisms to regulate their firing rate, such as *spike accommodation*. The next sections will first discuss the excitatory effect that locally released neuropeptides exert on MNC and second, the mechanisms regulating spike accommodation will also be addressed.

1.4.1. Depolarizing neuropeptides: angiotensin II and neurotensin

Several neuropeptides have been shown to exert an impact on the excitability of MNC. In this section, the excitatory and inhibitory role of angiotensin II (Ang II), which is synaptically released onto MNC during hypovolemia (Potts et al., 2000), and the excitatory role of neurotensin (NT), which is putatively released on SON cells via SCN synaptic afferents (Cui et al., 1997), will be discussed.

Ang II is localized in different neuronal regions including the SfO, which sends afferents onto SON cells (Jhamandas et al., 1989). Importantly, *in vivo* experiments have shown that neurons of the SfO become excited during hypovolemia (Potts et al., 2000), a condition characterized by a decrease of ECF volume, notably via blood loss. Bath application of Ang II was found to increase the firing rate of different groups of neurons located in the SON, the SfO and within the AV3V region (Okuya et al., 1987). The membrane depolarization and the subsequent increase in the firing rate observed in MNC, following exposure to Ang II, is mediated by angiotensin type-1 (AT1) receptor activation, because this effect is blocked by the AT1 receptor antagonist DuP753 (Yang et al., 1992). Interestingly, a previous study has also shown that Ang II can modulate synaptic transmission onto MNC. Indeed, upon osmotic activation of the OVLT, application of Ang II over the SON suppresses the synaptic excitation of OT neurons while it potentiates the glutamatergic activation of VP neurons (Stachniak et al., 2014). More specifically, it appears that binding of Ang II onto OT cells triggers the release of endocannabinoids (EC) that inhibit glutamatergic transmission, whereas Ang II promotes nitic oxide release from VP cells and thus, enhances excitatory transmission. In the context of hypovolemia, these data support the idea that an increase in VP release is required to induce water reabsorption from the kidneys, while natriuresis (elaborated in section 1.1.4.3) must be suppressed via an inhibition of OT neurons in order to keep the plasma isotonic.

Using immunohistochemistry, it was shown that the SCN contains NT expressing neurons (Watts and Swanson, 1987). The SCN could be a potential source of endogenous NT released onto MNC, because this nucleus sends afferents onto the SON (Cui et al., 1997). Exogenously applied NT on rat hypothalamic explant was also shown to depolarize MNC and to increase their firing rate (Kirkpatrick and Bourque, 1995). This effect is achieved via activation of the NT receptors type 1 (NTS1) and type 2 (NTS2) (Pelaprat, 2006).

Ang II and NT depolarize and increase the firing rate of MNC via a common mechanism. These neuropeptides bind to GPCR (Pelaprat, 2006; Godin and Ferguson, 2012; Harikumar et al., 2013) and induce a slow and long lasting depolarization via SIC channel activation (Chakfe and Bourque, 2001). Under current clamp condition, exogenous application of Ang II or NT on SON cells triggers a depolarizing response reaching its peak within 30-40 seconds. This response remains in the presence of TTX, excluding the effect that these peptide might have on synaptic transmission (Chakfe and Bourque, 2001). This study reached the conclusion that this depolarizing effect is mediated via an increase in cation conductance measured by steady-state current-voltage (I/V) analysis. Ionic substitution experiment indicated that these two peptides depolarize MNC via a non-selective cationic conductance. Moreover, bath application of Gd^{3+} abolished the inward current response generated by ANG II and NT application, suggesting that these peptides act on SIC channels (see section 1.1.5.2b). Lastly, this study has shown that the increase in MNC firing rate after application of a hypertonic solution (i.e. +30 mM mannitol) is potentiated in the presence of NT. In other words, these results indicate that synaptically released neuropeptides can impact MNC excitability. As shown above, NT and Ang II can target SIC channel activity, and during hypovolemia, MNC excitability is controlled via the release of second messengers impacting glutamatergic neurotransmission, following the release of Ang II.

1.4.2 Calcium-activated potassium channels

Calcium-activated potassium (Ca^{2+}-activated K^+) channels are of critical importance in the shaping of MNC spiking activity, as described in section 1.3.2. (Hu and Bourque model of clustering activity). Indeed, by modulating action potentials as well as the ISI, these channels directly affect peptidergic neurosecretion at the axon terminal (see section 1.3.3). A study using immunofluorescence has revealed the presence of large/big-conductance (BK) and small-conductance (SK) Ca^{2+}-activated K^+ channels (i.e. SK3) in MNC (Greffrath et al., 2004). Therefore, this section will discuss the role of BK and SK channels in spike frequency accommodation in MNC.

1.4.2.1. Large-conductance calcium-activated potassium channels

The activity of BK channels contributes to the repolarization phase of the spike and to the fast component of the after-hyperpolarizing potential (fAHP) (Faber and Sah, 2003). These channels are voltage- and Ca^{2+}- dependent with a single channel conductance of ~100-200 pS and can be blocked by low concentration of tetraethyl ammonium (TEA) (Adelman et al., 2012) as well as charybdotoxin (ChTX) (Garcia et al., 1995). Molecularly, changes in membrane potential are detected by the voltage sensor domain and a rise in intracellular calcium is sensed by the large cytosolic tail domain. These two mechanisms mediate the gating of BK channel and therefore, the outflow of K^+ to repolarize the cell (Yang et al., 2015).

It was observed that the hyperpolarizing after potential (HAP) amplitude, following an action potential, progressively increases in a spike train when a depolarizing current is injected into a MNC. This gradual increase of the HAP amplitude seems to be correlated to a progressive calcium influx within a spike train (Greffrath et al., 2004). More specifically, this study has shown that the progressive increase in the HAP amplitude is in part attributable to the presence of the fast component of the HAP (fHAP) that is mediated via BK channels activation, because ChTX application significantly decreases the fHAP

amplitude. Moreover, application of cadmium (Cd^{2+}, a calcium channel blocker) also prevented this gradual increase in fHAP amplitude, confirming the involvement of calcium for BK channel activation in MNC. However, exposing the cells to ChTX did not significantly affect the spike-frequency *accommodation*, a mechanism by which MNC convert their initial high firing frequency into a lower frequency of discharge. This result indicates that despite the role that the BK channels plays in the regulation of the fHAP amplitude, these channels do not appear to be the major contributor in the spike accommodation of SON neurons. The next section will investigate the contribution of the slow HAP (sHAP) in this spike-frequency accommodation mechanism, considering that the impact of the sHAP is significantly correlated to the regulation of ISI within a train of action potentials.

1.4.2.2. Small-conductance calcium-activated potassium channels

The identification of SK channels comes from an experiment where Hahn and Leditschke (1936) injected the bee venom toxin, apamin, into mice and this resulted into motor impairments such as convulsions. In 1984, it was proposed that apamin acts by blocking Ca^{2+}-activated K^+ channels based on the idea that the K^+ efflux from liver cells is abolished following apamin application (Habermann, 1984). Tetrameric SK channels have a single channel conductance of ~10-20 pS, are voltage-independent and are gated by submicromolar intracellular calcium concentration (Adelman et al., 2012). More precisely, each subunit contains a calmodulin binding domain where intracellular calcium binds, which in turn induces conformational changes that mediates the channel opening and subsequent K^+ outflow.

In MNC, studies using in situ hybridization (Stocker and Pedarzani, 2000) as well as immunocytochemistry (Greffrath et al., 2004) have only revealed the presence of SK3 channels (i.e. no SK1 or SK2). The sHAP, induced by SK channel activation, can be generated after discharge of high frequency spikes, whereas it was found to be nearly absent (or only weakly expressed) after the induction of a single spike or during a slow tonic discharge (Kirkpatrick and Bourque, 1996; Greffrath et

al., 2004). The purpose of the sHAP is to convert the initial high firing frequency into a lower frequency of discharge. This can be achieved via an increase in the ISI which is positively correlated to the sHAP amplitude. It was also demonstrated that spike-frequency accommodation is strongly attenuated in the presence of exogenously applied apamin (Greffrath et al., 2004), because the gradual increase in ISI within a spike train is reduced. Moreover, this study has shown that the sHAP was blocked by Cd^{2+}, supporting the role of calcium in this response. Together, these results suggest that the spike accommodation mechanism in MNC relies mainly on the sHAP, which is induced via SK channel activation and subsequent calcium influx, leading to a repolarizing K^+ efflux.

1.4.3. Neurotensin and the after hyperpolarizing potential

A burst of action potentials in SON cells leads to the emergence of an AHP that relies on the activation of a Ca^{2+}-activated K^+ conductance and for which the amplitude is proportional to the number of spikes elicited (Bourque et al., 1985). Importantly, it was shown that this AHP depends on SK channel activity because exogenously applied apamin completely suppresses the Ca^{2+}-activated K^+ current in SON cells, revealing the presence of a DAP that was masked prior to the drug application (Bourque and Brown, 1987) (see section 1.3.1 for the role of the DAP in phasic burst initiation). Neurotensin, a 13 amino acid peptide known for its depolarizing effect and for increasing the firing activity of MNC (described in section 1.4.1), was shown to also inhibit the AHP amplitude and to decrease the spike frequency accommodation in SON cells from hypothalamic explants (Kirkpatrick and Bourque, 1995). More precisely, in this study, application of the active NT fragment (i.e. amino acid 1-13 or 8-13) led in average to a 64% reduction of the AHP amplitude compared to the control condition (i.e. no drug or application of the NT inactive fragment; 1-8). Moreover, exposing the cells to NT 8-13 led to a decrease in the ISI duration as well as an increase in the mean firing frequency. Interestingly, application of apamin on VP cells displaying a phasic activity does not significantly affect the silent pause between bursts, but was shown to decrease burst length by about 50% (Kirkpatrick and Bourque, 1996).

Additionally, this study has demonstrated that bath application of apamin decreases the spike accommodation observed at the onset of a phasic burst and increases the intraburst frequency as well. Taken together, these results suggest that NT, by activating its receptor, exerts a depolarizing and an excitatory effect on MNC and also suppresses repolarizing conductances, therefore impacting SON cell firing activity. Because the AHP and the sHAP are both mediated by SK channel activity and shape the firing seen in different types of electrical pattern such as clustering (Hu and Bourque, 1992) and phasic activity, understanding the role of the neuromodulator NT on the firing activity of MNC will be further addressed in this thesis.

1.4.4. Hypothesis two

Clustering activity was shown to be extremely sensitive to voltage variations due to the Mg^{2+} block of NMDA receptors (see section 1.3.2). As described in section 1.4.1 and 1.4.3, the neuromodulator NT was shown to exert a depolarizing and excitatory effect on MNC and to decrease the AHP amplitude of these cells. Based on these findings, the second hypothesis elaborated during my PhD studies is that *NT, via its depolarizing effect, will impact the induction of NMDA-induced clustering activity and will also increase the cluster length, the intra-cluster frequency and will decrease the AHP amplitude, thus modulating this rhythmic firing.*

1.5. Somato-dendritic release

In sections 1.1.4.2, 1.3.1 and 1.3.2, we have discussed different types of firing activities in MNC, such as the lactation burst as well as phasic and clustering activity, and we saw that modulating the parameters involved in these types of electrical activity exerts a direct influence on peptide secretion from the nerve terminal (section 1.3.3). In the second part of this thesis, we will explore how messengers are released at the somato-dendritic level. Importantly, how somato-dendritic release modulates

glutamatergic neurotransmission (see section 1.5.6) and how calcium plays a role in this response (see section 1.6) will also be addressed.

1.5.1. First evidence about somato-dendritic release

Early studies using electron microscopy (EM) have shown that the location of peptides and neurotransmitters is not restricted to the axon/synaptic terminal, since both types of molecules can be found in the dendritic compartment. Indeed, this technique was used to show the presence of noradrenergic small core vesicles in close apposition to the dendritic plasma membrane of sympathetic nerves (Taxi and Sotelo, 1973). Two years later, it was proven that dendrites of dopaminergic neurons in the substantia nigra also contain vesicles enclosing dopamine, suggesting a role for dendritic exocytosis (Bjorklund and Lindvall, 1975).

In MNC, the first evidence that neurosecretory granules (NSG, also called large dense core vesicles ; LDCV) containing OT and VP peptides are present in the dendritic compartment was provided in 1989 (Pow and Morris, 1989). This study using EM and distinctly targeting OT and VP vesicles with specific antibodies has shown that several NSG were located in close apposition to the plasma membrane and some vesicles were seen as undergoing the process of exocytosis (Figure 1.5.1). Morphologically, it was observed that SON cells possess in average between 1 and 3 dendrites (Dyball and Kemplay, 1982). More precisely, each MNC contains at least one dendritic process and 60% of these cells contain 2 dendrites, while fewer cells possess 3 dendrites (about 15% of MNC). Using Lucifer Yellow to visualize SON cells, it was shown that the short diameter of MNC soma is about 12 μm, while their long axis is about 25 μm (Randle et al., 1986b). In rats, the dendrites of MNC are ~300-400 μm long (Stern and Armstrong, 1998), show a weak spine density (which varies considerably among neurons and within the same dendrite) and secondary branches are a common feature (Armstrong, 1995). The use of EM has revealed the presence of both rough and smooth ER within MNC dendrites, with no trace of

Golgi apparatus, suggesting that peptides might be synthesized in dendrites, but must then reach the soma to be packaged into vesicles. It is important to note that ribosomal as well as poly(A) mRNA was found in close apposition to the dendritic plasma membrane (Steward, 1997), indicating a local control of synapse-related proteins. Lastly, it is also worth mentioning that MNC possess axon collaterals. Indeed, axon collaterals have been found to originate from SON neurons in rhesus macaque (LuQui and Fox, 1976). In rats, axon collaterals in OT neurons were found to synapse onto amygdala neurons (Knobloch and Grinevich, 2014) and OT release onto this nucleus was shown to attenuate fear-related responses (see section 1.1.2).

1.5.2. Depolarization-induced suppression of excitatory and inhibitory transmission

Depolarization-induced suppression of excitatory (DSE) and inhibitory (DSI) transmission is achieved when a postsynaptic neuron is depolarized. The subsequent release of endocannabinoids (EC) targets presynaptic axon terminals to decrease their excitatory or inhibitory drive onto that same postsynaptic neuron (Lovinger, 2008). The discovery of DSI and DSE is an important one because it was the first functional evidence to support the idea that messengers released from dendrites can exert an impact on synaptic inputs. The first evidence of DSI comes from experiments that were performed in the early 1990s. More precisely, depolarizing pulses elicited in cerebellar Purkinje cells were found to decrease the frequency of spontaneous inhibitory GABAergic currents arising from local neurotransmitter release from basket and stellate afferents (Llano et al., 1991). Moreover, despite the fact that the mechanism responsible for this form of inhibition was not clear back then, these authors hypothesized that this inhibitory effect might rely on the liberation of a lipid-soluble second messenger such as arachidonic acid (i.e. a type of EC). Another key experiment concerning DSI, performed in the hippocampus, led to the conclusion that eliciting a train of action potentials in CA1 cells resulted in a suppression of sIPSP frequency and also significantly decreased the evoked IPSC (eIPSC) amplitude (Pitler and Alger, 1992). This retrograde inhibition of GABAergic transmission was also shown to be dependent

on postsynaptic calcium rise since this effect was prevented in BAPTA-filled cells. However, in both cases, it was still unknown if this form of inhibition was mediated via the release of messengers from the somato-dendritic region.

About a decade later, several laboratories found evidence that EC were the lipid mediators involved in DSI and DSE (Kreitzer and Regehr, 2001; Maejima et al., 2001; Ohno-Shosaku et al., 2001). As an example, depolarization of Purkinje cells was found to inhibit the excitatory drive of parallel and climbing fibers, and this effect was prevented upon application of the cannabinoid receptor type 1 (CB1) antagonist AM251, whereas the CB1 receptor agonist WIN55,212-2 occluded this effect (Kreitzer and Regehr, 2001). Importantly, it was observed that CB1 receptors are located on presynaptic terminals within the central nervous system (Freund et al., 2003). Binding of EC to their $G_{i/o}$ -coupled GPCR CB1 receptors was shown to inhibit adenylyl cyclase activity, to phosphorylate/activate extracellular signal-related kinase (ERK), to activate G-protein-activated inwardly rectifying potassium channels (GIRK) and other types of K^+ channels, and to inhibit voltage-gated calcium channels (VGCC) (Lovinger, 2008). The use of calcium imaging techniques has shown that DSE emerging from CB1 receptor activation on granule cells (synapsing onto Purkinje cells), leads to an inhibition of N- P/Q- and R-type VGCC that decreases the amount of presynaptic calcium influx and therefore, reduces presynaptic glutamate release (Brown et al., 2004).

1.5.3. Dendro-dendritic synapses

Although dendrites are now known to mediate output signals such as DSI and DSE via release of membrane permeable EC, these processes can also produce output signals via conventional transmitters. This form of communication can be found at the *dendro-dendritic synapse* where dendrites and somata on two distinct neurons can communicate together by releasing neurotransmitter on their neighboring cell. The first evidence that dendro-dendritic synapses exist came from a study where these type of

synapses were shown to be located in the olfactory bulb of the rat (Rall et al., 1966). Using EM, synapses were observed between dendrites of mitral and granule cells and clusters of vesicles were shown to be located within both types of dendrites. In the lateral geniculate nucleus of the squirrel monkey, dendro-dendritic as well as somato-dendritic synapses were shown to be present within the magno- and parvocellular layers (Wong, 1970). Importantly, the somata and dendrites involved in these synapses were filled with synaptic vesicles that were clearly seen at the site of interaction. The first functional evidence that dendrites from different neurons can communicate via synapses came from a study where olfactory neurons were inhibited following the antidromic stimulation of the lateral olfactory tract (Westecker, 1970). More precisely, mitral cells, which form dendro-dendritic synapses with granular cells, showed a temporal correlation in their activation with granular cells, when the later were stimulated antidromically.

In MNC, despite the fact that no evidence of dendro-dendritic synapses has been reported at the functional or EM level, the percentage of membrane involved in direct dendro-dendritic appositions in adult female rats was shown to significantly increase by the 21st day of gestation (prepartum period) and stays elevated during the first post-partum days compared to virgin rats (Perlmutter et al., 1984). Moreover, the number of dendrites per *bundle* (i.e. define as a minimum of 2 dendrites in close proximity without glia interposition between them) was found to be enhanced in the lactating, prepartum and postpartum groups compared to the control group. In another experiment, rats were chronically dehydrated (i.e. drinking 2% NaCl water for 10 days) or acutely dehydrated (i.e. 4-24h water deprived) and then rehydrated (Perlmutter et al., 1985). The results have shown that the number of dendrites per bundles as well as the percentage of membrane in dendro-dendritic appositions significantly increased in acutely and chronically dehydrated rats, and these values returned to the control condition upon rehydration. These morphological changes in dendro-dendritic juxtapositions found during dehydration, lactation and gestation occurs because glia retract their astrocytic processes

and thus, enhance the proportion of dendro-dendritic membrane seen in apposition (Tweedle and Hatton, 1977; Hatton and Tweedle, 1982). The presence of dendro-dendritic appositions, in both studies, does not rule out the possibility that neighboring cells might influence their excitability via dendro-dendritic synapses, but additional studies will be required to elucidate this question, considering that dye-coupling and gap junctions have been observed between SON cells (Andrew et al., 1981). Nonetheless, peptides secreted via the somato-dendritic compartment of MNC play an important role in the excitability of these cells as well as in the shaping of their morphology during early development. Therefore, the next section will discuss the role of somato-dendritic release in young rats.

1.5.4. Role of somato-dendritic release during early development

During early development, OT and VP peptides are released from their respective neurons. The experiments described below suggest that somato-dendritic release of these peptides is involved in the maturation of SON neurons. Indeed, it was shown that in rats aged of 20 days (post natal day 20; P20) or less, exogenous application of V1a and V2 receptor antagonist resulted in a decreased firing activity in VP cells and also induced a hyperpolarization, while OT receptor antagonist had the same inhibitory effect on OT cell (Chevaleyre et al., 2000). On the contrary, application of VP and OT, respectively on OT and VP neurons, led to a depolarizing effect as well as an increased firing activity and this effect was first seen at P4 to then reach its peak at P7, and started to decrease at P16. Lastly, V1a and V2 receptor agonist applied on VP isolated cells resulted in a pronounced increase in the release of this peptide, analyzed via radioimmunoassay, while the same potentiation was observed in OT cells upon OT receptor agonist application, and this peptidergic facilitation showed a twofold increase from P3 to P13.

The morphological development of MNC evolves quickly within the first postnatal days. To investigate this aspect, rats were injected daily with a subcutaneous dose of OT and VP receptor antagonists. These rats showed a 36% decrease in the total number of dendritic branches compared to

control rats (Chevaleyre et al., 2002). Interestingly, incubating half of a hypothalamic slice (i.e. one SON for 3-8 hours) with OT and VP receptor agonist increases the number of dendritic branches by 53% compared to the control SON (i.e. no drug) between P3 and P6, whereas this effect became non-significant from P7 to P9. In another subset of experiments, the NMDA receptor blocker MK801 was injected daily subcutaneously, from birth to P6, considering that glutamatergic EPSP start to appear near postnatal week 2 (Chevaleyre et al., 2001). Similarly to the OT/VP agonist effect on dendritic branching, daily injection of MK801 resulted in a 27% decrease of the total number of dendritic branches. Importantly, it was shown that the electrical activity of SON cells play a major role in the development of dendritic branches, because TTX application upon administration of other drugs (i.e. NMDA, OT and VP agonist) led to a decrease in the total amount of dendritic branches. However, taken as an isolated variable, the electrical activity of MNC itself is not solely responsible for a proper dendritic development. More specifically, application of high K^+ concentration (i.e. to depolarize and activate MNC) when NMDA, OT and VP receptor were blocked did not lead to an increase in the number of dendritic branches.

Taken together, these results indicate that OT and VP receptors in young rats start to be functional at P4 and that MNC electrical activity is modulated via somato-dendritic release during early development (i.e. before P20). Moreover, an appropriate formation of dendritic branching is possible upon activation of NMDA, VP and OT receptors and a neuronal electrical activity is also required.

1.5.5. Somato-dendritic release in adult MNC: a general perspective

An *in vitro* study provided the evidence that isolated SON can secrete OT and VP from their somato-dendritic compartment (Moos et al., 1984). Interestingly, application of VP on both cell types did not affect peptidergic release, whereas OT application had a facilitatory effect only for OT releasing neurons (see section 1.5.5.2 for VP facilitatory effect on its own release *in vivo*). The idea that MNC can secrete peptides from their soma and dendrites was more firmly established when isolated SON nuclei,

stimulated electrically, were found to efficiently release OT and VP in the presence of TTX, whereas application of D-600 (a calcium channel blocker) significantly decreased the amount of peptide secreted (Di Scala-Guenot et al., 1987). These results indicate that the release observed was not attributable to axon collaterals since synaptic transmission was blocked and these findings highlighted the importance of intracellular calcium rise in this form of peptidergic secretion. Additionally, it was shown that somato-dendritic OT and VP release can be triggered when plasma osmolality rises (Ludwig et al., 1994). More precisely, this group has shown that i.p. and i.v. injection of NaCl *in vivo* leads to a rapid increase of systemic peptide release (i.e. within 30 minutes), while a delay of 2.5 to 3.5 hours is required for intranuclear somato-dendritic release, measured via a microdialysis probe. Interestingly, synaptic communication, following an osmotic challenge, appears to be involved in the triggering of intranuclear release of OT and VP *in vivo*. Indeed, systemic osmotic stimulation (i.e. i.p. injection of NaCl) elicited an increase in intranuclear release that was prevented upon TTX application within the SON (Ludwig et al., 1995). On the other hand, central administration of TTX as well as NaCl via a microdialysis probe did not abolish intranuclear release. This last result also supports the fact that somato-dendritic release can be elicited without action potentials.

Using capacitance membrane measurement, it was shown that induction of a 2 ms depolarizing pulse in isolated MNC or administration of an action potential elicit somato-dendritic release of about 40-45 LDCV (de Kock et al., 2003). It was also found, using nucleated outside-out patch, that NMDA application increases capacitance measurement when the cell is maintained below action potential threshold (i.e. -70 mV), supporting the fact that somato-dendritic release can occur with or without any firing activity (de Kock et al., 2004). Because calcium plays an important role in the exocytosis from the somato-dendritic compartment, this topic will be addressed in section 1.6.

1.5.5.1. Intanuclear somato-dendritic release from oxytocin cells

It was observed that administration of oxytocin within the 3rd ventricle (i.e. a region encompassed by the hypothalamus) leads to an increase in the firing rate of the slow firing OT cells and has a dose-dependent facilitatory effect on the milk ejection reflex, mainly via an increase in the amplitude and the frequency of these "lactation bursts" recorded extracellularly in the PVN (Freund-Mercier and Richard, 1984). Interestingly, this study has also shown that administration of OT antagonist into the 3rd ventricle delayed the appearance of the first milk ejection reflex as well as the frequency of this response, suggesting that activation of intranuclear OT receptors is an important part of the milk ejection reflex. Soon after this discovery, another *in vivo* approach was used where the neurohypophysis of lactating rats was stimulated in order to antidromically activate OT cells in the PVN (Negoro et al., 1985). This group has shown that stimulation of the posterior pituitary elicited typical lactation bursts, recorded extracellularly in the PVN, that were temporally correlated to an increase in intra-mammary pressure resulting in milk ejection. These authors proposed that somato-dendritic OT release might be responsible for the appearance of lactating bursts rather than OT release from the neurohypophysis because it was previously shown that i.v. injection of OT does not induce this type of burst (Lincoln, 1974) and that this peptide does not cross the blood brain barrier (Zaidi and Heller, 1974).

Analogously, it was shown that OT release within the SON, measured via a push-pull cannula *in vivo*, increases during the milk ejection reflex, and to a smaller degree following stimulation of the neurohypophysis (Moos et al., 1989). Several important conclusions were drawn from this study. First, the increase in intranuclear OT release was seen before the milk ejection reflex, more precisely as soon as the pups started suckling. Second, when suckling did not elicit the milk ejection response, no increase in intra-SON secretion was observed. Third, an i.p. osmotic stimulation of hypertonic saline did not lead to an enhancement of intanuclear OT over the 75 minutes of perfusion. Electrophysiologically, it was shown that administration of an OT antagonist within the SON or the PVN during suckling decreased the

burst amplitude and the firing rate of OT cells within the injected nucleus, and also reduces these parameters in the recorded contralateral nucleus (Lambert et al., 1993). On the other hand, injection of an OT agonist had the opposite result (i.e. an increase in the burst amplitude and in the firing rate of OT neurons). Finally, it is proposed that somato-dendritic OT release might be responsible for the synchronization of busting activity observed among OT cells during parturition and lactation (Ludwig and Stern, 2015). Taken together, these findings indicate that local OT release from SON and PVN neurons, which subsequently binds to OT receptors on the soma and dendrites of these neurons, plays an important role in the initiation and the shaping of lactation bursts.

1.5.5.2. Intranuclear somato-dendritic release from vasopressin cells

It was demonstrated *in vivo* that infusion of lysine VP (LVP; no cross-reactivity with VP when performing radioimmunoassay analysis) with a microdialysis probe within the SON increases VP secretion in this nucleus, whereas administration of a V1/V2 receptor antagonist had no effect on basal intranuclear VP release compared to the control (vehicle; normal ACSF) condition (Wotjak et al., 1994). Moreover, this study has shown that perfusion of a hypertonic solution inside the SON increases VP release within this nucleus. This effect was prevented upon application of a V1/V2 receptor antagonist, suggesting that during a hypertonic challenge, endogenous VP activates VP receptors to potentiate its own peptidergic release. Finally, this study has also shown that infusion of LVP during this central hypertonic challenge failed to further enhance VP secretion within the SON, indicating that endogenous VP already had a saturating effect.

Interestingly, it appears that VP secretion from the somato-dendritic compartment either enhances or decreases the firing frequency of these cells depending on their initial firing rate (in contrast to the excitatory role of this peptide during early development, see section 1.5.4). It has been demonstrated *in vivo* that application of VP within the SON, via a microdialysis probe, decreases the

firing frequency of phasic or continuously active VP neurons and in some instances, a complete silencing was observed (Ludwig and Leng, 1997). Upon application of the V1 receptor antagonist OPC 21268, spontaneously active phasic VP cells showed an increase in their firing rate as well as an increase in their intraburst firing frequency. Importantly, neither the application of VP nor the VP receptor antagonist affected the firing rate of OT cells which remained constant. Another *in vivo* study also investigated the firing activity of VP-containing neurons upon application of this peptide inside the SON and the PVN and provided slightly different results (Gouzenes et al., 1998). Indeed, it was shown that VP application on quasi silent neurons (slow firing) triggered phasic activity, while application of this drug on phasic cells displaying very short period of activity elongated the burst duration and decreased the silent period duration, thus establishing a more robust phasic firing. When a spontaneous phasic pattern was clearly seen for a sustained period of time, VP application did not alter at all any parameters of the phasic firing. Finally, for cells displaying a fast continuous activity, application of this peptide decreased the firing rate and progressively induced a phasic firing.

Taken together, these results indicate that somato-dendritic VP release excites slow firing neurons to promote a phasic firing and decreases the activity of continuously active cells to induce a phasic firing, or considerably reduce their activity. The only contradictory result between these studies is about whether somato-dendritic VP release decreases or maintains phasic firing when this phenotype is clearly established. It was proposed that somato-dendritic VP release acts on neighboring VP cells to favor more exocytosis of this peptide (Ludwig and Stern, 2015). However, during times of high peptidergic demand such as dehydration, it might be preferable to not exceed a certain threshold of electrical activity since radioimmunoassay studies have shown that going over ~15 Hz for VP cell does not lead to an additional increase in VP release from the neurohypophysis (Bicknell, 1988). However, whether this is the case at the somato-dendritic level remains to be determined.

As discussed in section 1.3.1, it was demonstrated that DYN released from VP cells during phasic activity is involved in burst termination by decreasing the DAP amplitude (Brown and Bourque, 2004). Moreover, application of nor-BNI (i.e. a κ-opioid receptor antagonist) *in vivo* within the SON was shown to decrease the probability of burst termination, suggesting that endogenous DYN release plays an important role in burst cessation (Brown et al., 2006). It is also important to mention that this autocrine inhibition is further enhanced along the releasing process, probably because κ-opioid receptors, enclosed in VP vesicles, are rapidly inserted into the membrane upon exocytosis (Shuster et al., 1999).

1.5.6. Somato-dendritic release of messengers inhibits presynaptic excitatory neurotransmitter release

Within the last 20 years, several articles were published concerning how somato-dendritic peptides released from MNC modulate presynaptic neurotransmitter secretion. Indeed, an effort was made in the field of MNC to investigate how somato-dendritic release affects presynaptic GABAergic neurotransmission (de Kock et al., 2003; de Kock et al., 2004; Oliet et al., 2007). As previously described in section 1.2.1, the increase of sEPSP frequency in MNC is correlated to the degree of osmotic stimulation over the OVLT, with no change for the frequency of sIPSP. This finding suggests that the increased excitability of MNC, following an osmotic stimulation of the OVLT, is attributable to glutamatergic afferents activity rather than a suppression of GABAergic activity. Therefore, how somato-dendritic release from both OT and VP cells regulates presynaptic excitatory neurotransmission will be discussed in the next sections.

1.5.6.1. Somato-dendritic release of messengers from oxytocin cells inhibits excitatory neurotransmission

The first study investigating the functional role of dendritic release in SON neurons came to the conclusion that OT, released from the somato-dendritic compartment, acts as a retrograde messenger to decrease presynaptic glutamate release (Kombian et al., 1997). In this study, it was shown that bath

application of OT as well as postsynaptic depolarization via current injection (i.e. 200 pA for 1 s.; 2-4 times) into SON cells resulted in a decrease of the eEPSC amplitude. This decrease of the eEPSC amplitude was blocked by OT receptor antagonists such as Manning compound (MC) and vasotocin. It was also determined that the locus of action of OT is mainly presynaptic based on several lines of evidence. First, steady-state I/V curves generated (i.e. from -120 mV to -30 mV) in the presence or in the absence of OT were not significantly different within the same cell, suggesting that OT does not affect postsynaptic conductance. Second, bath application of an OT agonist (OT-AG) resulted in an increase in the paired-pulse ratio (PPR; ratio of the EPSC amplitude: $EPSC_2/EPSC_1$). Third, AMPA-induced current amplitude in MNC were similar in the presence or in the absence of OT application, suggesting that OT release does not lead to changes in the density nor the properties of postsynaptic AMPA receptors. Taken together, these results indicate that OT acts presynaptically to depress the EPSC amplitude.

A couple of years later, the same group reported new findings to further elucidate this mechanism. Indeed, it was proposed that OT exocytosis exerts an autocrine effect that triggers EC release, which in turn acts presynaptically to inhibit glutamate release (Hirasawa et al., 2004). Importantly, this study used immunocytochemistry to shown that CB1 receptors are located presynaptically (i.e. on asymmetric and symmetric synapses contacting MNC dendrites). Moreover, exogenous application of WIN55,212-2, an EC receptor agonist, was shown to cause a decrease of the eEPSC amplitude, an increase in the PPR and a decrease in the miniature EPSC frequency, suggesting an EC-mediated inhibitory effect targeting presynaptic terminals. As shown previously, bath application of OT led to a decrease of the eEPSC amplitude, but this effect was occluded in the presence of the CB1 receptor antagonist AM251, indicating that EC receptor activation is necessary in this form of presynaptic inhibition. Moreover, depolarization of the postsynaptic cell (i.e. 0 mV, 1 second) induced a decrease of the eEPSC amplitude that was prevented upon AM251 application.

1.5.6.2. Somato-dendritic release of messengers from vasopressin cells inhibits excitatory neurotransmission

It was shown that exogenous application of AVP decreases the eEPSC amplitude (Kombian et al., 1997) but when this observation was made, the subtype of receptor involved in this response was ambiguous, despite the fact that it is was already known that the OT peptide does not activate VP receptors and vice versa (see sections 1.5.5 and 1.6.1). In other words, it was unknown whether this effect was mediated via activation of OT or VP receptors because the cell phenotype (i.e. OT or VP) was not clearly established (Pittman et al., 2000). About a decade later, it was found that exogenous application of either DynA or U69593 (i.e. two κ-opioid receptor agonists), led to a presynaptic depression of glutamatergic transmission, measured via a decrease of the eEPSC amplitude (Iremonger and Bains, 2009). This DYN-mediated inhibition acts at a presynaptic locus as shown by an increase in PPR, a decrease of mEPSC frequency as well as a decrease in the coefficient of variation (calculated as $1/CV^2$) of the eEPSC. Moreover, postsynaptic depolarization of identified VP cells (from -60 to 0 mV for 100 ms, 240 times) in the presence of AM251 (i.e. to block the contribution of EC) resulted in a long lasting inhibition of the eEPSC that was prevented upon nor-BNI application. This study has also shown that DYN is released in a SNARE-dependent manner because pipettes filled with an internal solution containing Botulinum toxin type-C, a toxin that cleaves syntaxin to interfere with the exocytosis machinery, prevented this DYN-mediated presynaptic inhibition.

Because activation of the presynaptic κ-opioid receptor, coupled to the $G_{i/o}$ subunit, was shown to inhibit transmitter release via different mechanisms such as activation of K^+ channels (Simmons and Chavkin, 1996) or inhibition of VGCC (Kelamangalath et al., 2011), different experiments were performed to investigate how this DYN-mediated presynaptic inhibition is regulated. Blockade of either N-type or P/Q-type Ca^{2+} channels, respectively with ω-conotoxin GVIA and ω-agatoxin IVA, did not occlude the inhibitory effect of the DYN receptor agonist U69593, suggesting that these VGCC are not inhibited

following presynaptic κ-opioid receptor activation. Moreover, external solution containing BAPTA-AM, a Ca^{2+} chelator that permeates and accumulates in the cell, did not prevent the reduction in mEPSC frequency following application of U69593. It also appears that presynaptic K^+ channels are not required in this DYN-mediated presynaptic inhibition. Indeed, after the application of 4-AP, a decrease of the EPSC amplitude upon U69593 application was still observed in a solution containing low external Ca^{2+} (low external Ca^{2+} was used because K^+ channel blockade leads to an enhanced presynaptic Ca^{2+} influx). Moreover, when TTX was bath-applied, addition of 4-AP had no effect on mEPSC frequency, whereas administration of U69593 under the same conditions caused a decrease in the frequency of mEPSC. Based on the findings mentioned above and the fact that mEPSC persist despite the absence of external Ca^{2+} (Inenaga et al., 1998), it was therefore proposed by these authors that κ-opioid inhibition is mediated by direct modulation of the vesicle release machinery. The latter result suggests that this DYN-mediated presynaptic inhibition is downstream of calcium entry.

Another study has investigated the inhibitory role of somato-denditic release from VP cells on glutamatergic neurotransmission and concluded that EC are involved in short term depression (STD), while DYN is responsible for a long term depression (LTD) of excitatory afferents (Iremonger et al., 2011). More specifically, EC mediate a STD by activating presynaptic CB1 receptors, which in turn decreases glutamate release and therefore, reduces postsynaptic metabotropic glutamate receptors (mGluR) activation. This decrease of mGluR activity subsequently reduces the amount of postsynaptic DYN release and thus, prevents the synapses from undergoing LTD. Bursts of postsynaptic spikes (current clamp; 10 s. of activity at 10-20 Hz, 10 s. of pause, repeated 10 times) to mimic phasic activity were elicited and resulted in a short and transient (1<min) reduction of the eEPSC amplitude that was blocked upon exogenous application of AM251, suggesting an EC-mediated presynaptic inhibition. On the other hand, pairing of presynaptic stimulation (10 s. on, 10 s. off, 10 times) with a postsynaptic stimulation induced a sustained depression that recovered to baseline values after 30 minutes. This prolonged

inhibition was prevented by the group I/II mGluR antagonist MCPG and was also abolished when the postsynaptic cell was dialyzed with GDP-βs, an inhibitor of G-protein signaling, thus confirming the role of postsynaptic mGluR activation in this sustained inhibition. Interestingly, LTD (i.e. an inhibition lasting >30 minutes) could only be achieved during the burst pairing protocol when AM251 was exogenously applied. This LTD could be reversed into STD upon nor-BNI application. In other words, activation of CB1 receptors induced a STD by limiting presynaptic glutamate release and subsequent postsynaptic mGluR activation and thus, decreased the amount of DYN release from VP cells. However, when CB1 receptors are antagonized with AM251, the DYN-mediated presynaptic inhibition is unmasked and leads to a LTD. Based on these findings, we can therefore postulate that LTD can be prevented upon EC release.

1.5.7. Hypothesis three

It has been demonstrated that peptide release from MNC axon terminals occurs in an activity-dependent manner. For example, the neurohypophysis elicits more secretion at higher frequencies of stimulation or when stimulated with a clustering phenotype (compared to a tonic stimulation, see section 1.3.3). Indeed, several studies led to the conclusion that exocytosis from the neurohypophysis is modulated by several parameters such as the frequency of stimulation, the pattern of activity and the pauses between bursts of action potentials. However, little is known about how these parameters affect somato-dendritic release from MNC. One of the aims of this thesis is to understand how somato-dendritic release is regulated by the pattern of electrical activity and the frequency of stimulation. This can be achieved by measuring to which extent retrograde messengers, released from the soma and dendrites of MNC, inhibit glutamate release (see section 1.5.6). Therefore, my third hypothesis is that *SON cell firing frequency will be positively correlated to a decrease of presynaptic excitatory neurotransmission, measured via a reduction of the eEPSC amplitude in MNC. Moreover, I propose that a clustering stimulation will have a greater inhibitory impact on excitatory neurotransmission compared to a tonic stimulation, using the same number of action potentials in all conditions.*

1.5.8. Hypothesis four

Previous studies have shown that somato-dendritic release from MNC inhibits presynaptic glutamatergic secretion via the release of retrograde messengers (see section 1.5.6). However, the cell phenotype (i.e. OT or VP) was most of the time not clearly established, therefore providing ambiguous conclusions. It has also been shown that using electrophysiological parameters to assess the cell phenotype is not a reliable approach (da Silva et al., 2015). Moreover, the experiments described in section 1.5.6.2 were performed on transgenic rats expressing enhanced green fluorescent protein (eGFP) cells to identify the cell phenotype and therefore, cells that did not display fluorescence were classified as OT neurons (i.e. negative-eGFP cells). Targeting the right cell type with this approach can be misleading because a small proportion of transgenic VP neurons do not express fluorescence (Ueta et al., 2005). Indeed, identifying a negative-eGFP cells as an OT neuron can be misleading. Moreover, previous studies used a stimulation to elicit somato-dendritic release that was either very high in terms of firing frequency or not constant across successive stimulations. In order to assess the cell phenotype with greater confidence, I will use VP eGFP as well as OT monomeric red fluorescent protein 1 (mRFP1) transgenic rats to perform my experiments and I will also use a physiological and constant stimulation (i.e. 10 Hz, 100 spikes). Lastly, previous findings have shown the involvement of different retrograde second messengers in the inhibition of glutamate release, such as EC for OT cells and DYN as well as EC for VP neurons (see section 1.5.6.1 for OT and 1.5.6.2 for VP). My fourth hypothesis is that *somato-dendritic release from identified VP cells will inhibit excitatory neurotransmission via activation of κ-opioid and CB1 receptors and will therefore transiently reduce the eEPSC amplitude. On the other hand, activation of presynaptic CB1 receptor via EC release from identified OT cells will decrease glutamate release and will thus transiently reduce the eEPSC amplitude.*

1.6. Role of calcium in somato-dendritic release

We have seen in sections 1.1.4.1 and 1.1.5.1 that calcium must invade the synaptic terminal to trigger the process of exocytosis from the neurohypophysis. In the next sections, we will explore how calcium regulates the release of messengers from the soma and dendrites of MNC.

1.6.1. Basal calcium and priming

It has been shown using isolated SON cells (i.e. a preparation containing MNC soma and residual proximal dendrites) that the resting intracellular Ca^{2+} concentration $[Ca^{2+}]_i$ is close to 43 nM and this value rises in OT cells upon exogenous application of OT in a dose-dependent manner (i.e. 100 μM OT induced ~+340 nM $[Ca^{2+}]_i$; 1000 nM OT induced ~+420 nM $[Ca^{2+}]_i$) (Lambert et al., 1994). The source of this rise in $[Ca^{2+}]_i$ following OT application comes from the liberation of intracellular calcium stores, because thapsigargin (TG; an ER Ca^{2+}-ATPase blocker) treatment enhances $[Ca^{2+}]_i$ with no further increase after OT application. Moreover, this Ca^{2+} response following OT application is long lasting and stays elevated until the end of the treatment. It was also shown that VP application onto VP neurons elicits a transient increase in $[Ca^{2+}]_i$ (i.e. recovery to baseline level in < than 1 min) in a dose-dependent manner (i.e. resting $[Ca^{2+}]_i$ ~70 nM up to ~480 nM after application of VP) (Dayanithi et al., 1996). Moreover, this rise in $[Ca^{2+}]_i$ upon VP application was completely abolished in the presence of an external solution containing low Ca^{2+} and EGTA and was partially blocked when TG was applied, suggesting that the VP-mediated response is partially dependent on extracellular Ca^{2+} influx via VGCC and the liberation of intracellular Ca^{2+} stores from the ER. There was also no cross-reactivity in the activation of both OT and VP receptor because application of SR49059, a V1 receptor antagonist, had no effect on the OT-induced Ca^{2+} response, while $d(CH_2)_5OVT$, an OT receptor antagonist, had no effect on the VP-induced Ca^{2+} response. Lastly, this study has shown that VP cells display a progressive desensitization (i.e. less

responsive in their calcium response) over repetitive application of their peptide, whereas OT cells show a constant Ca^{2+} response following repetitive stimulations with OT.

In MNC, *priming* can be defined as the mobilization of intracellular Ca^{2+} which in turn translocates the readily releasable pool (RRP) of vesicles close to the dendritic plasma membrane to make them available (i.e. ready for exocytosis) for a prolonged period, following spikes of activity (Ludwig et al., 2002). In other words, priming involves the translocation of LDCV close to the plasma membrane (i.e. within soma and dendrites) following mobilization of intracellular Ca^{2+} and thus, enhances somato-dendritic release when the cell displays a subsequent period of electrical activity. As mentioned by these authors, a rise in intracellular Ca^{2+} *per se* is not responsible for the priming effect because exposure to high K^+ alone does not trigger this mechanism. Interestingly, it was shown *in vivo* that administration of TG (i.e. used as a Ca^{2+} mobilizer) into the SON via a microdialysis probe significantly enhanced somato-dendritic OT release following an i.p. injection of NaCl compared to the control condition (i.e. no TG) (Ludwig et al., 2002). Additionally, i.p. injection of NaCl was shown to enhance plasma OT, but no difference was observed when comparing the TG-treated and the control groups, suggesting that mobilization of Ca^{2+} stores enhance intranuclear OT release rather than exocytosis from the neurohypophysis. In the same study, isolated neurohypophyses were stimulated with K^+ and subsequently with TG, the latter having no effect on OT release. On the other hand, TG applied onto isolated SON had a significant effect on OT release and potentiated the effect of K^+-induced release, suggesting a priming effect in the somato-dendritic compartment. Importantly, this potentiation induced by TG could only be observed after a minimal delay of 30 minutes between TG application and the K^+ stimulation because shorter delays between these two tests were ineffective at enhancing the K^+-induced exocytosis. Moreover, exogenous application of OT onto isolated SON cells enhanced intranuclear OT release and also potentiated the K^+-induced exocytosis.

In VP neurons, it was shown that intra-SON VP release is enhanced *in vivo* after i.p. injection of NaCl in the TG-treated group compared to control rats, and the K^+-induced VP release was also potentiated after TG application on isolated VP cells (Ludwig et al., 2005). Contrarily to OT cells, VP application did not potentiate the K^+-induced VP release, suggesting that this peptide is not involved in the priming of vesicles. In other words, the liberation of Ca^{2+} stores via TG treatment potentiates somato-dendritic release of VP, but binding of this peptide on VP cells does not appear to participate in the priming response.

To summarize, these authors propose that considering that the rise in $[Ca^{2+}]_i$ induced by TG returns to baseline levels after only 5-10 minutes, the long lasting effect of TG on OT intranuclear release might be attributable to the fact that the vesicles (or RRP) are translocated close to the dendritic plasma membrane when $[Ca^{2+}]_i$ increases, specifically as a result of Ca^{2+} release from internal stores. The idea that LDCV are translocated in close proximity to the dendritic plasma membrane upon liberation of Ca^{2+} stores has been confirmed by the use of EM (Tobin et al., 2004). Importantly, when counting the number of LDVC within 500 nm of the dendritic plasma membrane (i.e. in close proximity to the dendritic membrane), there was a higher incidence of LDVC in the group that received a TG treatment *in vivo* (i.e. before their brain was removed) compared to the control group that did not receive TG.

1.6.2. Voltage-gated calcium channels

We have seen in the previous section that the liberation of calcium from intracellular stores is involved in the priming as well as the intranuclear release of OT- and VP-containing vesicles. However, Ca^{2+} influx via VGCC can also participate in the release of these peptides from the somato-dendritic compartment. A study using immunohistochemistry and electrophysiology has shown that different types of high voltage-activated VGCC are localized on the soma and dendrites of isolated MNC (Joux et al., 2001). Ca^{2+} currents were measured during a voltage ramp to generate an I/V curve where SON cells

were depolarized from -50 mV up to +10 mV. This Ca^{2+} current started to activate at -35 mV to then reach its peak close to 0 mV (i.e. peak Ca^{2+} density of ~37 pA/pF). Moreover, Cd^{2+} completely abolished this inward Ca^{2+} current and no Ca^{2+} influx was found below -40 mV, suggesting the absence of low-activated T-type VGCC on the somato-dendritic compartment. Importantly, the L-type Ca^{2+} current appears to be the major contributor of Ca^{2+} influx into SON cells because application of nicarpidine (i.e. a L-type Ca^{2+} channel blocker) decreased this inward current to a higher extend compared to blockade of other high-activated VGCC (i.e. contribution of 19 pA/pF for L-type). In order of density, L-, P/Q-, R- and N-type Ca^{2+} currents all contributed to Ca^{2+} influx within the somato-dendritic area. Using immunohistochemistry, this study has shown that $Ca_v1.2$ and $Ca_v1.3$, both L-type Ca^{2+} channels subunits, were found to be localized on the soma and proximal dendrites of MNC. Moreover, $Ca_v2.3$ (i.e. an R-type VGCC subunit) was also present on the somato-dendritic compartment as well as $Ca_v2.1$ (i.e. a P/Q-type VGCC subunit). On the other hand, a weak expression of $Ca_v2.2$ (i.e. an N-type VGCC subunit) was observed in the soma of both OT and VP cell, whereas a strong expression was found in astrocytes.

Concerning T-type VGCC, it was shown using isolated MNC that this low-voltage activated current is present at -60 mV when performing a 10 mV depolarizing steps (Fisher and Bourque, 1995). Moreover, in VP guinea pig cell, a T-type current was shown to emerge at -64 mV during the DAP found within phasic burst, which could be blocked by nickel (Erickson et al., 1993). In another study using isolated rat MNC, no T-type current was observed at -60 mV when performing an I/V curve, and these authors proposed that this lack of consistency across studies concerning the existence of a T-type current might be due to differences in internal solutions, the strains of rats used or a difference in cell sampling (Foehring and Armstrong, 1996).

It was also shown that upon application of the N-type channel blocker ω-conotoxin GVIA, K^+-induced depolarization triggering OT release in SON explants of adult rats was blocked by 50% (Tobin et al., 2011). Moreover, the priming effect mediated via TG application (i.e. measured as OT release) was

attenuated when a K^+-induced depolarization was performed in the presence of either N- or L-type Ca^{2+} channel blockers. On the other hand, both P/Q- and R-type channel blockers had no effect on OT release following K^+-induced depolarization with or without TG treatment. These results suggest that Ca^{2+} influx via the N-type VGCC plays an important role in somato-dendritic release of OT and that the activation of both L- and N-type VGCC channel is involved in the priming response of this peptide.

Using immunohistochemistry, this study has shown the presence of all high voltage-activated VGCC Ca_v α1 subunits in the soma and dendrites of MNC. Interestingly, it was shown that the expression of Ca_v subunits is age- and physiological state-dependent. For example, the $Ca_v1.2$ subunit shows a higher expression for P8 rats compared to adults in both OT and VP cells. Moreover, $Ca_v1.3$ expression was found to be higher for lactating rats in both cell types compared to P8 and adult rats, indicating a dynamic remodeling of Ca_v subunit expression under different physiological contexts.

1.6.3. Vesicle fusion machinery

Many proteins associated with the soluble N-ethylmaleimide sensitive fusion protein attachment protein receptor (SNARE) complex have been identified in the axon terminals of MNC (Jacobsson and Meister, 1996; Zhang et al., 2009). However, it appears that the vesicle fusion machinery differs within the somato-dendritic compartment of these cells. The SNARE complex comprises three main proteins involved in the exocytosis process, which includes: the vesicle associated membrane protein 2 (VAMP-2, also referred to as synaptobrevin), syntaxin-1 and the soluble N-ethylmaleimide attachment protein-25 (SNAP-25). This SNARE complex interacts with additional regulatory SNARE proteins in close proximity to the plasma membrane (Speidel et al., 2003; Montecucco et al., 2005). Indeed, using immunocytochemistry, the only SNARE protein found in the soma and dendrites of MNC was syntaxin-1 (Tobin et al., 2012). Concerning accessory SNARE proteins, this study has revealed that Munc-18 (i.e. a protein that influences the conformation of the SNARE complex) and the Ca^{2+}-dependent activator

protein for secretion (CAPS-1; acts as a Ca^{2+} sensor for vesicle exocytosis) are both present in the somato-dendritic compartment. Since all proteins forming the SNARE complex were present within the pituitary and different results were obtained for the somato-dendritic compartment, these authors propose that different protein isoforms might be localized in MNC soma and dendrites. Because the protein VAMP-2, which co-localizes with OT and VP membrane vesicles, was only observed in the synaptic terminal but not in the somato-dendritic compartment, it could be possible that LDCV expressing VAMP-2 are preferentially shuttled to the neurohypophysis.

Despite the fact that no immunoreactivity was observed for VAMP-2 in the soma and dendrites of MNC, it was shown that impairing the functioning of synaptobrevin (referred to as VAMP-2) with TeTx (i.e. a drug that specifically cleaves synaptobrevin) prevents somato-dendritic release (de Kock et al., 2003). Indeed, this study has shown that pipettes filled with an internal solution containing TeTx were effective in preventing somato-dendritic release of OT and adenosine. More precisely, the decrease of sIPSC, caused by the release of these retrograde messengers (i.e. OT and adenosine), which inhibit GABAergic transmission, was significantly attenuated when TeTx was present in the recording electrode. As mentioned above, it might be possible to reconcile these divergent data by considering the fact that a different isoform of synaptobrevin might be found in the soma and dendrites of MNC.

1.6.4. Action potential broadening and calcium entry

A unique feature about MNC electrical activity is that the action potential width broadens under certain conditions (Andrew and Dudek, 1985; Bourque and Renaud, 1985). First, the action potential width broadens progressively during a spike train. Second, higher frequencies of discharge also lead to an increase in steady-state action potential duration. As an example, data acquired from intracellular recordings in hypothalamic explants have shown that the average action potential duration of a MNC at a firing frequency of 0.5 Hz is 1.7 ms, whereas the spike duration at a frequency of 10 Hz is 2.7 ms

(Bourque and Renaud, 1985). Moreover, this study showed that there is a gradual action potential broadening from the first spike to the 20th when spontaneous bursts are recorded or elicited via current pulse injections. Importantly, this frequency-dependent broadening relies on calcium entry because application of various Ca^{2+} channel blockers such as Co^{2+}, Mn^{2+} and Cd^{2+} and reduction of extracellular Ca^{2+} concentration with EGTA all led to a decrease of spike prolongation.

Concerning the mechanism responsible for action potential broadening in MNC, it was demonstrated that blocking K^+ conductance with either Cs^+ or TEA increases the action potential duration. However, the use of a Ca^{2+}-free ACSF (in combination with K^+ channel blockers) was shown to restore the spike duration to control values, underlying the importance of K^+ current in the repolarizing phase of the action potential as well as the role of Ca^{2+} influx in this broadening mechanism (Kirkpatrick and Bourque, 1991). Interestingly, cells injected with BAPTA showed an increase in spike width, which could be explained by the suppression of Ca^{2+}-activated K^+ currents, leading to a broader action potential (see section 1.4.2.1 for the role of BK channels in spike accommodation). Using isolated SON neurons, it was demonstrated that applying consecutive voltage pulses (i.e. from -60 mV to -50 mV for 10 ms, 10 times) led to a decrease of K^+ current amplitude in a frequency-dependent manner (O'Regan and Cobbett, 1993). In other words, higher frequencies of stimulation resulted in a more pronounced decrease of the K^+ current amplitude progressively over 10 repetitions compared to smaller frequencies. On the other hand, Ca^{2+} current amplitude remained stable over the 10 stimulations when performing the same experimental protocol. In accordance to the previous studies mentioned above, these authors propose that frequency-dependent action potential broadening can be explained first by a reduction of K^+ current and second, by a stable or a very small increase in Ca^{2+} current.

Importantly, it was shown that the frequency-dependent facilitation of secretion from the posterior pituitary (see section 1.3.3) can be explained by the presence of a spike frequency-dependent broadening mechanism that generates more Ca^{2+} entry, per action potential, at higher frequency of

stimulation (Jackson et al., 1991). As mentioned above, higher frequency of stimulation were shown to be correlated with a larger action potential width in the soma of MNC, but if this mechanism is also linked to a higher Ca^{2+} influx per spike within the soma and dendrites and therefore leads to an enhanced secretion from this compartment is still unknown.

1.6.5. Calbindin, calretinin and calcium buffering

The sections above have highlighted the important role of Ca^{2+} in the priming of LDCV, in the action potential broadening mechanism of MNC, as well as in how different VGCC impact somato-dendritic release. However, many types of neurons express proteins that can modulate the magnitude and time course of Ca^{2+} signals, therefore regulating several cellular processes that require Ca^{2+}. In SON neurons, such candidates are calbindin, a protein with high affinity Ca^{2+}-binding sites (i.e. up to 6 binding sites) from the EF-hand family of Ca^{2+}-binding proteins (Leathers et al., 1990) and calretinin, a Ca^{2+}-binding protein that also belongs to the same family (Persechini et al., 1989). Using immunofluorescence, it was observed that calbindin is preferentially found in OT-rich regions (Li et al., 1995; Voisin et al., 1996) and co-localizes with OT cells in the SON (Arai et al., 1994). Importantly, using triple-labeling immunofluorescence and confocal microscopy, the differential expression of calbindin and calretinin in OT- and VP-containing neurons was investigated (Arai et al., 1999). The results have shown that 70% of the OT-labeled cells were stained for both calbindin and calretinin, whereas 73% of the VP-labeled cells were neither stained for calbindin nor calretinin, suggesting that only low proportion of VP neurons express these Ca^{2+}-binding proteins.

Interestingly, it was demonstrated that addition of calbindin into the recording electrode of SON neurons is effective at converting a phasic firing (i.e. putative VP cells) into a continuous discharge (Li et al., 1995). Moreover, this conversion from a phasic to a continuous firing was also accompanied with a suppression of the DAP. On the other hand, introducing anti-calbindin antiserum into cells displaying a

continuous activity with no DAP (i.e. putative OT cells) led to a phasic phenotype of firing activity with the emergence of DAP. Finally, this study has shown that elevating intracellular Ca^{2+} concentration (i.e. electrodes filled with 0.1 mM Ca^{2+}) resulted in the emergence of a phasic firing with the apparition of DAP, whereas addition of BAPTA into the recording electrode led to a continuous electrical activity linked with an absence of DAP. These results indicate that in principle, both cell types are capable of displaying phasic firing and importantly, the presence of calbindin plays a role in restricting intracellular calcium availability and somehow, prevents the emergence of DAP and phasic firing in OT neurons. Altogether, these findings indicate that modulating intracellular Ca^{2+} concentration with Ca^{2+}-binding proteins can have a direct influence on the cell firing activity, but if this Ca^{2+} modulation could potentially regulates somato-dendritic release is still not known.

1.6.6. Hypothesis five

It was previously shown that stimulation of the posterior pituitary leads to an enhanced peptidergic secretion in a frequency-dependent manner (see section 1.3.3). Importantly, this frequency-dependent facilitation of secretion at the posterior pituitary can be explained by the presence of a spike frequency-dependent broadening mechanism that generates more Ca^{2+} entry per action potential at higher frequencies of stimulation (see section 1.6.4). Despite the fact that somatic action potentials also show a spike frequency-dependent broadening that relies on a Ca^{2+} current, nothing is known concerning how Ca^{2+} levels are regulated within OT and VP dendrites upon different frequencies of stimulation. Additionally, calbindin and calretinin were shown to play a potent role in Ca^{2+} buffering, preferentially in OT cells, but if these proteins impact Ca^{2+} influx within dendrites is also not known. Based on these findings, my fifth hypothesis is that *dendritic Ca^{2+} level will be positively correlated to the firing frequency of OT and VP neurons and a lower absolute increase in dendritic Ca^{2+} values will be observed for OT cells.*

1.7. Summary

As described in section 1.3.2, relatively little attention has been given to clustering activity, as well as to which parameters modulate this rhythmic firing. Therefore, the first aim of this thesis is to elucidate how clustered firing is induced synaptically *in situ* (*Hypothesis one*, section 1.3.4) and to further characterize which parameters play a determining role in the shaping of this short rhythmic oscillation (*Hypothesis two*, section 1.4.4). These questions will be investigated in *Chapter III*.

The second aim of this thesis is to characterize whether excitatory transmission is inhibited in a spike frequency- and pattern-dependent manner (*Hypothesis three,* section 1.5.7 and *Hypothesis four*, section 1.5.8), following somato-dendritic release of retrograde messengers from OT and VP neurons, considering that previous studies have shown that postsynaptic depolarizations in MNC suppress glutamate release (see section 1.5.6). These two hypotheses will be examined in *Chapter IV*. Lastly, *Chapter V* will investigate whether intra-dendritic calcium rises in a frequency-dependent manner in OT and VP neurons and if this intra-dendritic calcium increase is differentially regulated in both cell types (*Hypothesis five*, section 1.6.6). The next Chapter, *Methods*, will provide a detailed overview of the procedures and analysis used to test the hypotheses mentioned above.

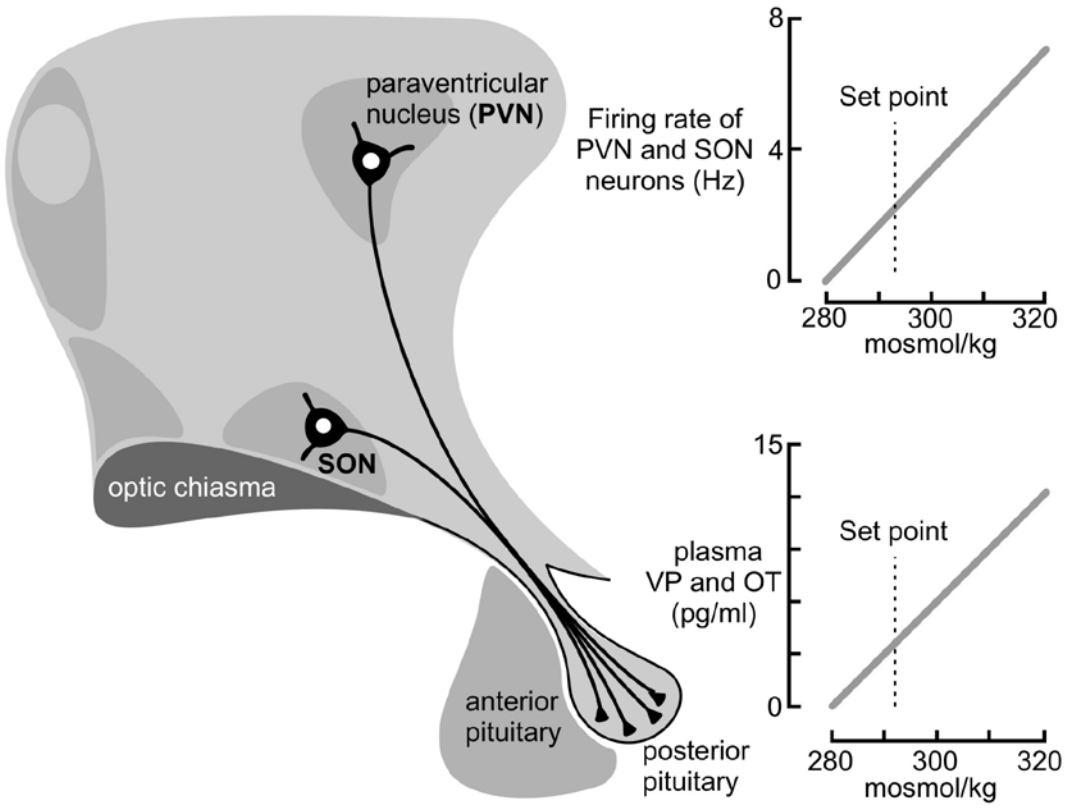

Figure 1.1.2. MNC are localized in PVN and SON nuclei

Magnocellular neurosecretory cells (MNC) somata are found in PVN and SON nuclei and send their axonal projection into the posterior pituitary. Previous studies have shown a positive relationship between rise in plasma osmolality and peripheral release of OT and VP, as well as between the firing rate of MNC and hormone release from the posterior pituitary (see sections 1.1.5.2b and 1.3.3)

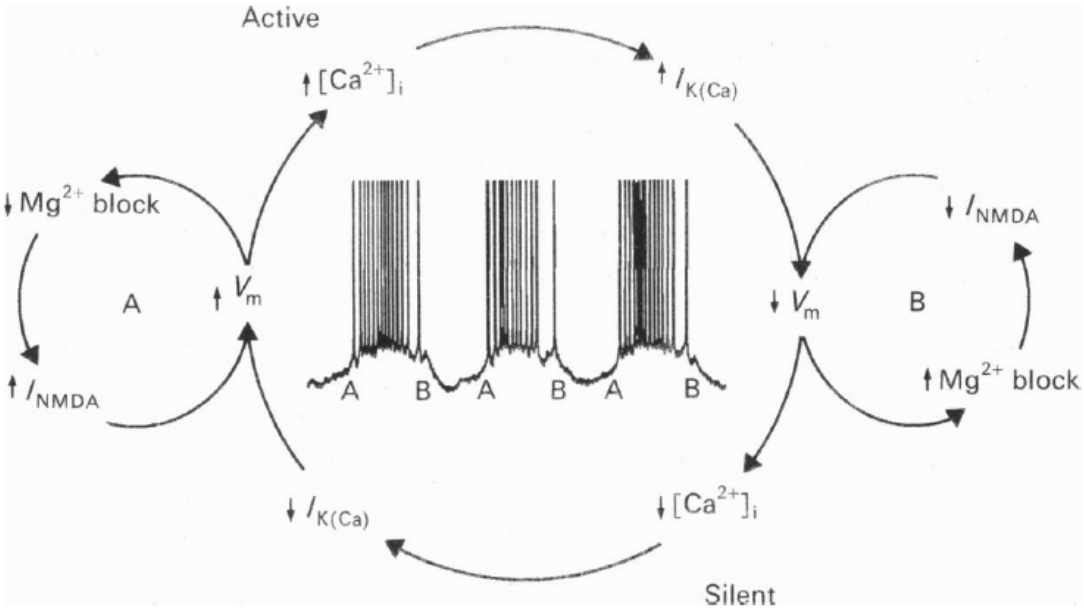

Figure 1.3.2. Hu and Bourque model of NMDA-induced clustering activity

The large circle depicts activity-dependent changes in intracellular Ca^{2+} concentration ($[Ca^{2+}]_i$) and resulting effects on the apamin-sensitive Ca^{2+}-activated K^+ current ($I_{K(Ca)}$). The lateral loops illustrate the regenerative consequences of membrane depolarization ($\uparrow V_m$; *A*), or hyperpolarization ($\downarrow V_m$; *B*), which are attributed to the Mg^{2+}-sensitive voltage dependence of the NMDA channels. The inset trace shows the respective portions of the burst cycle which are thought to result from processes in *A* and *B*.

(With permission, from Hu and Bourque, 1992; *Journal of Physiology* (458) p.684, Fig.16)

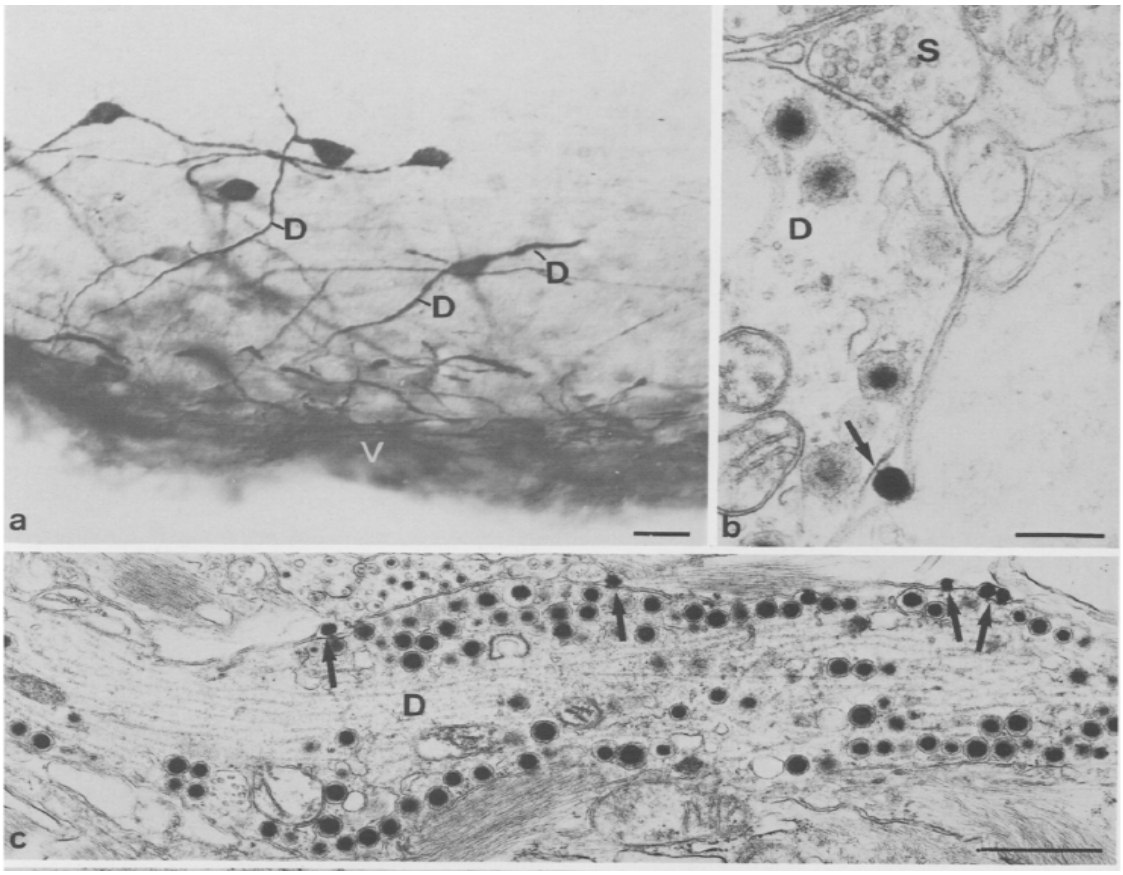

Figure 1.5.1. Vesicles undergoing exocytosis from the somato-dendritic compartment of MNC visualized with electron microscopy

A, VP dendrites visualized with light microscopy. **B**, A VP vesicle is undergoing exocytosis (where the arrow points) in close apposition to the dendritic plasma membrane. **C**, Longitudinal section of a dendrite with several vesicles undergoing the process of exocytosis (see arrows). (D; dendrite, S; synaptic button, V; ventral glial laminae)

(With permission, from Pow and Morris, 1989; *Neuroscience* (32) p.436, Fig.1)

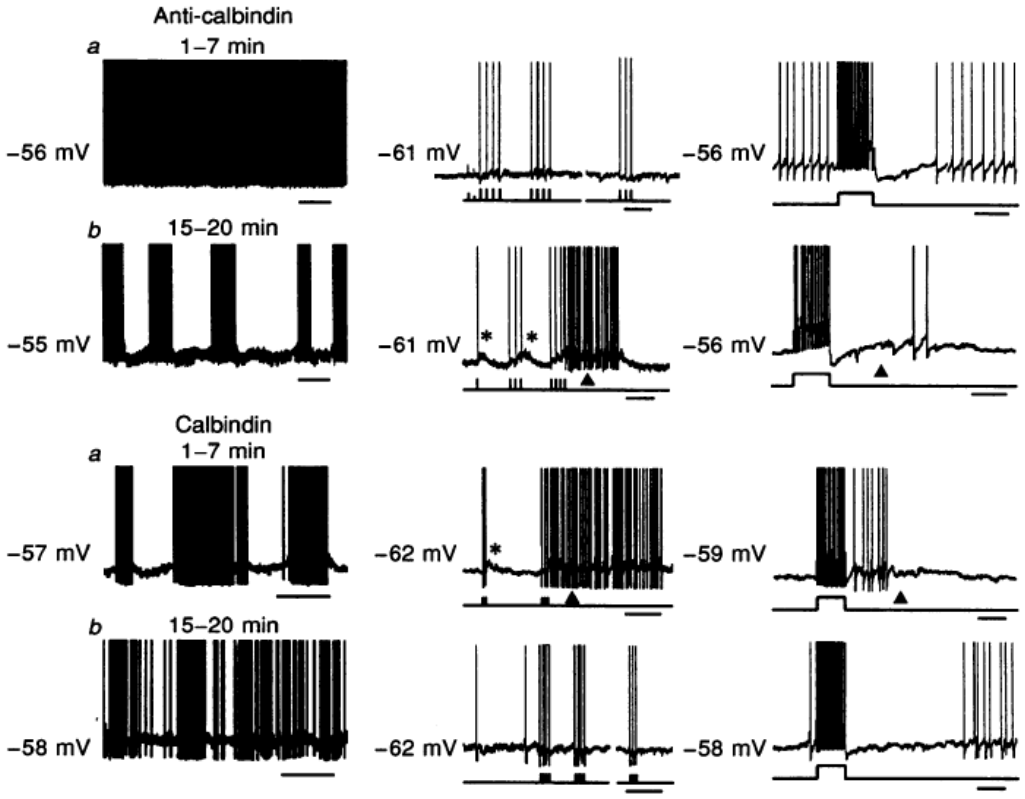

Figure 1.6.5. Calbindin converts a phasic firing into a continuous discharge

Addition of anti-calbindin antiserum into a cell displaying a continuous activity with no DAP (i.e. putative OT cells; **1st trace**) led to a phasic phenotype of firing activity with the emergence of DAP (**2nd trace**) about 15-20 minutes from the onset of the recording. On the other hand, introducing calbindin into the recording electrode of a SON neuron is effective at converting a phasic firing (i.e. putative VP cells, **3rd trace**) into a continuous discharge (**4th trace**). Moreover, this conversion from a phasic to a continuous firing was also accompanied with a suppression of the DAP. (***** represents DAP; ▲ plateau potential; current monitor below electrophysiological traces and underlying short bars on the left represent the segments analyzed on the right).

(With permission, from Li and Hatton, 1995; *Journal of Physiology* (488), p.603, Fig.1)

II: METHODS

Now that the background literature leading to the formulation of specific hypotheses was provided in *Chapter I*, the current chapter will thus focus on the experimental procedures used to test these hypotheses. Importantly, all experiments have been performed in accordance to the guidelines from the Animal Care Committee of McGill University and the Canadian Council on Animal Care (protocol 1190).

2.1. Animals

Two different rat strains were used for the experiments reported in this thesis. Male Long Evan rats (purchased from Charles River Laboratories, Wilmington, MA, U.S.A.) have been used for the data acquired from the experiments investigating the NMDA-induced clustering in magnocellular neurosecretory neurons, while transgenic male and female Wistar rats (eGFP and mRFP1, further explained in section 2.1.1. and 2.1.2.) have been used for the frequency- and pattern-dependent somato-dendritic release experiments. Rats were housed in the McGill Animal Facility with free access to food and water and weighted in average between 80 and 180 g on the day of the experiment.

2.1.1. Transgenic rats expressing enhanced green fluorescent protein

In order to correctly identify the cell phenotype (i.e. VP or OT neurons), male and female Wistar rats expressing enhanced green fluorescent protein (eGFP) in VP cells were used to visualize these cells under differential interference contrast (DIC) microscopy. This transgenic rat line has been generated in 2005 in Japan (Ueta et al., 2005). More precisely, within the C-terminus, an arginine vasopressin (AVP-) eGFP transgene was inserted into the exon III of the AVP gene. The fluorescence expressed by the VP peptide is therefore found within VP-containing vesicles and immunostaining data provided by the group of Ueta has shown a robust eGFP expression in the SON (including the posterior pituitary), the PVN and

the SCN, with no ectopic expression. Due to frequent intra-breading of this transgenic line in our laboratory, we breaded some transgenic rats with wild-type Wistar rats to avoid genetic diseases acquired via a lack of gene variability. To confirm that the new born rats were expressing the eGFP transgene, ear punch samples were send to a genotyping company (Transnetyx inc., Cordova, TN, U.S.A.) and rats expressing the transgene were then used for subsequent breading.

2.1.2. Transgenic rats expressing monomeric red fluorescent protein 1

In order to visualize OT cells under DIC microscopy, we used transgenic OT monomeric red fluorescent protein 1 (mRFP1) rats, a line also created in Japan (Katoh et al., 2011). Using the same experimental approach as for the eGFP rats, a chimeric OXT mRFP1 bacterial artificial chromosome clone transgenic construct was purified for microinjections into fertilized oocytes. Fluorescence for OT mRFP1 is expressed within OT vesicles and was observed in the SON, the PVN, the internal layer of the median eminence and the posterior pituitary. Even if no quantification was provided in their article, the majority of labeled OT cells also expressed mRFP1, suggesting that targeting OT cells with this approach is highly reliable. Again, to avoid genetic diseases, mRFP1 rats were breaded with wild-type Wistar rats and the expression of the mRFP1 transgene was also assess via DNA genotyping from ear punch samples and sent to a genotyping company (Transnetyx inc., Cordova, TN, U.S.A.).

2.2. Solutions

Artificial cerebrospinal fluid (ACSF) for the horizontal hypothalamic slices contained (in mM): 120 NaCl, 4 KCl, 1.46 $MgCl_2$, 26 $NaHCO_3$, 2 $CaCl_2$, 1.23 NaH_2PO_4, and 10 D-glucose (all from Sigma-Aldrich Co., Oakville, Ontario, Canada) and was adjusted to 295 mOsml·kg^{-1} with mannitol, as needed. The slicing solution contained the same ACSF preparation. For the hypothalamic explant preparation, the ACSF contained (in mM): 104 NaCl, 26 $NaHCO_3$, 1.23 NaH_2PO_4, 3 KCl, 1 $MgCl_2$, 2 $CaCl_2$, 10 D-glucose, and mannitol was added again, as needed (pH 7.35).

2.3. Experimental tissue preparations

2.3.1. Superfused hypothalamic explants preparations

Rats were handled in restraining cones and rapidly guillotined. Their brain was quickly extracted and unnecessary tissue was removed (i.e. the edges if the brain) with razor blades to get a hypothalamic explants (~8 X 8 X 2 mm) which preserved the SON, the OVLT and the optic chiasm. The explants were pinned on a Sylgard base chamber (~30°) and surface membranes overlying both the OVLT and the SON were removed with small forceps. The temperature was controlled (31–33°C) via perfusion (~1 ml/min) of warm oxygenated ACSF (95% O_2/5% CO_2). Importantly, this preparation was used because the connections between the OVLT and SON neurons are preserved (Yang et al., 1994; Richard and Bourque, 1995).

2.3.2. Acute angled hypothalamic sections

In accordance with the hypothalamic slice preparation preserving the connectivity between the SCN, the OVLT and the SON (Trudel and Bourque, 2003) rat brains were quickly extracted (as described in section 2.3.1), glued on a horizontal platform (38°) and immersed into ice-cold, corbogenated ACSF (95% O_2/5% CO_2). A horizontal brain slice (400 um thick) was made using a VT1200 vibrating blade microtome (Leica Microsystems, Wetlzar, Germany). The slice was then immediately transferred into a recording chamber, kept at a temperature of 30-32°C via the perfusion of a carbogenated ACSF (95% O_2/5% CO_2) at a rate of 2 mL·min for one hour prior to recording. The temperature as well as the perfusion rate was kept constant throughout the entire experiment.

2.4. Electrophysiological recordings

2.4.1. Extracellular recordings

Recording glass micropipettes prepared with a vertical puller (Narighige International USA, INC., East Meadow, NY) were filled with 1 M NaCl (10–20MΩ) and advanced using an IVM micromanipulator (Scientifica, Uckfield, UK). Voltage recorded via an Axoclamp-2A (Molecular Devices Corp, Sunnyvale, CA, U.S.A.) was filtered (0.5−1.2 kHz) before capture using Clampex 10 software (Molecular Devices). For the clustering experiments, cells with a basal firing frequency >10 Hz or a basal rate of clustering >12 clusters per minute (CPM) were excluded from analysis. The number of CPM was calculated in control condition during a 30 seconds segment right before the stimulation of the OVLT (with a bipolar stimulating electrode; 10 Hz, 60 s., Fig. 2.4.1). Following the electrical stimulation of the OVLT, the number of CPM was calculated during five consecutive 30 second segments. Because electrically evoked clustering activity was short lived, the number of interspike intervals detected during this period was insufficient to produce a histogram that could be adequately fitted with a single exponential function. Therefore individual clusters recorded in explants were arbitrarily defined as a grouping of two or more action potentials preceded and followed by pauses greater than 400 ms, and where interspike intervals within the cluster were smaller than 400 ms, as described previously (Hu and Bourque, 1992).

2.4.2. Intracellular recordings

2.4.2.1. Current clamp

Whole-cell current clamp recordings (D.C.-2 kHz) were performed using an Axopatch-1D amplifier (Axon Instruments), displayed on an oscilloscope and digitized using pCLAMP 8.0 software (10 KHz). Pipettes were prepared with a P-87 puller (Sutter Instrument, Novato CA) and filled with a solution comprising (in mM): 110 $KMeSO_4$, 10 Hepes, 10 KCl, and 1 $MgCl_26H_2O$ (2–5 MΩ). Concerning the NMDA-

induced clustering activity via bath application of this drug, clusters were detected using a procedure modified from the Poisson surprise technique (Ko et al., 2012), where individual clusters were identified as groupings of ≥2 action potentials separated by interspike intervals lasting more than the pause criterion (PC), defined as the duration beyond which fewer than 1% of the interspike intervals are expected to occur as determined by fitting a single exponential to the falling phase of the interspike interval distribution measured in each cell. In order to assess the number of CPM at different voltages, cells were hyperpolarized until silenced and then a staircase of incrementing current steps (+5 pA, 30 s. each) was delivered until the cell was strongly depolarized. To elicit an AHP in MNC, a depolarizing pulse (200 ms and 400 ms, +800 pA) was triggered to elicit between 6-12 action potentials, leading to the formation of an AHP. For the gramicidin perforated patch-clamp recordings, recordings started when the pipette resistance dropped to values between 40 and 80 MΩ, and a 200 ms pulse (+800 pA) was delivered to subsequently measure the AHP amplitude. To elicit somato-dendritic release in another subset of experiments, spike trains were induced in MNCs at different frequencies (0.1, 0.5, 1, 3, 5, 10, 30 and 50 Hz) or using different patterns of electrical activity (clustering vs tonic; see Fig.2.4.2.1). Spike trains always contained the same number of action potential (i.e. 100).

2.4.2.2. Voltage clamp

Whole-cell voltage clamp recordings (D.C.-2 kHz) were performed using an Axopatch-1D amplifier (Axon Instruments), displayed on an oscilloscope and digitized using pCLAMP 8.0 software (10 KHz). To evaluate changes in evoked excitatory postsynaptic current (eEPSC) amplitude, identified MNC (i.e. OT or VP) were patched with an electrode filled with an internal solution comprising (in mM): 140 mM potassium gluconate, 2 mM $MgCl_2$, 10 mM HEPES, 2 mM di-sodium ATP and 0.4 mM sodium GTP (pH adjusted to 7.25 with NaOH). Upon seal rupture, MNC were held at -70 mV. To induce an eEPSC, the OVLT or glutamatergic afferents synapsing onto the SON were stimulated with a bipolar electrode at a frequency of 0.2 Hz (i.e. every 5 s). The eEPSC charge transfer was assessed 5 minutes prior to and after

the postsynaptic cell conditioning (postsynaptic stimulations are described in section 2.4.2.1). The inhibition of the eEPSC charge transfer was calculated by fitting an exponential function (exponential decay, single, 3 parameters; f = y0+a*exp(-b*x)) to the eEPSC amplitude values obtained following the postsynaptic conditioning (see Fig. 2.4.2.2). Then, the change in the amplitude of eEPSC (i.e. a in the formula) was divided by the average baseline value of the eEPSC amplitude (i.e. during 110 s. of eEPSC acquisition in control) obtained prior to the postsynaptic spike conditioning. This final value was multiplied by 100 to get the percent of inhibition (% inhibition; see Fig. 2.4.2.2). Cells displaying a percent of inhibition smaller than 10% were not considered for the final analysis. Values were corrected for time-dependent loss of short-term facilitation (also explained in the *General Discussion*, section 6.2). More precisely, during the induction of action potentials in MNC, the OVLT was not stimulated, which led to a decrease of the eEPSC amplitude upon reintroduction of the OVLT stimulation, but only when the OVLT was not stimulated for > than ~ 30 s. For every frequency of postsynaptic stimulation tested (i.e. from 0.1-50 Hz), we used the corresponding duration (e.g. 0.1 Hz = 1000 s.) and did not stimulate the OVLT for equivalent durations. Then, we reintroduced the OVLT stimulation and measured the % inhibition of the eEPSC charge transfer (see Fig. 6.2.2.B). These values were used as a correction factor and subtracted from the spike frequency-dependent inhibition values obtained in *Chapter IV*, for Figure 4.2.1.D.

To measure the PPR, two depolarizing pulses were elicited 50 ms apart. In order to obtain a ratio, the charge transfer of the second EPSC was divided by the charge transfer of the first EPSC. The amplitude of asynchronous events was measured during a 200 ms segment following the onset of second EPSC, when its amplitude was back to the original holding membrane voltage (i.e. baseline).

2.5. Tissue and single cell PCR

Blocks of SON tissue were placed in RNAlater (Life Technologies Inc., Burlington, ON, Canada) or processed as previously decribed to isolate MNCs(Sharif Naeini et al., 2006). Tissue RNA was purified and

converted to cDNA using RiboPure and RETROscript kits (Life Technologies). For single cell analysis, MNCs were aspirated into a micropipette containing 1.5 µl Hepes buffer with RNAseIN (10 U μl^{-1}) and then expelled into a tube containing 0.5 µl DNAse I (1 U μl^{-1}) and 0.5 µl buffer (Fermentas), incubated at 37°C for 30 min, after which 1 µl 25 mM EDTA was added. Retrotranscription was performed with 1 µl 50 µM Random Hexamer primers, 0.25 µl RNAseIN (10 U μl^{-1}), 1 µl 0.1 M DTT, 1 µl 50 mM MgCl2, 1 µl 10 mM (each) dNTPs mix (Qiagen), 2 µl First Strand Buffer and 0.25 µl SuperscriptIII (200 U μl^{-1}) (Life Technologies). The mix was incubated at 50°C for 2 h and the resulting cDNA was stored at −20°C. PCR detection of NT receptors 1 (NTS1) and 2 (NTS2) was performed using a nested approach with Phusion High Fidelity Polymerase (New England Biolabs, Whitby, ON, Canada). Primers targeting NTS1 were: external pair, forward (5'GGTAGCCGTGTGTGCGCTCC3'), reverse (5'AAAGGGCTGGGCATCGGGTTC3'), expected product 489 bp; internal pair, forward (5'ATCTGGAGGTCCGTAGCAGCCC3'), reverse (5'GTTGAGGTGCATGGTGGGTGCC3'), expected product 322 bp. For NTS2, the primers were: external pair, forward (5'GCTGTCACTGGTCTGGGTCGC3'), reverse (5'GTGCTGGAGGCTGCGGATCTG3'), expected product 418 bp; internal pair, forward (5'AGCACGAAGTGGAAAGCGCGG3'), reverse (5'CGTGATGAAGCCCAGGAGGCC3'), expected product 272 bp.

2.6. Two-photon calcium imaging

Patch pipettes (4-6 MΩ) were pulled from medium-wall capillaries using a P-97 or P-1000 electrode puller (Sutter Instruments) and were filled with internal solution comprising (in mM): 140 mM potassium gluconate, 2 mM $MgCl_2$, 10 mM HEPES, 2 mM di-sodium ATP and 0.4 mM sodium GTP. On the day of the experiment, Alexa 594 (17 µM; Invitrogen, Carlsbad, CA) was added to the internal solution in order to see the cell morphology, and Fluo-5F pentapotassium salt (180 µM; Life technologies, Burlington, Ontario, CA) was also included to assess changes in intracellular calcium concentration. Neurons were patched at 400x or 600x magnification using customized microscopes (SliceScope, Scientifica Ltd; or Olympus BX51WI, Olympus, Melville, NY) with infrared video Dodt

contrast (Luigs and Neumann, Ratingen, Germany). Most laser-scanning imaging was performed using three 2PLSM workstations (Denk et al., 1990), custom-built according to standard procedures (Tsai and Kleinfeld, 2009) from BX51WI (Olympus, Melville, NY) or SliceScope (Scientifica) microscopes, using hand-selected R3896 bialkali photomultipliers, C9525-51 high-voltage PSUs, and C7319 preamplifiers from Hamamatsu, or Stanford Instruments SRS570 preamplifiers. One SliceScope was fitted with an MDU (Scientifica). Scanners were Cambridge Technologies 6215H 3-mm or Thorlabs GVSM002/M 5-mm galvanometric mirrors and photomultipliers were in epifluorescence configuration.

Two-photon excitation was achieved using a MaiTai BB (Spectraphysics) or a Chameleon XR (Coherent) Ti:Sa laser, tuned to 800-820 nm for Fluo-5F and Alexa-594, or to 880-900 nm for GFP. Gating was achieved using Thorlabs SH05/SC10 or Uniblitz LS6ZM2/VCM-D1 shutters. Laser power was manually attenuated using a polarizing beam splitter (Melles Griot PBSH-450-1300-100 or Thorlabs GL10-B with AHWP05M-980 half-wave plate) while monitoring output with a power meter (Thorlabs PM100A/S121C or Melles Griot 13PEM001/J) by picking off a fraction of the beam with a glass slide.

Imaging data was acquired with PCI-6110 boards (National Instruments) using custom modified versions of ScanImage v3.5-3.7 (Pologruto et al., 2003) running in Matlab (MathWorks, Natick, MA), and was analysed off-line using in-house software running in Igor Pro. Calcium imaging experiments commenced approximately 15-30 minutes after break-through, to allow for dye equilibration. Identified OT and VP neurons were filled with Alexa 594 to visualize the cell morphology and select areas where 1000 line scans per 1.12 s. were performed onto proximal dendrites (i.e. perpendicularly to their long axis). Cells were also filled with the calcium-sensitive dye Fluo-5F in order to assess changes in intracellular dendritic calcium level, measured as the change in the green Fluo-5F fluorescent signal (dG) normalized to the red Alexa 594 (R) fluorescent signal (dG/R). Electrophysiology and imaging boards were synchronized by a trig signal, which provided sub-sample precision.

2.7. Pharmacology

The drugs listed below are expressed as a final concentration when used on the day of the experiment. The SK3 channel blocker apamin (Sigma-Aldrich, St-Louis, MO) was diluted in water and dissolved in ACSF as needed (100 nM or 4 nM for the IC_{50} concentration). Neurotensin (NT) and NT 1-7 (Sigma-Aldrich, St-Louis, MO) were dissolved in water and added to the ACSF (0.3-3 μM). The NT antagonist SR46892 was dissolved in DMSO, kept frozen and dissolved as needed into ACSF (0.3-3 μM; provided by Dr P. Sarret, France). NMDA (50 μM) and the NMDAR antagonist D,L-amino-phosphono-valeric acid (APV; 100 μM, both from Sigma-Aldrich, St-Louis, MO) were freshly dissolved into ACSF. To block IPSC, bicuculine methochloride was dissolved in water and added to the ACSF (5 μM; Tocris Bioscience, Bristol, UK). For some experiments, BAPTA was included in the internal solution (10 mM; Sigma-Aldrich, St-Louis, MO) and potassium gluconate concentration was lowered (from 140 mM to 95 mM). The CB1 receptor blocker AM251 was dissolved in water and included in the ACSF (5 μM; Tocris Bioscience, Bristol, UK). Tetrahydrolipstatin (THL, 5 μM; Sigma-Aldrich, St-Louis, MO) was incorporated in the internal solution to inhibit the diacylglycerol lipase (i.e. involved in 2-AG synthesis). Manning compound, an OT and VP receptor antagonist (10 μM; Tocris Bioscience, Bristol, UK) and SR49059, a V1a receptor antagonist (10 μM; Sigma-Aldrich, St-Louis, MO) were dissolved in water and added to the ACSF. nor-Binaltorphimine (nor-BNI, 1 μM; Tocris Bioscience, Bristol, UK) was dissolved in water and incorporated to the ACSF. For the gramicidin perforated patch-clamp experiments, gramicidin (Sigma-Aldrich, St-Louis, MO) was dissolved in DMSO at a stock concentration of 0.05 mg/ml and diluted 1:500 into the internal solution. The information and the concentration used regarding Alexa 594 and Fluo-5F are explained in section 2.6.

2.8. Data and statistical analysis

All values are reported as means ± standard error of the mean (SEM) and Sigmaplot 12 (Systat Software Inc., Chicago, IL, USA) was used to perform statistical tests including: Student's *t* test, paired *t* test; one-way ANOVA, followed by the Holm–Sidak *post hoc* test; one-way repeated measures (RM) ANOVA, followed by the Holm–Sidak *post hoc* test. A value of $P < 0.05$ was considered statistically significant. Data acquired via two-photon calcium imaging were analyzed with Igor pro 6.35A5 (WaveMetrics, Lake Oswego, Oregon, U.S.A.).

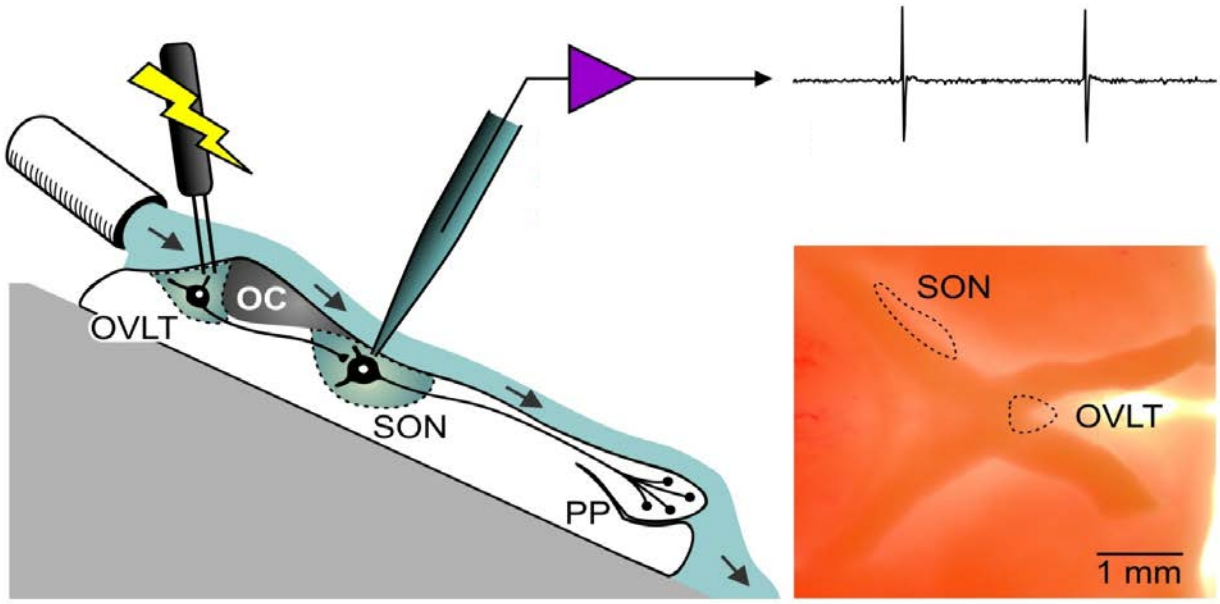

Figure 2.4.1. Protocol used to elicit glutamate release onto MNC via the electrical stimulation of the OVLT

The OVLT, which sends glutamatergic afferents onto SON neurons, was stimulated with a bipolar electrode for 60 s. at 10 Hz. The electrical activity of SON neurons was monitored via extracellular single-unit recordings. (OC, optic chiasm; PP, posterior pituitary).

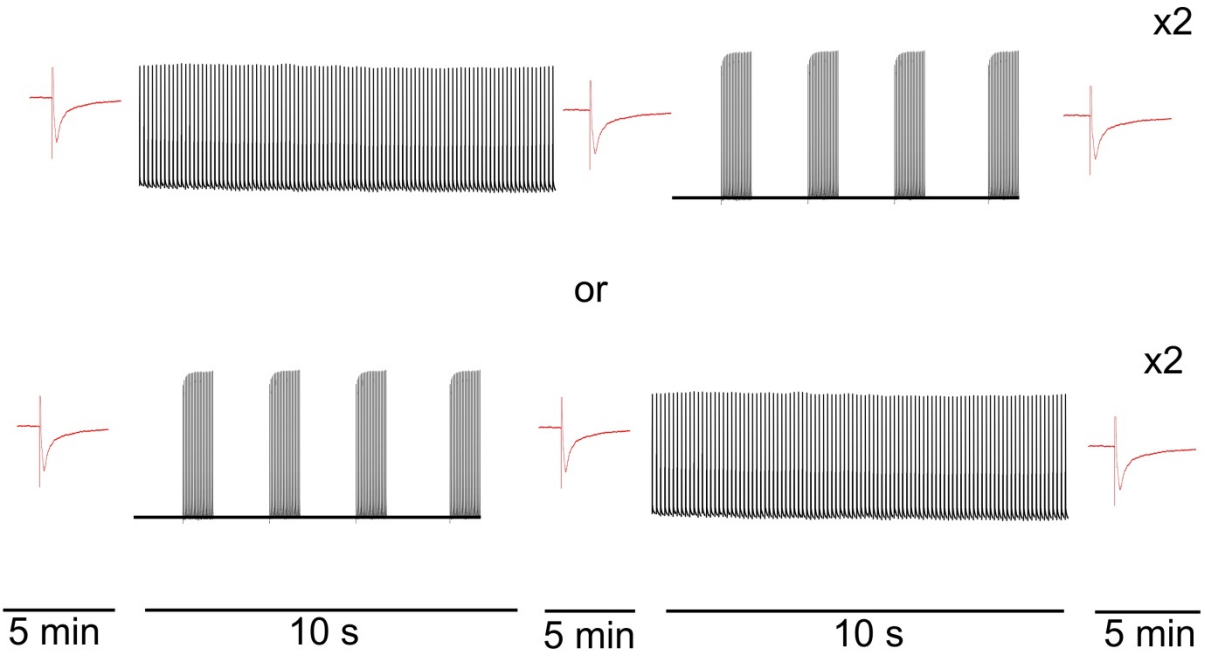

Figure 2.4.2.1. Protocol used to elicit a tonic and a clustered firing in MNC

The eEPSC amplitude was monitored for a control period of 5 minutes after which action potentials were elicited to either mimic a tonic or a clustered firing, in OT and VP neurons (100 spikes, mean frequency of 10 Hz). Following the postsynaptic stimulation, the eEPSC was again monitored for 5 minutes. A variation in the order of presentation (tonic or clustering) was also included for every new cell tested.

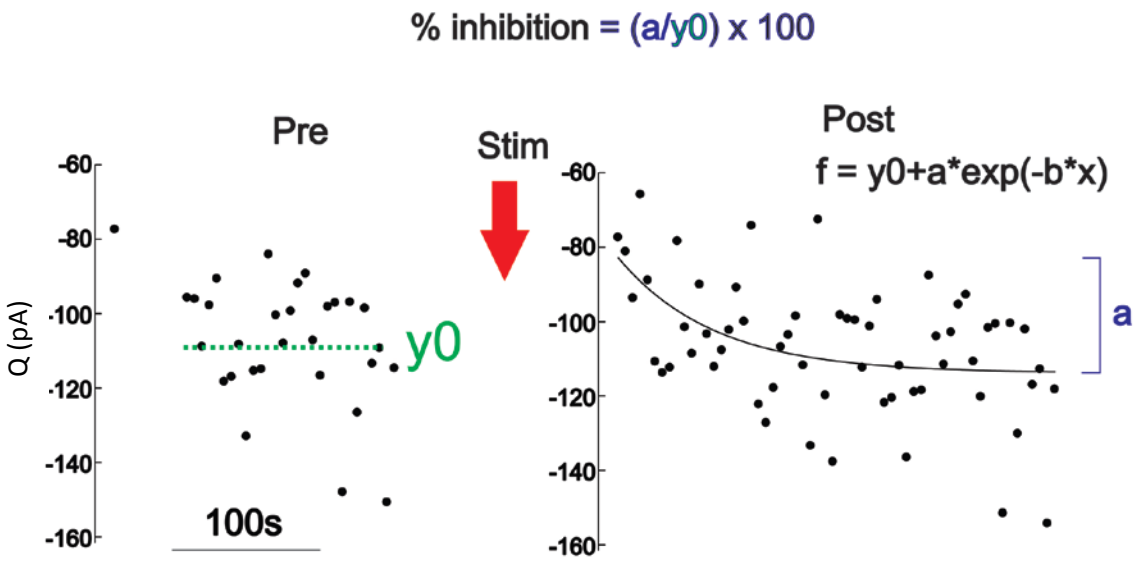

Figure 2.4.2.2. Method of analysis to calculate the percent of inhibition of the eEPSC amplitude

The average eEPSC amplitude (y0) was analyzed for the last 110 s. in control condition (left; Pre). Following the induction of postsynaptic spikes (red arrow), the eEPSC amplitude was monitored in Post (right) and an exponential function was fitted. The variation of the eEPSC amplitude (a) was then divided by y0 and multiplied by 100 to be expressed as a % of inhibition (% inhibition).

III : MODULATION OF SPIKE CLUSTERING BY NMDA RECEPTORS AND NEUROTENSIN IN RAT SUPRAOPTIC NUCLEUS NEURONS

In *Chapter II*, the different experimental procedures used to test the hypotheses presented in *Chapter I*, *Summary* (see section 1.7) were extensively described. Therefore, the current chapter aims to evaluate whether the release of endogenous glutamate, following stimulation of the OVLT, leads to cluster formation in MNC (*Hypothesis one*, see section 1.3.4) and to investigate how this rhythmic oscillation is modulated via neurotensin and SK3 channels (*Hypothesis two*, see section 1.4.4).

3.1. Overview

In contrast to the considerable amount of information that has been accumulated concerning in one hand, phasic activity from VP cells (see section 1.3.1) and on the other hand, electrical bursts from OT cells such as seen during lactation and parturition (see section 1.1.4.2), very few studies have investigated clustering activity. As described in section 1.3.2, clustered firing was shown to emerge *in vivo* following dehydration within the OT and VP neuronal populations. Additionally, stimulating the neurohypophysis with a clustering phenotype maximizes VP release, compared to a tonic stimulation (Cazalis et al., 1985). It was also demonstrated that clustering activity can be initiated *in vitro* via bath application of NMDA and that this regenerative rhythmic firing depends on SK3 channel activation (see section 1.3.2). However, it is still unknown if endogenous glutamate release *in situ* can trigger clustered firing in MNC.

Because of the Mg^{2+} block of NMDA receptors, slight voltage variations were shown to impact NMDA-induced clustering activity, by directly modulating the shaping of clusters (Hu and Bourque, 1992). Therefore, it is interesting to understand how depolarizing peptides might also modulate this clustered firing. Neurotensin (NT) has been shown to exert a depolarizing effect on MNC and is thus a potent candidate in the shaping of clustered firing. It has also been shown that NT inhibits the AHP

amplitude in SON neurons (Kirkpatrick and Bourque, 1995). Importantly, the AHP, also responsible for pauses between clusters, is mediated via SK3 channel activity (see section 1.4.3), and if NT might directly modulate clustering activity via an inhibition of SK3 channels is still not known.

Osmosensitive neurons in the OVLT are excited under hyperosmotic conditions and these neurons send glutamatergic afferents onto MNC in the SON (see sections 1.1.5.2a and 1.2.1). This chapter will therefore examine first if activation of OVLT neurons can promote the emergence of NMDA receptor-dependent clustered firing in MNC via endogenous glutamate release. Second, if this clustering activity can be modulated by depolarizing peptides such as NT or via a modulation of the SK3-dependent pauses between clusters will also be addressed.

3.2. Results

3.2.1. Stimulation of the OVLT induces spike clustering in MNC

To determine if NMDAR-dependent clustering can be induced by endogenous glutamate release, we examined the effects of electrically stimulating the OVLT during extracellular recordings of single unit spiking activity from MNC in superfused explants of rat hypothalamus. As illustrated in Figure 3.2.1.A, repetitive electrical stimulation of the OVLT at 10 Hz for 60 seconds induced spike clusters that were not observed during the pre-stimulation period. The average rate of clustering measured during consecutive 30 seconds intervals returned exponentially to baseline following the end of the stimulus (τ = 49.6 s.; n = 5; Fig. 3.2.1.B). While OVLT stimulation at 10 Hz for 10−30 seconds did not affect the rate of clustering observed during the first 20 seconds after the end of the train (n = 8; one-way repeated measures ANOVA with *post hoc* Holm–Sidak test; P = 0.842), stimulating the OVLT for 60 seconds caused a significant increase in clustering (from 4.6 ± 1.1 to 15.7 ± 4.0 CPM; n = 13; one-way RM ANOVA with *post hoc* Holm–Sidak test; P = 0.003; Fig. 3.2.1.C).

To determine if NMDA receptors (NMDAR) are involved in OVLT-mediated spike clustering, we examined the effects of blocking these receptors with APV (100 μM). In the presence of APV, stimulation of the OVLT for 60 seconds (10 Hz) no longer increased the rate of clustering (n = 7; one-way RM ANOVA with *post hoc* Holm–Sidak test; P = 0.882; Fig. 3.2.1.D and E). We next examined if OVLT-mediated clustering required the activity of SK channels. As shown in Figure 3.2.1.D and E, bath application of the SK channel inhibitor apamin (100 nM) prevented the increase in the rate of clustering induced by OVLT stimulation (n = 6; one-way RM ANOVA with *post hoc* Holm–Sidak test; P = 0.909). Collectively, these results indicate that endogenous activity-dependent glutamate release can induce clustered firing in MNC, through a mechanism that depends on NMDAR activation and SK channel activity.

3.2.2. Variations in membrane potential modulate clustering activity

To determine if changes in membrane potential can affect clustered firing, we examined the effects of current injection on NMDAR-induced clustering activity during whole-cell patch clamp recordings in hypothalamic slices. As illustrated in Figure 3.2.2.A and B, bath application of 50 μM NMDA caused a depolarization of the membrane potential and the emergence of sustained clustering activity that persisted throughout the application. Cells were then hyperpolarized until silenced and a staircase of incrementing current steps (+5 pA, 30 s. each) was delivered until the cell was strongly depolarized. As illustrated in Figure 3.2.2.C, cells exposed to ACSF did not display clustering activity at any of the voltages examined, whereas cells exposed to NMDA displayed robust clustering activity. The relationship between the rate of clustering and voltage in NMDA-treated cells was bell shaped, with a maximum at −65 mV (ACSF n = 10, NMDA n = 35; Fig. 3.2.2.D). Based on the shape of this curve, we expect that membrane depolarization from initial voltages ≤ −65 mV would enhance clustering as long as voltage does exceed −65 mV, whereas depolarization from baseline voltages between −65 and −50 mV would reduce clustering activity. Indeed as illustrated in Figure 3.2.2.E, depolarizing current steps applied from −83 and −65 mV respectively induced or suppressed clustered firing. These results suggest that neurotransmitters

capable of changing the membrane potential could regulate the rate of NMDAR-driven clustering activity in MNC.

3.2.3. Inhibition of SK channels modulates clustered firing

In agreement with previous work (Hu and Bourque, 1992), NMDAR-dependent clustering activity was fully inhibited by bath application of a saturating concentration of apamin to block SK channels (100 nM; Fig. 3.2.3.A). To determine if a more partial inhibition of SK channels can modulate clustered firing we examined the effects of a submaximal dose of apamin. Using whole-cell recording we found that the AHP following a current-induced spike train was only partly (~25%) yet significantly reduced by 4 nM apamin (n=12; paired *t* test; P=0.001; Fig. 3.2.3.B and C). We therefore examined the effects of 4 nM apamin on NMDA-evoked clustered firing using the staircase protocol described earlier. Apamin (4 nM) caused a significant decrease in the rate of NMDA-evoked clustering at voltages between −62.5 and −52.5 mV, and completely eliminated the presence of clustering activity at voltages $\geq$ −50 mV (n = 12 for apamin and NMDA; paired *t* test; Fig. 3.2.3.D). The duration of clusters recorded at equal levels of holding current was increased by 4 nM apamin (Fig. 3.2.3.E). Moreover, 4 nM apamin decreased the mean maximal rate of clustering observed in the cells (from 10.6 ± 0.7 to 6.1 ± 1.3 CPM; P = 0.002; n = 12; Fig. 3.2.3.F) and this effect was accompanied by a significant increase in cluster duration (from 1.24 ± 0.14 to 4.76 ± 2.35 s.; n = 12; paired *t* test; P = 0.003; Fig. 3.2.3.F), but no change in mean intraburst spiking frequency (paired *t* test; P = 0.464; Fig. 3.2.3.F). Therefore partial inhibition of SK channel activity can effectively modulate NMDAR-induced clustering activity in MNC.

3.2.4. Neurotensin receptor activation modulates NMDA receptor-dependent clustering activity

Previous work showed that NT can both depolarize the membrane potential and reduce the AHP amplitude in MNC (Kirkpatrick and Bourque, 1995). We therefore examined if NT could modulate NMDAR-dependent clustered firing. We first determined which G-protein coupled NT receptors (NTS) are

expressed in the SON using tissue RT-PCR. As illustrated in Figure 3.2.4.A, transcripts encoding both NTS1 and NTS2 could be detected within the SON. However, single cell RT-PCR in acutely isolated SON neurons revealed that most MNC express NTS2 rather than NTS1. As shown in Figure 3.2.4.B–D, application of 0.3–3 μM $NT^{8–13}$, a fragment that activates NTS2 (Vincent et al. 1999), significantly reduced clustering activity (from 9.8 ± 1.7 to 4.4 ± 1.2 CPM in $NT^{8–13}$; n = 17; paired *t* test; P = 0.002). However, bath application of 3 μM $NT^{1–7}$, an inactive fragment of NT (Kirkpatrick & Bourque, 1995), did not affect the rate of NMDA-induced clustering (from 12.3 ± 1.7 to 11.3 ± 2.2 CPM in $NT^{1–7}$; n=6; paired *t* test; P = 0.625; Fig. 3.2.4.C and D). Moreover, the effect of $NT^{8–13}$ was prevented when tested in the presence of the NTS1/2 antagonist SR4692 (from 11.7 ± 1.5 to 10.1 ± 1.5 CPM; n = 12; paired *t* test; P = 0.071; Fig. 3.2.4.C and D). As illustrated in Figure 3.2.4.E, $NT^{8–13}$ also significantly increased cluster duration (from 4.5 ± 1.0 to 22.9 ± 6.1 s. in $NT^{8–13}$; n = 17; paired *t* test; P = 0.002) and this effect was also abolished by SR46892 (from 3.1 ± 0.4 to 3.2 ± 0.9 s.; n = 12; paired *t* test; P = 0.677). $NT^{1–7}$ had no effect on cluster duration (from 2.3 ± 0.4 to 2.9 ± 0.6 s.; n = 6; paired *t* test; P = 0.129; Fig. 4.E). To determine if the effects of $NT^{8–13}$ on clustering were mediated by the peptide's depolarizing action, we also compared NMDA-induced clustering parameters on cells whose voltage was adjusted to −60 mV. As shown in Figure 3.2.4.F, $NT^{8–13}$ had no significant effect on the rate of clustering observed at −60 mV (n = 11; paired *t* test; P = 0.492). However cluster duration (n = 11; paired *t* test; P = 0.024) and total number of action potentials recorded per 30 seconds test period (P = 0.029) were both significantly increased by $NT^{8–13}$ in cells maintained at −60 mV.

We then examined if NT can modulate NMDAR-dependent clustering induced by endogenous glutamate release in hypothalamic explants. As illustrated in Figure 3.2.4.G and H, bath application of $NT^{8–13}$ abolished the increase in spike clustering induced by electrical stimulation (10 Hz, 60 s.) of the OVLT (n = 12; one-way RM ANOVA with *post hoc* Holm–Sidak test; P = 0.952).

3.2.5. Neurotensin does not directly inhibit SK channels

Previous findings have shown that application of NT^{8-13} inhibits the AHP amplitude to about 60% of control values when performing intracellular recordings in superfused hypothalamic explants (Kirkpatrick and Bourque, 1995). Because the AHP is induced via SK channel activity in MNC, we decided to examine if application of NT^{8-13} could exert an impact on the rate of clustering induced via bath-application of MNDA. The rationale behind this experiment was that NMDA-induced CPM rate would be significantly altered in the presence of the NT active fragment when the membrane voltage is kept constant, suggesting that NT GPCR signaling modulates SK channel function and hence, CPM activity. More precisely, if NT^{8-13} modulates SK channel activity, we should expect a significant decrease in NMDA-induced clustering activity at voltages above ~ -60 mV, since partial inhibition of SK channels was found to increase cluster duration, and thus decrease the rate of clustering, from this membrane voltage (see section 4.2.3). To investigate if NT modulates the NMDA-induced rate of clustering at different membrane voltages, cells were hyperpolarized and progressively depolarized with a staircase of incrementing current steps (+5 pA, 30 s. each) until cells were strongly depolarized. This staircase protocol was performed in the presence of NMDA (50 μM) and a subsequent staircase protocol was elicited after the addition of NT^{8-13} (0.3-3 μM). The relationship between the rate of clustering and voltage was examined by interpolating and aligning data obtained from different cells in 2.5 mV increments and was bell shaped for these two conditions (i.e. NMDA and NMDA + NT^{8-13}). The results shown in Figure 3.2.5.A indicate that application of NT^{8-13} does not modulate the rate of clustering obtained above -67.5 mV, nor the maximal rate of clustering found at −60 mV (*t* test; P = 0.392). However, the presence of NT^{8-13} led to a significant increase in the rate of clustering at −67.5 mV (from 2.73 ± 1.09 to 8.83 ± 1.88 CPM; NMDA n = 15; NT^{8-13} n = 12; *t* test; P = 0.007) and at −70 mV (from 0.87 ± 0.87 to 5.83 ± 1.7 CPM; NMDA n = 15; NT^{8-13} n = 12; *t* test P = 0.011). The latter observation indicates that NT^{8-13} increases the number of clusters at membrane voltages below the CPM max (i.e. from -70 mV

to -67.5 mV). However, since an increase in clustering activity, rather than a decrease, was observed between -70 and -67.5 mV following NT^{8-13} application, activation of additional conductances might have participated in this response. Additional work needs to be done to elucidate this finding.

Because NT^{8-13} was shown to inhibit the AHP amplitude of MNC in hypothalamic explants (Kirkpatrick and Bourque, 1995) and for the reason that this peptide increased the CPM rate in the experiment described above, we therefore decided to investigate if application of NT^{8-13} could decrease the AHP amplitude in SON slices. MNC were held at a constant voltage and a depolarizing pulse (+800 pA, for 200 ms and 400 ms) was injected to elicit an AHP. The amplitude of the AHP was calculated from the difference between the baseline voltage and the voltage at the peak amplitude of the AHP. As illustrated in Figure 3.2.5.B, exposure to NT^{8-13} neither significantly reduced the AHP amplitude following a 200 ms pulse (n = 5; paired *t* test; P = 1.0) nor to a 400 ms pulse (n = 5; paired *t* test; P = 0.573). Because NT GPCR signaling could be altered via a dialysis effect inherent to the whole cell-patch clamp technique (Penner et al., 1987), we performed additional experiments using gramicidin perforated patch-clamp recordings to avoid any possible interruptions with downstream signaling. However, the amplitude of the AHP was still not significantly reduced in the presence of NT^{8-13} (from 6.71 ± 0.64 mV to 7.01 ± 0.64 mV; n = 12; paired *t* test; P = 0.568; Fig. 3.2.5.C). Taken together, these data do not suggest that NT^{8-13} inhibit SK channel activity. Indeed, even if the rate of clustering was increased at specific negative membrane voltage (i.e. from -70 mV to -67.5 mV) when performing a staircase protocol, the AHP amplitude recorded during gramicidin perforated-patch was not reduced when the cell was held at similar membrane voltage baselines (i.e. from -75 to -64 mV).

3.3. Discussion

3.3.1. Stimulation of the OVLT elicits clustering activity via endogenous glutamate release

A considerable amount of information has been accumulated concerning phasic activity in SON neurons (Wakerley et al., 1978) and effective computational models have been developed using quantitative electrophysiological data (Roper et al., 2004; MacGregor and Leng, 2012). However, little is known about clustered activity, a firing pattern that emerges during hyperosmolality (Bourque and Renaud, 1984; Poulain et al., 1988) and which enhances activity-dependent hormone release from the posterior pituitary (Cazalis et al., 1985). Our findings show that sustained electrical stimulation of the OVLT, which contains neurons that are excited by hyperosmolality and which release glutamate from axon terminals in the SON (Armstrong et al., 1996; Bourque, 2008), causes an enhancement of spike clustering in MNC. This effect was prevalent at a stimulation frequency of 10 Hz, a value which corresponds to the firing rate of rat OVLT neurons exposed to a hypertonic stimulus (Vivas et al., 1990). Indeed, previous work has shown that stimulation of the OVLT can activate NMDAR (Yang et al., 1994; Panatier et al., 2006), and our current data indicate that OVLT-mediated clustering is inhibited by blocking NMDAR. Taken together, these observations indicate that endogenous glutamate release can induce clustering in MNC through the activation of NMDAR.

The neurons recorded in our study were not specifically identified as vasopressin releasing MNC. Previous studies have shown that the rat SON also contains oxytocin-releasing neurons, which account for approximately 35% of the total population of MNC in this nucleus (Rhodes et al., 1981). It is therefore likely that both types of MNC were sampled in our experiments. However, we found that all neurons recorded (n = 70) could display pronounced clustering activity upon exposure to NMDA, suggesting that both OT- and VP-releasing MNC are capable of expressing NMDAR-dependent clustering activity. Interestingly, previous studies have shown that bursting activity can also facilitate the release of oxytocin

from the neurohypophysis (Bicknell, 1988). Although we believe that the results reported in our study are applicable to both OT- and VP-releasing MNC, additional work is needed to establish if the modulation of clustering activity contributes to the regulation of both types of hormones *in vivo*.

OVLT-mediated clustering activity persisted for a significant amount of time following the end of a stimulation trial. Specifically, kinetic analysis revealed that the rate of clustering returned to baseline following an exponential time course with a time constant of ~50 s. The basis for this persistence remains to be determined, but several mechanisms could be involved. First, MNC express a high density of GLUN2D (Doherty and Sladek, 2011), an NMDAR subunit that features an unusually slow offset decay (τ ~5 s (Monyer et al., 1994)). Second, it has been shown that quantal glutamate release persists for tens of milliseconds following the arrival of a single action potential into presynaptic axon terminals contacting MNC (Iremonger and Bains, 2007). Moreover, repetitive stimulation of afferents at 10 Hz has been shown to enhance glutamate release probability for $\geq$ 60 s after the end of a stimulus (Kombian et al., 2000). Third, it is possible that prolonged high frequency stimulation of the OVLT causes an accumulation of glutamate that exceeds the capacity of local transporters such that synaptic NMDAR remain activated for a protracted period following a train of stimuli. Fourth, it is also possible that repetitive activation of axon terminals causes a spill-over of glutamate into the extrasynaptic space, where it could lead to a prolonged activation of extrasynaptic NMDAR. Indeed, a recent study has shown that extrasynaptic NMDAR contribute to the excitation of MNC during dehydration (Joe et al., 2014). Additional studies are required to define the mechanisms responsible for the persistent activation of clustering after OVLT stimulation in MNC.

3.3.2. SK channel activity and neurotensin receptor activation both modulate clustered firing

NMDAR-mediated rhythmic clustering activity has been shown to depend on apamin-sensitive (SK type) calcium-dependent K^+ channels (Hu and Bourque, 1992) which play an important role in

controlling burst duration by promoting an activity-dependent after-hyperpolarization (Bourque and Brown, 1987). Indeed bath application of a saturating concentration of apamin completely suppressed NMDAR-induced clustering and caused the cells to fire tonically. Interestingly, a partial inhibition of SK channels (~25%) with 4 nM apamin caused a significant decrease in the rate of spike clustering and an increase in cluster duration. These results show that even partial modulation of SK channels could provide an effective mechanism for the regulation, or fine tuning, of spike clustering in MNC. Previous studies have shown that receptor-dependent modulation of SK channels can be achieved through membrane trafficking (Faber, 2009) or phosphorylation (Adelman et al., 2012).

To determine if NMDAR-dependent spike clustering can be modulated by the activation of other receptors we investigated the effect of the tridecapeptide NT, which has been reported to inhibit the SK channel-mediated after-hyperpolarization and to depolarize MNC in the SON (Kirkpatrick and Bourque, 1995; Chakfe and Bourque, 2000). Although the SON was found to express both NTS1 and NTS2 receptors, single cell RT-PCR analysis showed that MNC preferentially express the NTS2 receptor. Bath application of NT^{8-13}, which activates NTS2 (Vincent et al., 1999) significantly increased cluster duration and reduced the overall rate of spike clustering in MNC. These effects were abolished by SR46892, an antagonist of both NTS1 and NTS2 receptors (Pelaprat, 2006) and could not be induced by the inactive agonist NT^{1-7}. Interestingly the effects of NT^{8-13} on the rate of clustering were eliminated when cell voltage was restored to control value (Fig. 3.2.4.F), suggesting that this effect depends mainly on the peptide's depolarizing effect. However, NT^{8-13} significantly prolonged cluster duration and increased the total number of action potentials recorded per test segment, even when voltage was maintained at an equivalent level in the absence and presence of the peptide (Fig. 3.2.4.F). Thus the effects of NT^{8-13} on these parameters may involve additional actions, such as the regulation of other conductances. The mechanisms by which NT^{8-13} modulate these parameters remains to be determined.

3.3.3. Neurotensin receptor activation does not directly inhibit SK channels in SON slices

Despite the fact that previous findings have shown that NT inhibits the AHP amplitude in MNC when performing intracellular recordings in hypothalamic explants (Kirkpatrick and Bourque, 1995), our results show that application of this drug does not affect the AHP amplitude when performing whole cell patch-clamp recordings in SON slices (Fig. 3.2.5.B) nor the AHP amplitude when using the perforated patch technique (Fig. 3.2.5.B), to avoid any interruption in NT downstream signaling. Such divergent data are difficult to interpret and will need further investigation. It might be possible that other conductances get activated following NT signaling, thus increasing the rate of clustering activity observed from -70 to -67.5 mV (Fig. 3.2.5.A). However, this increase on the rate of clustering activity is unlikely to rely on the inhibition of SK channels via NT signaling since application of apamin had no effect on the rate of clustering between -70 mV and – 67.5 mV (see Fig. 3.2.3.D). Additionally, even if the synaptic connections between the SON and the OVLT are preserved in the horizontal hypothalamic slice used in our experiments (Trudel and Bourque, 2003), the fact that the integrity of the synaptic network is largely preserved in the superfused explant preparation might account in the discrepancy observed between our data and what was previously shown. Indeed, we cannot exclude the possibility that additional synaptic connections containing NT receptors somehow participate in the decrease of the AHP amplitude in the explant preparation, whereas it might not be the case for the horizontal slice.

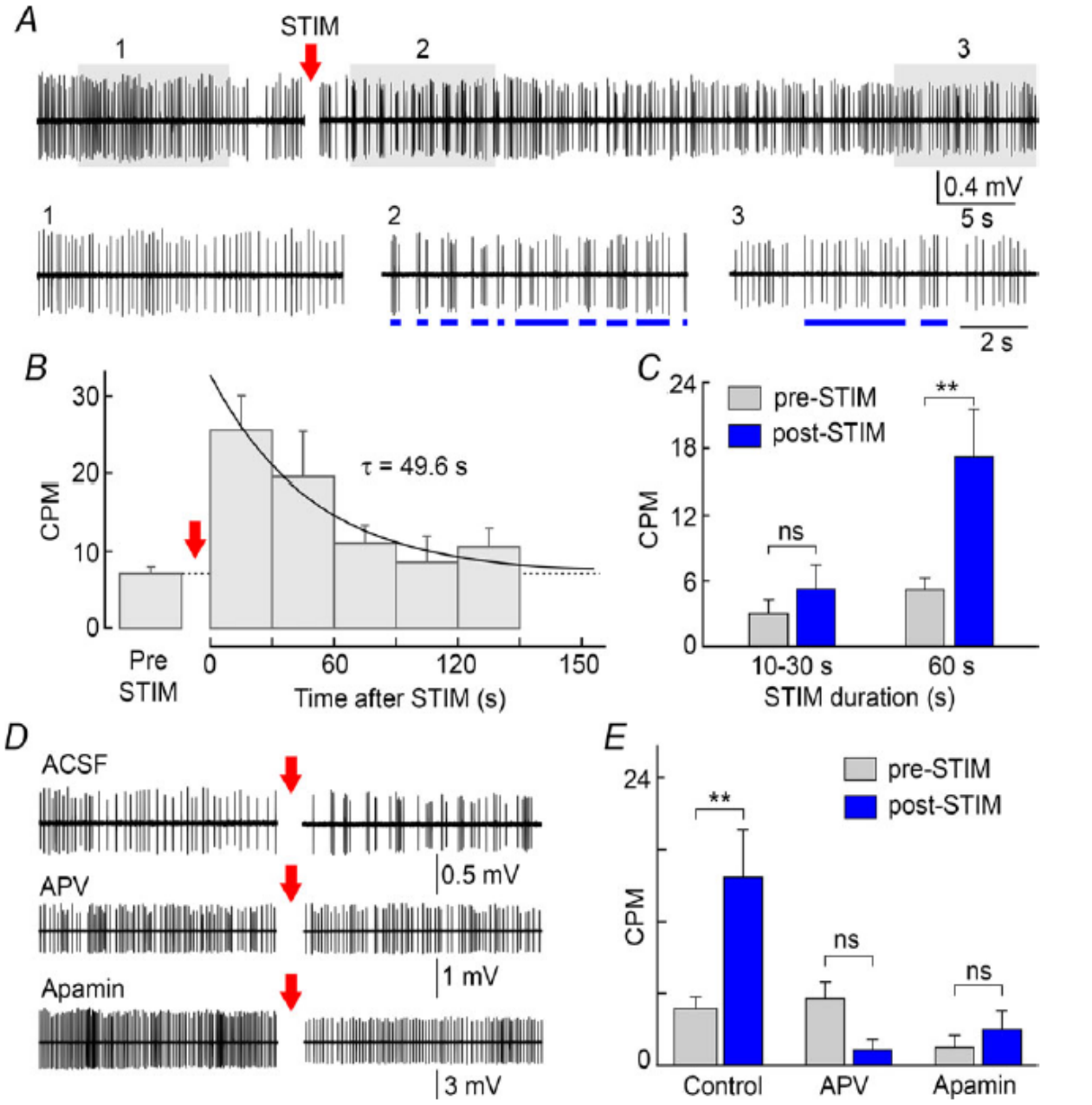

Figure 3.2.1. OVLT stimulation induces spike clustering in MNC

A, single unit spiking activity recorded from a SON MNC in a hypothalamic explant shows the effect of OVLT stimulation at 10 Hz (STIM) for 60 s (segment removed). Lower traces are segments expanded from the shaded parts of the main trace. STIM caused a reversible increase in spike clusters (blue lines). **B**, graph shows mean (± SEM) rate of clustering (clusters per minute, CPM) before (pre-STIM; dashed line) and during 5 consecutive 30 s segments after STIM (post-STIM). Continuous line is a mono-exponential fit. **C**, bar graphs show mean (± SEM) CPM pre-STIM and during the first 20 s post-STIM observed when STIM was applied for 10–30 s or 60 s. **D**, spiking activity recorded from MNC before and after STIM in control conditions (ACSF), or in the presence of APV or apamin. **E**, bar graphs show mean CPM observed pre- and post-STIM in different conditions.**P < 0.01; ns, not significant. (Gagnon et al., 2014; *Journal of Physiology*)

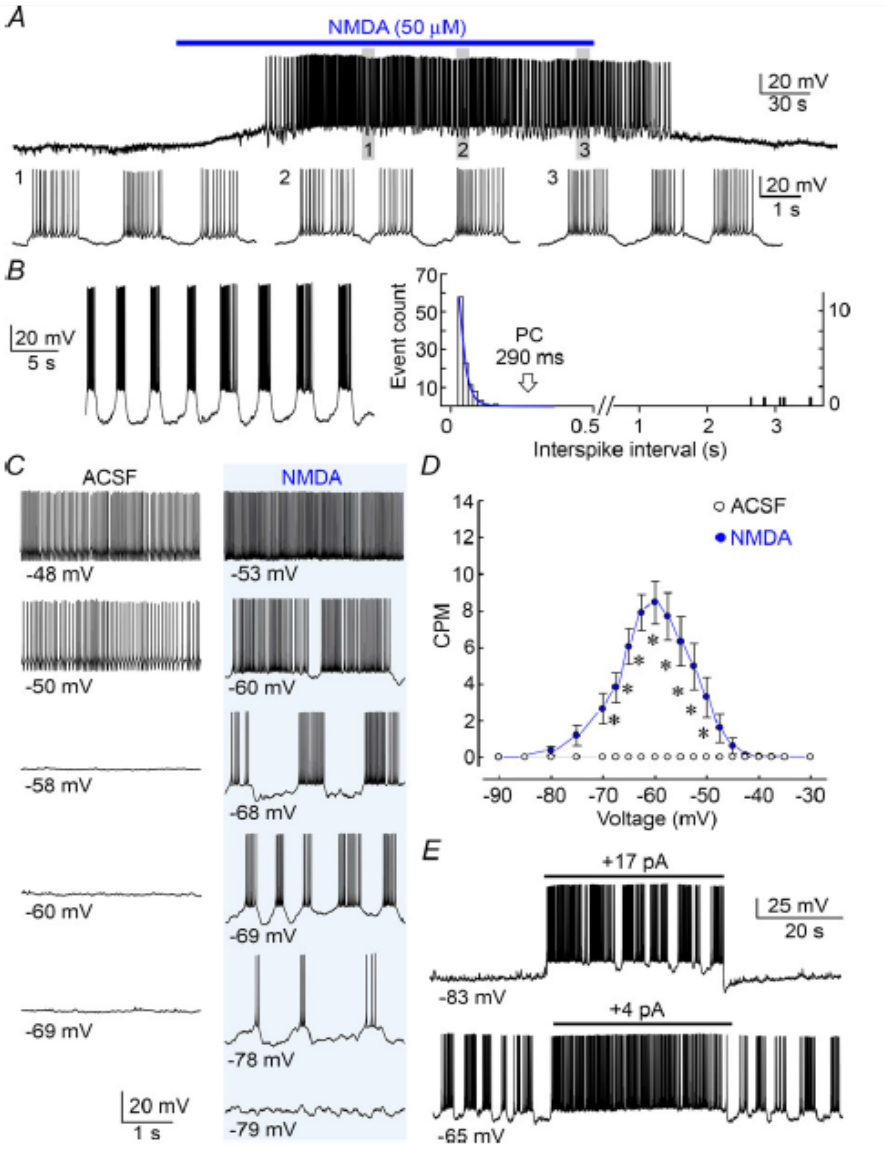

Figure 3.2.2. Voltage dependence of NMDA receptors-induced clustering

A, upper trace shows a whole-cell voltage recording from a MNC in a hypothalamic slice (excerpts shown below). Bath application of NMDA (bar) caused a reversible depolarization and sustained clustering activity. **B**, left trace shows an example of NMDA-induced clustering in another MNC. The histogram at right plots the distribution of interspike intervals for the corresponding cell. The blue curve is a single exponential fit of the falling phase of the distribution. The arrow points to the pause criterion (PC), beyond which intervals of greater duration are defined as pauses (see Methods). **C**, recording segments from a single MNC illustrate the relation between voltage (average of all points, indicated below) and firing pattern in absence (ACSF) or presence of NMDA. Each trace was recorded with different levels of holding current (not shown). **D**, graph shows mean (±SEM) clustering rate at different voltages in ACSF and NMDA (∗P < 0.05). **E**, traces from MNC exposed to NMDA show the effects of depolarizing current pulses (bars) applied from different baseline voltages. (Gagnon et al., 2014; *Journal of Physiology*)

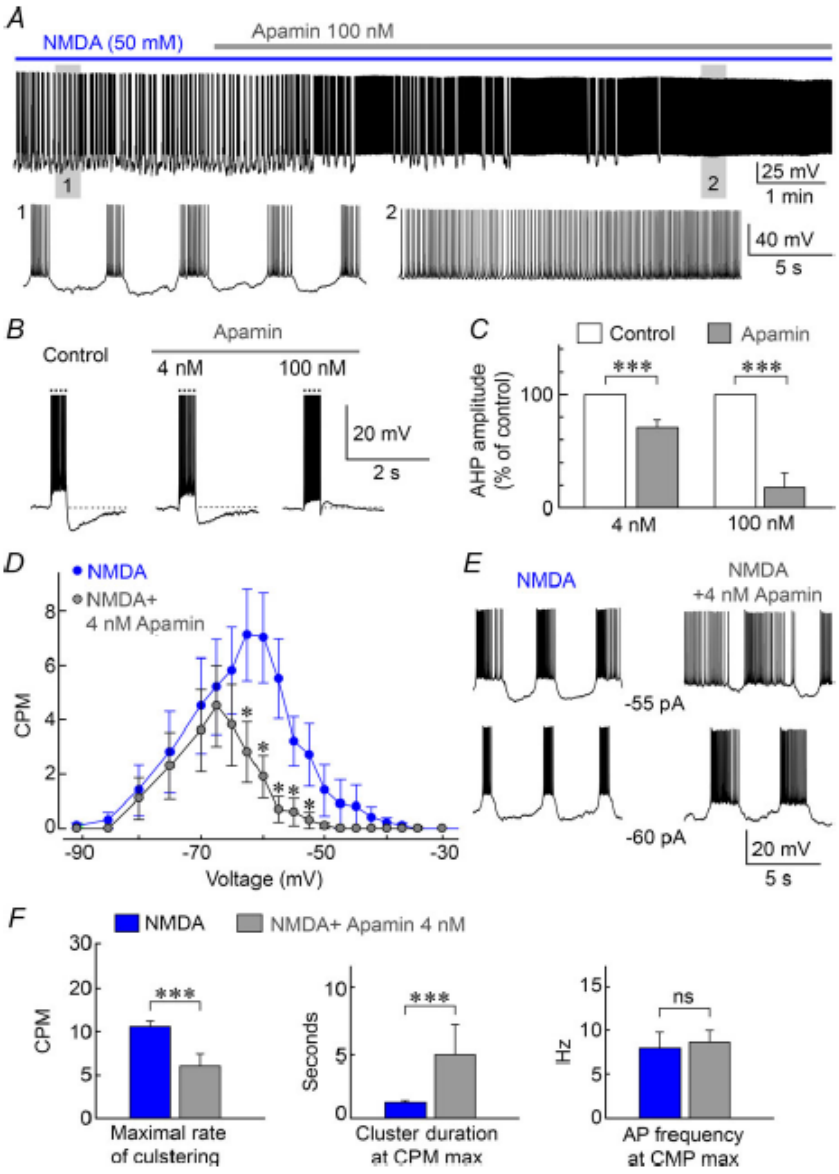

Figure 3.2.3. Inhibiting SK channels modulates spike clustering

A, voltage recording shows the effect of 100 nM apamin (grey bar) on NMDA-induced clustering (blue bar). Lower panels show excerpts of the full trace (as indicated by numbers). **B**, traces show the effects of apamin on after-hyperpolarizations (AHPs) induced by spike trains triggered by depolarizing current pulses (dotted lines). **C**, bar graphs show the effects of 4 nM and 100 nM apamin on mean (±SEM) AHP amplitude expressed as percentage of control. **D**, graph shows the effect of 4 nM apamin on mean (±SEM) clustering rate observed at different voltages. **E**, traces show the effects of apamin on NMDA-induced clustering activity at fixed levels of current injection (shown). **F**, bar graphs show the effects of 4 nM apamin on mean (±SEM) maximal clustering rate (CPM max), as well as cluster duration and intracluster spiking frequency at CPM max. $*P < 0.05$; $***P < 0.005$; ns, not significant. (Gagnon et al., 2014; *Journal of Physiology*)

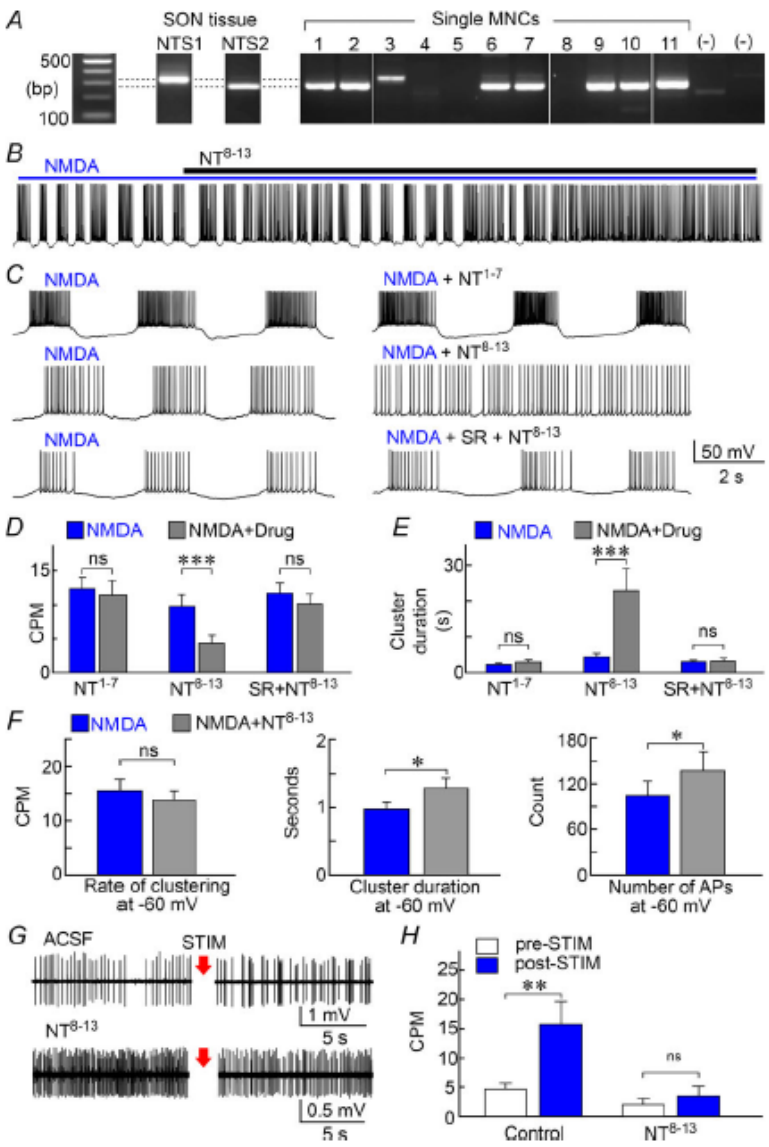

Figure 3.2.4. NT receptors modulate NMDA receptor-dependent clustering in MNC

A, PCR detection of mRNA coding for NTS1 and NTS2 in SON tissue, and in 11 single MNC ((–) lanes are controls). **B**, whole-cell recording from a MNC exposed to NMDA shows that addition of $NT^{8–13}$ inhibits clustering. **C**, excerpts taken from 3 cells show NMDA-induced activity recorded before (left) and after (right) addition of $NT^{1–7}$, $NT^{8–13}$ or $NT^{8–13}$+SR46892 (SR). **D** and **E**, bar graphs show the mean (±SEM) rate of clustering **(D)** and cluster duration **(E)** observed in the presence of NMDA alone (blue) or in the presence of NMDA and various drugs (grey bars, drugs indicated below each set). **F**, bar graphs show mean (±SEM) values of clustering rate, cluster duration and total number of action potentials (count) in the absence (blue) and presence of $NT^{8–13}$ (grey) in cells whose voltage was adjusted to a value of −60 mV for both conditions. **G**, single unit recordings from MNC in hypothalamic explants show the effects of stimulating the OVLT for 60 s at 10 Hz (STIM; arrows) in the absence (ACSF) and presence of $NT^{8–13}$. **H**, bar graphs show the effect $NT^{8–13}$ on mean (±SEM) rates of clustering induced by OVLT stimulation. $*P < 0.05$; $**P < 0.01$; $***P < 0.005$; ns, not significant. (Gagnon et al., 2014; *Journal of Physiology*)

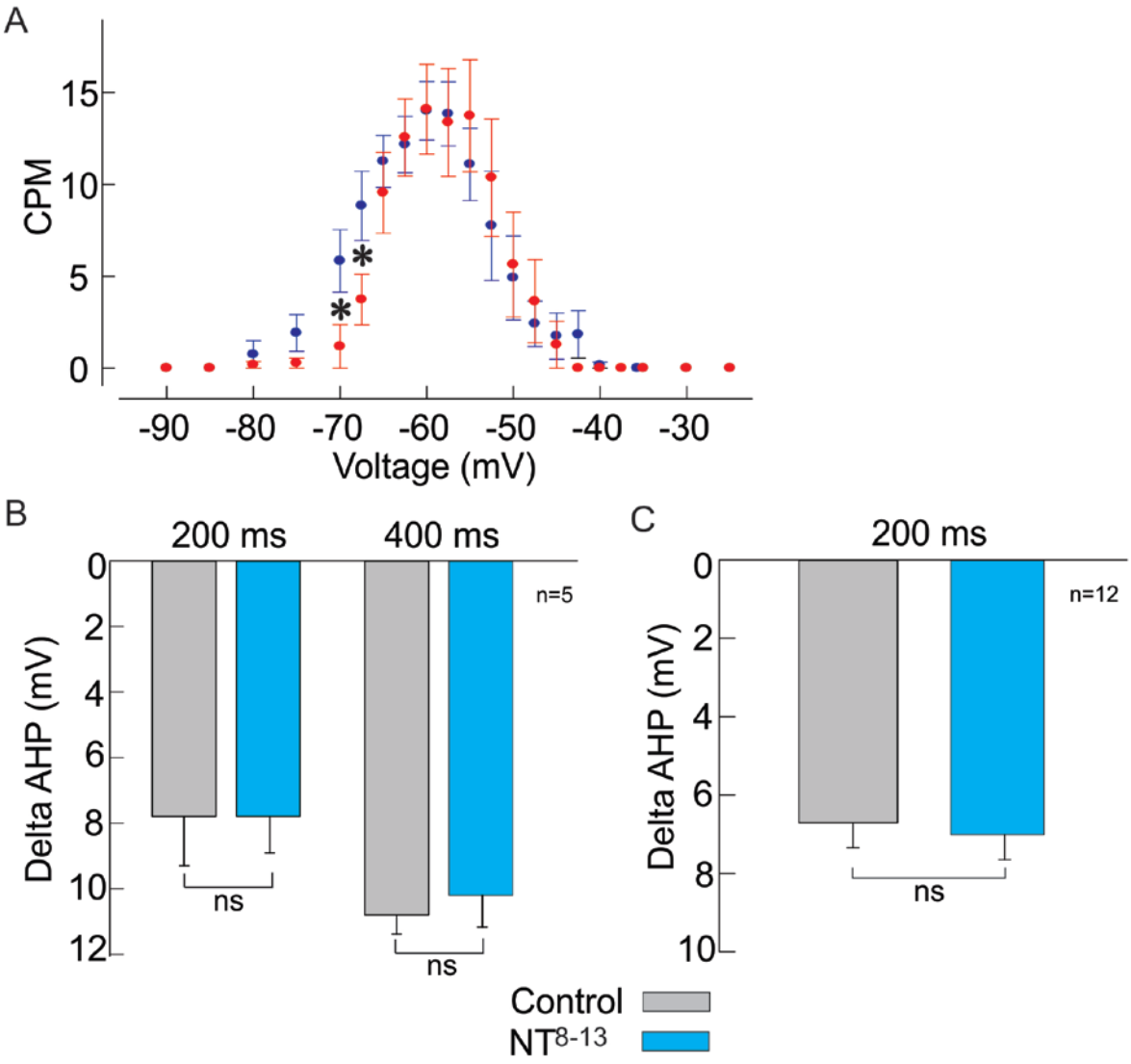

Figure 3.2.5. Neurotensin does not inhibit SK channels in MNC

A, Staircase protocol investigating the impact of 50 μM NMDA (red) and NMDA + 0.3-3 μM NT^{8-13} (blue) on the NMDA-induced CPM rate at various membrane voltages (∗a significant difference in CPM activity was only observed from -70 mV to -67.5 mV). **B**, The AHP amplitude (delta) measured following the induction of a depolarizing pulse (lasting 200 or 400 ms) was not altered in the presence of NT^{8-13} (3 μM) when performing whole-cell patch clamp recordings. **C**, The AHP amplitude (delta) was also not reduced after the application of NT^{8-13} (3μM) when performing gramicidin perforated patch-clamp recordings in MNC, to avoid any dialysis effect. ∗$P < 0.05$; ns, not significant.

IV: SOMATO-DENDRITIC RELEASE IS REGULATED IN

A SPIKE- AND FREQUENCY-DEPENDENT MANNER TO IBHIBIT GLUTAMATERGIC NEUROTRANSMISSION

In *Chapter III*, we saw that endogenous glutamate release, following stimulation of the OVLT induced clustered firing in MNC, and that this fast rhytmic oscillation is modulated by neurotensin and SK3 channels. The present chapter will investigate whether activity-dependent somato-dendritic release of retrograde messengers inhibits excitatory transmission in a pattern- (*Hypothesis three*, see section 1.5.7) and frequency-dependent manner (*Hypothesis four,* see section 1.5.8).

4.1. Overview

Previous studies have extensively examined the effects of the pattern- and frequency-dependent facilitation of peptide release by the axon terminals of MNC at the level of the neurohypophysis (see section 1.3.3). Those studies showed that higher frequencies of stimulation enhance neurosecretion from the neural lobe (Dreifuss et al., 1971). Moreover, certain patterns of electrical activity were shown to be more effective at eliciting peptide release from the neurohypophysis. More precisely, electrical stimulation protocols mimicking a phasic or a clustering activity were shown to elicit more VP release at the nerve terminal compared to a tonic stimulation, even when the mean firing frequency and the total number of action potentials were kept constant. Additionally, administration of a pattern of electrical activity mimicking a lactation burst, derived from *in vivo* templates, was shown to be more potent at triggering OT secretion, compared to a continuous stimulation (see section 1.3.3). As elaborated in section 1.5.1, messengers can be released from the somato-dendritic compartment of SON neurons, sometimes independently from the release process at the level of the neurohypophysis (see section 1.5.5). Therefore, an important question arising is whether a frequency- and pattern-dependent facilitation of release, such as seen in the neural lobe, is also observed at the level of the somato-dendritic compartment.

Intranuclear release of OT and VP has been shown to play important physiological roles *in vivo*. For example, it was shown that OT release within the SON of lactating female rats, measured via a push-pull cannula *in vivo*, increases during the milk ejection reflex (Moos et al., 1989) and that administration of an OT antagonist within the SON or the PVN during suckling by the pups decreased the burst amplitude and the firing rate of OT cells, within the injected nucleus (Lambert et al., 1993). These findings suggest that activation of OT receptors on the soma and dendrites of PVN neurons can alter the milk ejection reflex. Regarding the VP-containing neurons, it was observed that application of this peptide *in vivo* within the SON decreases the firing rate of fast firing cells, maintains the firing activity of moderately active cells and enhances the electrical activity of slow firing neurons (see section 1.5.5.2 for intranuclear release from VP cells).

About two decades ago, several groups started to investigate the impact of retrograde messengers, released from the somato-dendritic compartment of MNC, onto excitatory and inhibitory neurotransmission (see sections 1.5.6, 1.5.6.1 and 1.5.6.2). Indeed, modulating transmitter release by presynaptic afferents, via somato-dendritic release, is an efficient way to control the synaptic input of MNC and hence, to regulate the secretion of OT and VP into the bloodstream. Importantly, investigating how excitatory neurotransmission is inhibited by the release of retrograde messengers from the soma and dendrites of SON neurons is critical to understand how these neurons auto-regulate their electrical activity and hence, their hormone output from the nerve terminal. Previous studies have shown that electrical stimulation of SON cells leads to an inhibition of excitatory transmission via the release of retrograde messengers. More specifically, it was observed that VP neurons mediate this presynaptic inhibition by releasing endocannabinoids and dynorphin, while OT cells mediate this effect via the release of OT and endocannabinoids (Hirasawa et al., 2004; Iremonger et al., 2011).

Based on these previous findings, the first aim of this chapter will be to investigate if presynaptic glutamate release is inhibited in a frequency- and pattern-dependent manner via the release of

messengers from the somato-dendritic compartment. The second aim will be to elucidate which retrograde messengers are involved in this suppression of excitatory neurotransmission following the induction of action potentials in the physiological-relevant range in identified OT and VP cells (see *Method*s, section 2.1.1 and 2.2.2.), to assess without ambiguity the cell phenotype that corresponds to the release of these retrograde messengers.

4.2. Results

4.2.1. Frequency-dependent inhibition of glutamatergic transmission via somato-dendritic release

It was previously shown that higher frequencies of stimulation enhance neurosecretion from the neurohypophysis (Dreifuss et al., 1971), but if such frequency-dependent facilitation mechanism is present at the level of the somato-dendritic compartment is not known. To answer this question, we elicited action potentials at frequencies between 0.1 Hz and 50 Hz in identified OT-mRFP1 (red) and VP-eGFP (green) neurons (Fig. 4.2 and 4.2.1.A). The variation in the strength of excitatory afferents was measured via changes of the evoked EPSC (eEPSC) charge transfer (ΔQ; pC) in OT and VP neurons. The amount of charge transfer, rather than the eEPSC peak amplitude, was analyzed to integrate asynchronous events considering that they participate in the evoked response since glutamate quanta were shown to fuse up for tens of milliseconds in MNC following the termination of presynaptic stimulation (Iremonger and Bains, 2007). To evoke an EPSC, the OVLT was stimulated at a frequency of 0.2 Hz and bicuculine (5 μM) was included in the ACSF to block IPSC. Values were corrected for time-dependent loss of short-term facilitation as explained in the sections *Methods* (2.4.2.2) and *Discussion* (6.2).

As illustrated in Figure 4.2.1.B and C, induction of a spike train (10 Hz, 100 action potentials) in either OT or VP neurons caused a decrease of the eEPSC. The eEPSC charge transfer was assessed during a control period prior to the postsynaptic cell conditioning and the charge transfer, which decreased

following a 10 Hz stimulation in OT and VP neurons, recovered to baseline values after ~30 seconds with no difference between both cell types (OT τ = 28.06 ± 6.34 s., n = 8; VP τ = 32.44 ± 7.43 s., n = 7; *t* test; P = 0.658; Fig. 4.2.1.B). Therefore postsynaptic firing of 100 spikes at 10Hz can cause a transient inhibition of the eEPSC in both VP and OT MNC.

To determine if postsynaptic firing can inhibit the eEPSC in a frequency-dependent manner, we examined the effects of applying a train of 100 action potentials (from 0.1-50 Hz) in both cell types. Importantly, OT and VP neurons showed a frequency-dependent inhibition of the eEPSC charge transfer (Fig. 4.2.1.D). An exponential function was fitted to the data obtained. More specifically, lower frequencies of discharge led to a reduction of the eEPSC close to 0%, whereas higher frequencies of stimulation (i.e. $\geq$ 30 Hz) reached a maximum degree of inhibition of ~40%. Interestingly, a significant difference was found in the % of inhibition of the eEPSC charge transfer between OT and VP cells at 0.5 Hz (OT n = 13, VP n = 18; *t* tes*t*; P = 0.009; Fig. 4.2.1.D) and at 1 Hz (OT n = 16, VP n = 21; *t* test; P = 0.004; Fig. 4.2.1.D), suggesting that OT neurons are more effective at inhibiting excitatory transmission during lower frequencies of discharge. To make sure that no changes in series resistance occurred during our recordings, which could lead to the false assumption that the eEPSC amplitude was reduced if the patch pipette was blocked, the decay constant of the first EPSC was calculated by fitting an exponential function. No differences were found in the decay constant before and after the spike train conditioning for both OT cells (n = 14; paired *t* test; P = 0.839; Fig. 4.2.3.C) and VP cells (n = 10; paired *t* test; P = 0.133; Fig. 4.2.3.D), suggesting a stable series resistance was maintained during our recordings. Therefore, the results reported above are the first to demonstrate that both cell types mediate a frequency-dependent inhibition of excitatory neurotransmission, presumably via somato-dendritic release of retrograde messengers.

4.2.2. Pattern-dependent inhibition of glutamate release via somato-dendritic release

In *Chapter III*, we showed that clustering activity can be induced by activation of NMDA receptors via endogenous glutamate release. Moreover, a previous study has shown that stimulating the neurohypophysis with a clustering pattern elicited more VP release compared to a tonic stimulation (Cazalis et al., 1985). We therefore hypothesized that a clustered firing exerts a stronger inhibitory impact on glutamatergic transmission compared to a tonic firing. To test this hypothesis, we examined the effect of applying conditioning trains featuring both types of postsynaptic activity on EPSC evoked by OVLT stimulation at 0.2 Hz. Both types of stimulation contained 100 action potentials, displayed a mean frequency of 10 Hz and were repeated twice in OT and VP neurons (Fig. 4.2.2.A). Our results show that stimulating OT cells with the clustered pattern was no more effective than a tonic stimulation at inhibiting the eEPSC (Tonic = 28.37 ± 3.9% $_{inhibition}$; Clustering = 29.7 ± 4.3% $_{inhibition}$; n = 15; paired *t* test; P = 0.787; Fig. 4.2.2.B and D). However, stimulating VP neurons with a clustering phenotype significantly enhanced the activity-dependent inhibition of the eEPSC (Tonic = 39.74 ± 4.02% $_{inhibition}$; Clustering = 52.32 ± 4.09% $_{inhibition}$; n = 13; paired *t* test; P = 0.001; Fig. 4.2.2.C and E). Taken together, these results suggest that a clustering activity differently regulates somato-dendritic release from OT and VP neurons, the later cell type being more effective at inhibiting glutamatergic neurotransmission via a rhythmic clustered firing.

4.2.3. Locus of inhibition involved in the suppression of glutamate release

To investigate the locus of inhibition of the pattern- and frequency- dependent inhibition in MNC, we first investigated if a mild postsynaptic conditioning protocol (10 Hz, 100 action potentials) caused a reduction in the amplitude of asynchronous events, since every asynchronous event recorded in the postsynaptic cell reflects the impact of a single quantum of glutamate (Iremonger and Bains, 2007). More precisely, if a change in the amplitude of asynchronous events was observed following the

induction of our mild postsynaptic protocol, this would indicate modifications in postsynaptic receptor density/function and hence, a postsynaptic locus of inhibition. As illustrated in Figure 4.2.3.A and B, inducing a conditioning spike train did not significantly affect the amplitude of asynchronous events in either OT neurons (control = 34.71 ± 1.64 pA; post = 31.21 ± 1.71 pA; n = 15; paired *t* test; P = 0.064) and VP neurons (control = 21.8 ± 1.68 pA; post = 21.78 ± 2.54 pA; n = 13; paired *t* test; P = 0.992), suggesting no change on the postsynaptic cell responsiveness for both cell types.

To determine if the release of retrograde messengers suppresses excitatory synaptic transmission via a presynaptic locus of action, the PPR, which is inversely correlated to the probability of release, was assessed following the same spike conditioning in both cell types. In most cases, presynaptic inhibition of neurotransmitter release is mediated by a reduction in the efficacy of calcium influx through voltage-gated calcium channels (Fossier et al., 1999). When this presynaptic inhibition takes place, eliciting a second presynaptic impulse, ~40-50 milliseconds after the first one, leads to a temporal summation of presynaptic intra-terminal calcium, which facilitates the amount of transmitter release induced by this second pulse (Zucker, 1999). Calcium-dependent presynaptic inhibition of transmitter release is therefore associated with this increase in PPR (EPSC2/EPSC1). In agreement with this principle, a significant increase in PPR, measured as the averaged percent change compared to control, was observed in OT neurons ($PPR_{\%\ control}$ = 100 ± 0%; $PPR_{post\ (\%\ control)}$ = 105.81 ± 2.79%; n = 24; paired *t* test; P = 0.049; Fig. 4.2.3.E) as well as in VP cells ($PPR_{\%\ control}$ = 100 ± 0%; $PPR_{post\ (\%\ control)}$ = 104.67 ± 1.94%; n = 41; paired *t* test; P = 0.021; Fig. 4.2.3.F).

Together, these results suggest that inducing a conditioning spike train in OT and VP neurons caused a suppression of glutamate release via a presynaptic locus of action. However, a high proportion of OT cells (29%) and VP cells (24%) showed no increase in PPR despite the fact that most of these cells displayed a pronounced inhibition of the eEPSC amplitude (i.e. > 30% inhibition). This observation suggests the possibility of a presynaptic silencing mechanism following the induction of our mild

postsynaptic protocol. If the inhibition of excitatory afferents following the postsynaptic spiking protocol in OT and VP cells is partly due to a presynaptic silencing, this observation would suggest that the inhibition of excitatory synapses does not only involve a graded reduction in voltage-gated calcium influx, but also an all-or-nothing suppression of calcium-mediated transmitter release at a subset of the synapses. A similar presynaptic silencing mechanism has been shown to occur at the OVLT-MNC synapse (Trudel and Bourque, 2012) and has also been described in other brain regions (Tully et al., 2007) where a proportion of the nerve endings simply stop releasing glutamate, while some of the nerve terminals maintain a normal probability of release. Taken together, these results indicate a presynaptic locus of inhibition following the induction of our mild postsynaptic protocol, in both cell types.

4.2.4. Discovering the identity of retrograde messengers released from OT and VP neurons

Previous studies have shown that the inhibition of excitatory afferents, following intense spiking activity in MNC, is mediated by the release of OT and EC for OT neurons (Hirasawa et al., 2004), and via the release of EC and DYN in VP neurons (Iremonger et al., 2011). To investigate which messengers are involved in the suppression of glutamatergic neurotransmission when using the milder stimulation protocol described earlier (10 Hz, 100 spikes), we first looked at the contribution of different messengers secreted from OT and VP cells. Surprisingly, we found that blocking OT receptors with Manning compound (MC; 10 μM) did not significantly reduce the inhibitory effect of the conditioning train on eEPSC in OT neurons (Control = 24.31 ± 4.03%; MC = 23.78 ± 5.95%; n = 7; paired *t* test; P = 0.945; Fig. 4.2.4.A). Blocking V1a receptor with SR49059 (10 μM) in VP cells had also no effect on the eEPSC amplitude (Control = 42.8 ± 7.76%; SR49059 = 39.09 ± 10.37%; n = 8; paired *t* test; P = 0.683; Fig. 4.2.4.A). Thus the release of OT and VP does not appear to mediate the retrograde inhibition of glutamate release in response to mild postsynaptic activity.

Because previous studies have shown that EC can mediate the suppression of excitatory neurotransmission for both cell types in response to intense postsynaptic spike trains (Hirasawa et al., 2004; Iremonger et al., 2011), we next investigated if these compounds contribute to the suppression of glutamate release by blocking CB1 receptors with AM251 (5 μM). We found that blocking CB1 receptors significantly reduced the inhibitory effect of the conditioning train on eEPSC in both OT cells (Control = 43.39 ± 8.91%; AM251 = 7.86 ± 3.9%; n = 8; paired *t* test; P = 0.022; Fig. 4.2.4.B) and VP cells (Control = 34.51 ± 7.94%; AM251 = 7.71 ± 2.98%; n = 8; paired *t* test; P = 0.038; Fig. 4.2.4.B), suggesting that EC play a role in the suppression of excitatory transmission. 2-Arachidonoylglycerol (2-AG) and anandamide are the two best studied EC so far in the central nervous system (Hu et al., 2014). When the postsynaptic cell is depolarized, intracellular calcium levels rise and activate phospholipase C beta (PLCβ), which in turn leads to the production of diacylglycerol (DAG) that will be hydrolyzed via diacylglycerol lipase (DAGL) to generate 2-AG (Ohno-Shosaku and Kano, 2014). To investigate if DAGL activity is involved in the inhibition of glutamatergic transmission, we introduced tetrahydrolipstatin (THL, 5 μM), a DAGL α/β inhibitor, in the recording electrode. Interestingly, we found that the inhibition of the eEPSC caused by postsynaptic spiking was prevented in OT neurons (Control = 28.29 ± 5.9%; n = 15, THL = 13.82 ± 5.2%; n = 15; *t* test; P = 0.038; Fig. 4.2.4C), whereas this drug had no significant effect on VP cells (Control = 30.5 ± 4.74%; n = 12, THL = 29.82 ± 4.62%; n = 11; *t* test; P = 0.819; Fig. 4.2.4C). These findings suggest that intracellular DAGL activity is required for retrograde inhibition to occur in OT neurons, likely as a result of its ability to synthesize 2-AG. It is most likely that the DAG production was activated via rises in intracellular calcium concentration, following the conditioning spike train since, since DAG was shown to be generated via depolarization-induced calcium entry (Hu et al., 2014; Ohno-Shosaku and Kano, 2014). However our results also suggest that EC release from VP cells might not require the DAGL activity to produce EC.

Because it was previously shown that VP cells release dynorphin (DYN) and that this opioid peptide can lead to a long term depression of excitatory afferents upon specific conditions (Iremonger and Bains, 2009), we lastly examined if kappa (κ)-opioid receptors might be playing a role in the suppression of glutamatergic neurotransmission following our mild postsynaptic conditioning protocol (i.e. 10 Hz, 100 spikes). Interestingly, despite the fact that OT cells do not synthesize DYN while it is the case for VP-releasing neurons (Brown et al., 2000), we found that blockade of κ-opioid receptors with nor- Binaltorphimine (nor-BNI, 1 μM) led to a reduction in the percent of inhibition of the eEPSC in both OT neurons (Control = 53.76 ± 6.58%, nor-BNI = 7.51 ± 4.37%; n = 8; paired *t* test; P = 0.0003; Fig. 4.2.4.D) and VP neurons (Control = 49.83 ± 7.7%, nor-BNI = 29.71 ± 8.11%; n = 10; paired *t* test; P = 0.045; Fig. 4.2.4.D). This latter finding suggests that κ-opioid receptors are involved in the suppression of excitatory afferents following our mild stimulation protocol, in both cell types.

4.3. Discussion

4.3.1. Somato-dendritic release inhibits glutamatergic transmission in a frequency- and pattern-dependent manner

In this chapter, we demonstrated for the first time that release at the level of the soma and dendrites, measured via an inhibition of presynaptic glutamate release (i.e. the presynaptic locus of action is described in the next section), is regulated in a frequency- and pattern- dependent manner in both OT and VP neurons. As shown in Figure 4.2.1.D, lower frequencies of discharge were less effective at inhibiting glutamate release, whereas a higher degree of inhibition was observed at higher frequencies of discharge.

Our results show that following the induction of the conditioning spike trains, EC are involved in the suppression of glutamate release as well as the opioid DYN (see sections 4.3.3 and 4.3.4). Another interesting result observed in our study is the fact that inhibition of glutamate release following

induction of spike trains in OT cells was also present at low frequencies (i.e. from 0.5-1 Hz; $P < 0.05$; Fig. 4.2.1.D), while this was not the case when stimulating VP neurons at the same firing frequencies. However, whether the identity or the amount of retrograde messengers released from the somato-dendritic compartment is differently regulated in both cell types at lower frequencies of discharge will need additional investigations.

A previous study has shown that stimulating the neurohypophysis with a pattern of clustered firing elicited more VP release from the neural lobe, compared to a tonic stimulation (Cazalis et al., 1985). Analogously, we stimulated identified MNC with a clustering and a tonic pattern of electrical activity to investigate if these stimulations differentially regulated somato-dendritic release. Our results showed that stimulating VP cells with a clustering phenotype of electrical activity enhanced the percent of inhibition of glutamate release, whereas stimulating OT cells with a clustered firing suppressed excitatory transmission to the same extent as a tonic firing (Fig 4.2.2.D and E).

However, how the induction of a clustering pattern of activity, in VP neurons, did suppress more effectively glutamate release, compared to a tonic stimulation, remains to be determined. Despite the fact that both protocols (i.e. clustering and tonic) contained 100 spikes and a mean frequency of 10 Hz, the intra-cluster frequency during the induction of the clustering protocol reached 25 Hz, so it is thus possible that different retrograde messengers were recruited compared to those that might be release from a 10 Hz stimulation (i.e. during the tonic pattern), since intense postsynaptic spiking protocols were shown to recruit additional messengers than those reported in our study (Hirasawa et al., 2004). Therefore, whether VP participated in the suppression of glutamate release during the clustering stimulation remains ambiguous since blockade of VP receptors was not shown to play a role in the suppression of excitatory afferents (i.e. when stimulating VP cells at 10 Hz, 100 spikes), whereas the release of EC is required for both cell types when using the same stimulation protocol (see section 4.2.4). Moreover, it might be possible that a higher amount of EC was released from VP neuron during the

induction of the clustering pattern, due to a higher rise in calcium via VGCC, compared to the tonic stimulation. It is also surprising that the induction of a clustering pattern of electrical activity in OT neurons does not elicit more inhibition of glutamate release compared to a tonic stimulation, considering that lactation bursts, which last ~2-4 seconds and display a mean frequency of ~24-80 Hz (Wakerley and Lincoln, 1973), enhance somato-dendritic OT release within the SON (Moos et al., 1989). However, the results reported in section 4.2.4 showed that OT is not involved in the suppression of excitatory neurotransmission when stimulating this cell type at a frequency of 10 Hz. This finding suggests that the OT peptide is not recruited following the induction of a tonic pattern of discharge and is also probably not released from OT neurons following a clustering activity, considering that both conditions led to the same degree of inhibition. In summary, our results are the first to show that a clustering and a tonic activity differentially regulate the release of retrograde messengers from the soma and dendrites of VP neurons.

4.3.2. Presynaptic locus of inhibition for OT and VP neurons

Previous studies have shown that stimulating OT and VP cells leads to an inhibition of glutamatergic afferents measured via an increase in PPR, a decrease in the frequency of asynchronous events (Hirasawa et al., 2004; Iremonger and Bains, 2009) or a decrease in the coefficient of variation ($1/CV^2$) (Iremonger et al., 2011). Our results show that stimulating both OT and VP neurons at 10 Hz, with 100 spikes, led to a decrease of the eEPSC, while no change in the amplitude of asynchronous events was observed (Fig. 4.2.3.A and B). The later result suggests that no change occurred in the functionality or in the density (i.e. insertion/removal) of postsynaptic AMPA receptors following the stimulation protocol. Additionally, our results showed that stimulating OT and VP neurons at 10 Hz, with 100 action potentials, led to an increase in PPR. This finding indicates that the average probability of glutamate release was lowered following our stimulation protocol in these cells. However, 7 of 24 OT neurons (29%) as well as 10 of 41 VP neurons (24%) did not display any increase in the PPR despite a

substantial reduction of the eEPSC, following the induction of a 10 Hz postsynaptic spike train. This observation suggests that EC-mediated inhibition of excitatory transmission may also involve a presynaptic silencing mechanism.

Presynaptic silencing has been observed to occur in a number of regions. For example, this mechanism has been observed at the central amygdala (CeA) (Tully et al., 2007). More precisely, large EPSC are produced in the CeA upon glutamate release from parabrachial (PB) afferents that convey nociceptive information. During time of stress, noradrenaline is released via noradrenergic fibers onto the CeA and thus, decreases the EPSC amplitude recorded in the CeA region, presumably to suppress pain under high stress. Importantly, upon stimulation of the PB-CeA synapse, the PPR remained unchanged when noradrenaline was exogenously applied, suggesting that this effect was associated with a decrease in the number of sites of synaptic transmission without changes in the probability of release (Pr). Moreover, this decrease of the eEPSC amplitude relied on a presynaptic locus of inhibition rather than a postsynaptic one, since the quantal amplitude was not decreased by noradrenaline. This observation suggests that the inhibition of excitatory synapses does not only involve a graded reduction in voltage-gated calcium influx, but also an all-or-nothing suppression of calcium-mediated transmitter release at a subset of the synapses. In other words, these authors propose that using the PPR measurement to assess changes in the Pr might lack sensitivity if the Pr is already low at individual release sites. Additionally, a presynaptic silencing mechanism has also been observed at the OVLT-MNC synapse upon release of a unknown substance following electrical stimulation of the SCN (Trudel and Bourque, 2012). Indeed, the EPSC amplitude elicited in MNC during electrical stimulation of the OVLT was found to be attenuated following electrical stimulation of the SCN and importantly, no change in PPR was observed despite the reduction in the frequency of asynchronous events and an increase in the rate of synaptic failures (i.e. the percentage of trials in which no response was observed when stimulating the OVLT at low intensity). To summarize, it is possible that both mechanisms (i.e. a classical

inhibition of presynaptic VGCC and a presynaptic silencing at specific synapses) are involved in the suppression of glutamate release following the induction of our mild postsynaptic protocol.

4.3.3. Activity-dependent retrograde EPSC inhibition in oxytocin neurons

A previous study has shown that retrograde inhibition of glutamatergic transmission induced by intense postsynaptic spiking in OT neurons relies first, on an autocrine effect upon OT binding to its receptor and second, on the release of EC that binds to presynaptic CB1 receptors (Hirasawa et al., 2004). However, our findings showed that activation of OT receptors is not a necessary prerequisite in the suppression of excitatory afferents, whereas CB1 receptor activation is involved in this suppression of glutamate release (Fig. 4.2.4.A and B). The fact that OT receptors are not involved in this presynaptic inhibition, following our postsynaptic spiking protocol, might be attributable to the fact that the amount of peptide released with our stimulation protocol was too little to exert a significant inhibitory impact on glutamatergic transmission. Therefore, another mechanism might explain how EC were released from OT neurons following our mild postsynaptic protocol.

Interestingly, our experiments with THL suggest that a proportion of the EC involved in this suppression of excitatory transmission is synthesized via the DAGL pathway, because suppression of DAGL activity with this drug prevented the inhibition of glutamate release (Fig 4.2.4.C). DAG, which is hydrolyzed by DAGL to generate 2-AG, can be produced via rises in intracellular calcium concentration that activate PLCβ or via activation of the Gq11-PLCβ-DAGL pathway (Hu et al., 2014; Ohno-Shosaku and Kano, 2014). Since OT receptors, which activate Gq11, do not appear to be involved in this presynaptic inhibition, the most likely explanation would be that intracellular calcium rises, following our postsynaptic spiking protocol, led to the activation of PLCβ, which in turn produced DAG that generated 2-AG synthesis, via DAGL activity.

Our pharmacological analysis of the retrograde process also revealed that inhibiting κ-opioid receptors prevented the inhibition of glutamate release, despite the fact that OT neurons do not produce DYN, while it is the case for VP cells (Brown et al., 2000). As illustrated in Figure 4.3.3, a hypothetical mechanism might be that spontaneously active neighboring VP cells constitutively release DYN, hence producing an endogenous tone onto OT neurons, since OT and VP neurons contain κ-opioid receptors on their soma (Brown et al., 2000). Indeed, VP neurons recorded *in vivo* from rats, via extracellular single unit, display a spontaneous firing frequency between 4 and 8 Hz (Joe et al., 2014), suggesting a constitutive DYN release from these cells. Thus, activating somatic κ-opioid receptors and subsequently the Gi/o subunit might have contribute to the calcium-induced EC release following postsynaptic spiking, which in turn inhibited glutamate release. Indeed, previous studies have shown that activation of the Gi/o subunit led to the activation of PLC (Inoue et al., 2003; Murthy et al., 2004). Since all PLC isozymes convert PIP2 into the second messengers IP3 and DAG (Suh et al., 2008), activation of somatic κ-opioid receptors might have led to EC release via DAG production as well as a calcium-induced EC release via intracellular calcium rise following calcium store depletion upon IP3 binding on the endoplasmic reticulum.

4.3.4. Activity-dependent retrograde EPSC inhibition in vasopressin neurons

Previous findings have shown that bath application of exogenous VP on MNC causes a decrease of the eEPSC amplitude and that postsynaptic depolarization leading to an inhibition of the eEPSC, presumably via inhibition of glutamatergic neurotransmission via VP release, was blocked by MC (i.e. a OT and VP receptor antagonist) (Kombian et al., 1997). However, the cell types from which this EPSC inhibition was observed in this study were not clearly established. Interestingly, our results show that the activation of V1a receptors is not required in the suppression of excitatory afferents following our mild stimulation protocol in VP MNC, because blockade of these receptors with the V1a receptor antagonist SR49059 was ineffective at preventing a decrease of glutamate release (Fig. 4.2.4.A).

It has been previously demonstrated that intense postsynaptic depolarization induces EC release from VP neurons, which subsequently inhibits presynaptic release (Iremonger and Bains, 2009). Moreover, it was shown that simultaneously pairing a presynaptic stimulation and a postsynaptic depolarization in these cells triggers the release of EC as well as DYN, which causes a long-lasting suppression of glutamate neurosecretion (~30 minutes) from the presynaptic terminal (Iremonger et al., 2011). Our results indicate that EC and DYN are also involved in the suppression of glutamate release following mild postsynaptic activity, since blockade of CB1 receptor as well as κ-opioid receptors were shown to prevent this presynaptic inhibition (Fig. 4.2.4.B and D and Fig. 4.3.4). Contrarily to what we observed in OT neurons, we found that inhibiting DAGL in VP cells had no impact in the suppression of glutamate release (Fig. 4.2.4.C). This result could indicate that 2-AG is either not released in a sufficient amount from VP neurons to inhibit excitatory transmission or via a different pathway that does not required DAGL activity. Moreover, anandamide could be preferentially released from VP neurons, rather than 2-AG. Indeed, a study using immunocytochemistry has shown that the enzyme FAAH, which specifically degrades anandamide (Hu et al., 2014), was found in the soma of MNC (Hirasawa et al., 2004). However, despite the fact that both OT and VP neurons might have been sampled in the study mentioned above, whether the enzyme FAAH is a reliable marker of anandamide production or actively prevents its diffusion across the cell membrane after synthesis remains to be determined.

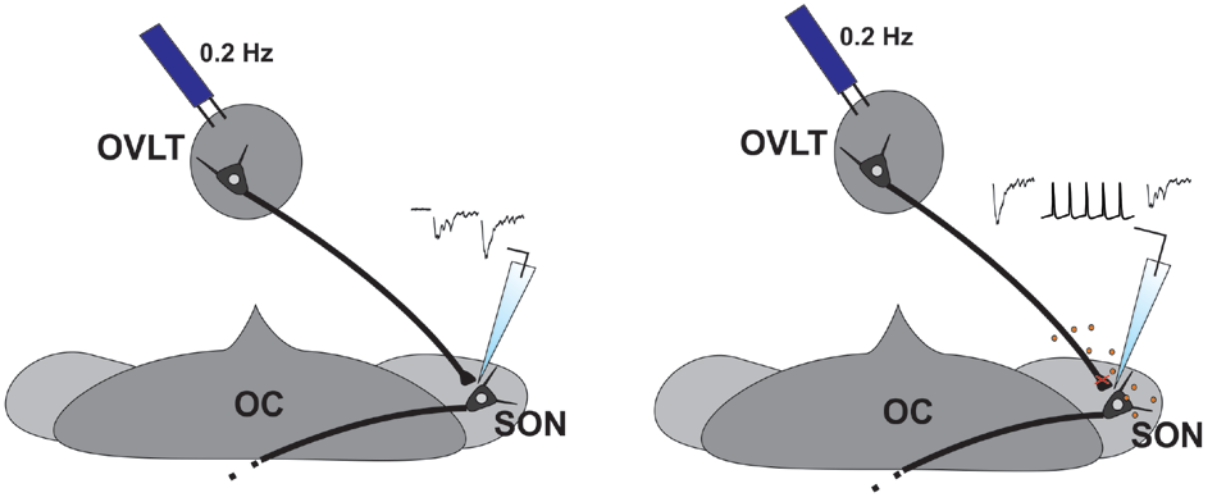

Figure 4.2. Protocol used to inhibit excitatory transmission via somato-dendritic release in MNC

(**Left**) Two stimulations were delivered to the OVLT 50 ms apart at a frequency of 0.2 Hz (i.e. every 5 s.) to elicit a pair of EPSC showing paired pulse facilitation in identified OT or VP neurons. (**Right**) After monitoring the eEPSC amplitude (in VClamp) for 5 minutes, trains of action potentials were elicited in the same cell (in IClamp) to cause somato-dendritic release of retrograde messengers. The inhibition of excitatory afferents was assessed via a reduction of the eEPSC (only the first EPSC is shown on the right for more clarity; OC, optic chiasm; SON, supraoptic nuucleus).

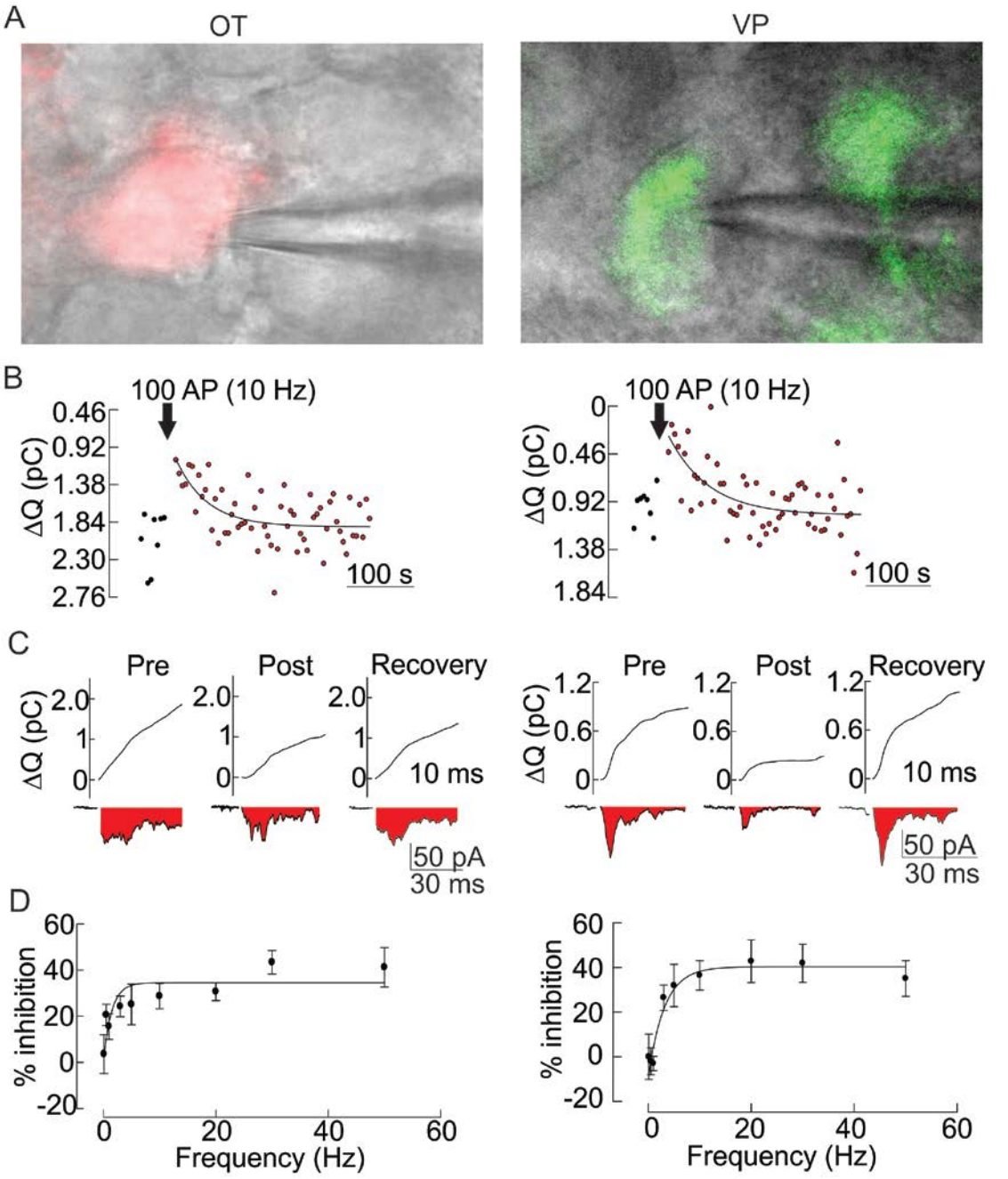

Figure 4.2.1. Frequency-dependent inhibition of excitatory transmission via somato-dendritic release

A, Whole-cell patch clamp recording from identified OT mRFP1 neuron (left) and VP eGFP neuron (right). **B**, Inhibition of the eEPSC charge transfer following our mild stimulation protocol (10 Hz, 100 spikes) in OT (left) and VP (right) neurons. **C**, Average eEPSC charge transfer during different phases of the stimulation protocol: pre (last 5 eEPSC), post (2 first eEPSC) and recovery (last 5 eEPSC) with their corresponding time course summation (top traces; in pC). **D**, A frequency-dependent inhibition of excitatory afferents is observed for OT (left) and VP (right) neurons.

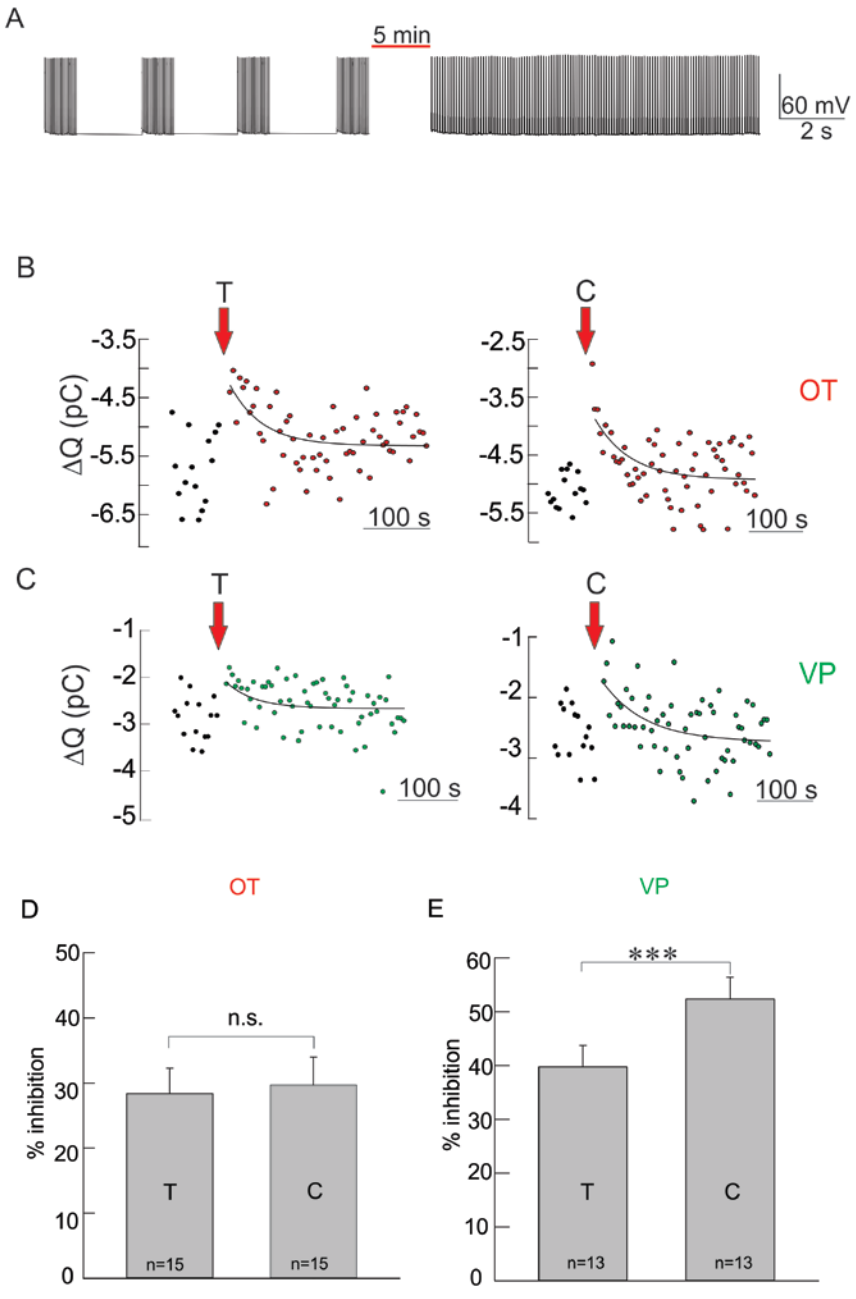

Figure 4.2.2. Pattern-dependent suppression of excitatory transmission

A, Protocol used to administer spikes mimicking a clustering and a tonic firing (see *Methods*), with corresponding examples showing the inhibition of the eEPSC in OT neurons (**B**) and VP neurons (**C**) following a tonic (T) and a clustering (C) stimulation. Inhibition of excitatory transmission (in % inhibition), measured as the decrease of the eEPSC amplitude following the induction of our protocol in identified OT (**D**) and VP neurons (**E**). ***P < 0.005; n.s., not significant.

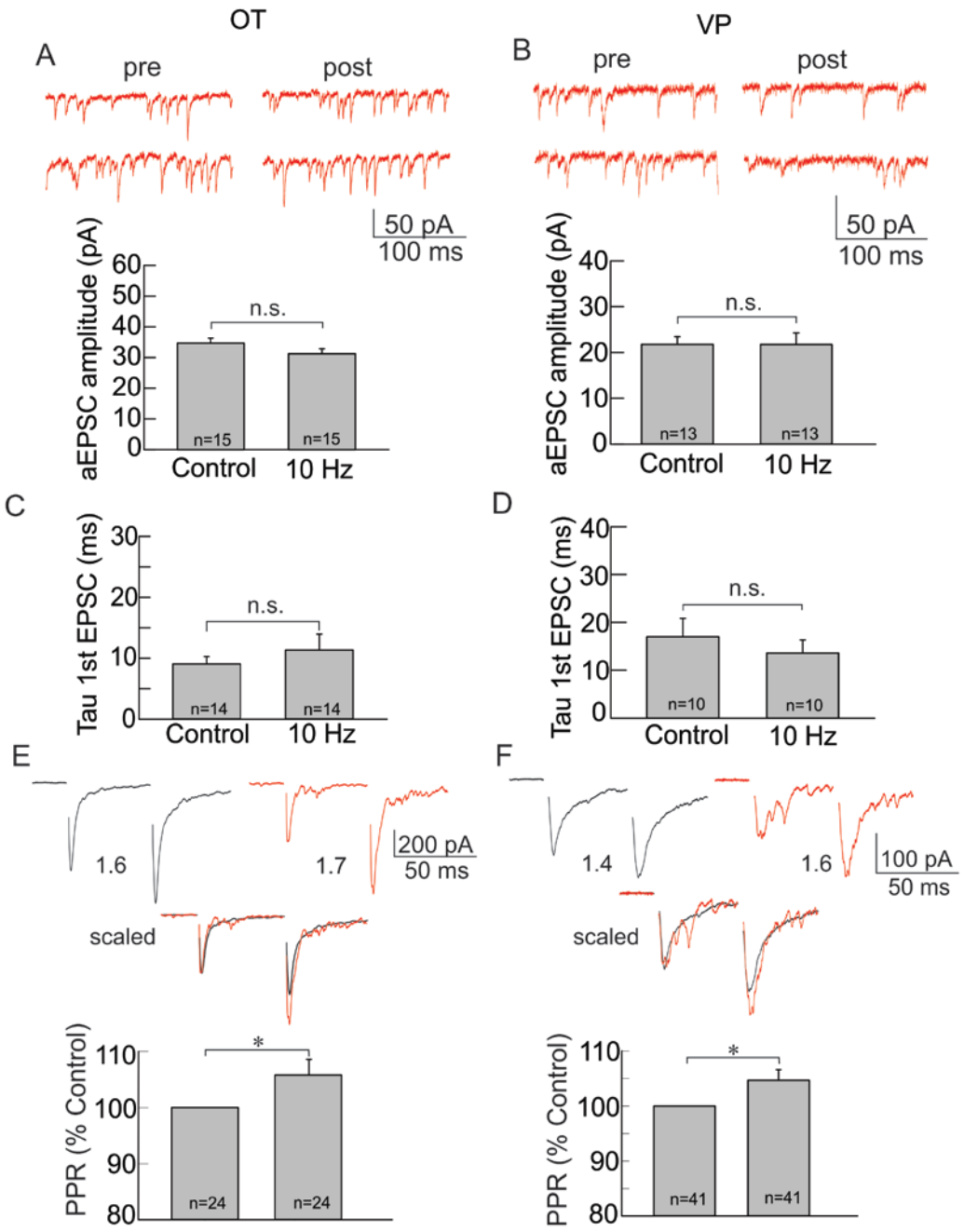

Figure 4.2.3. Presynaptic locus of inhibition for OT and VP neurons

Traces showing the amplitude of asynchronous events in OT neurons (**A**) and VP cells (**B**); no significant change in quantal amplitude was detected following the induction of our mild postsynaptic protocol (10 Hz, 100 spikes) in both cell types. **C**, No significant change in the decay constant of the first EPSC was observed following the administration of our mild postsynaptic protocol in OT neurons and VP neurons (**D**), suggesting a stable series resistance. **D-E**, OT and VP neurons displayed an increase in PPR following the induction of the same postsynaptic spike train, suggesting a presynaptic locus of inhibition. $*P < 0.05$; n.s., not significant.

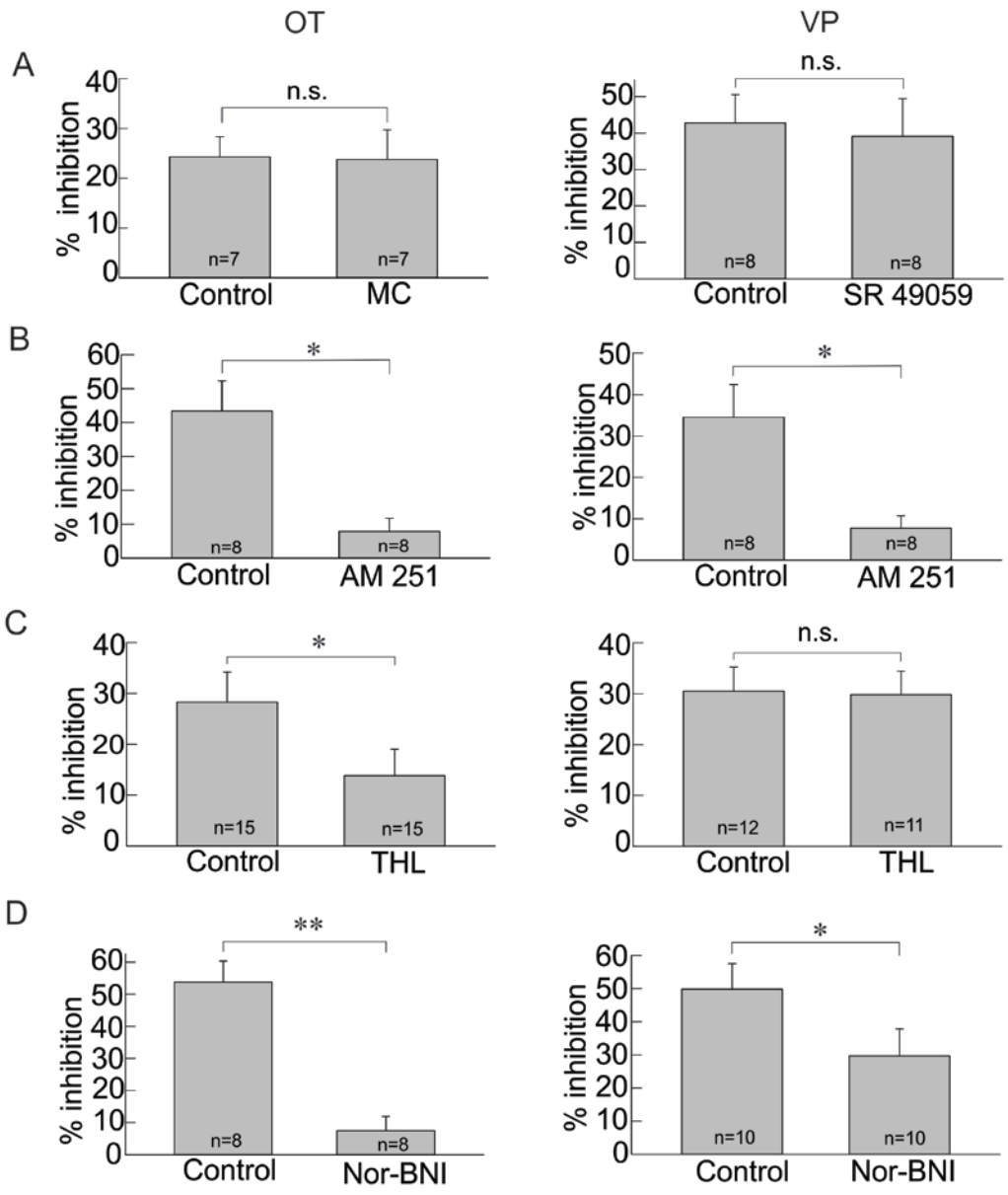

Figure 4.2.4. Contribution of different retrograde messengers released from OT and VP neurons in the inhibition of excitatory afferents

A, Following the administration of our mild postsynaptic protocol (10 Hz, 100 spikes), blocking OT receptors with Manning compound (MC; 10 μM) did not prevent the inhibition of excitatory afferents (in % inhibition) in OT neurons (left) and application of the V1a receptor antagonist SR49059 (10 μM) in VP cells also had no effect on glutamate release (right).**B**, Blocking CB1 receptors with AM251 (5 μM) in both cell types prevented the inhibition of excitatory transmission. **C**, Including the inhibitor of the DAGL enzyme, THL (5 μM), in the recording electrode prevented the inhibition of excitatory afferents in OT neurons (left) whereas this drug had no effect in VP neurons (right). **D**, Blockade of kappa-opioid receptors with nor-BNI (1 μM) significantly prevented the inhibition of glutamate release when performing our mild stimulation protocol in both cell types. $*P < 0.05$; n.s., not significant.

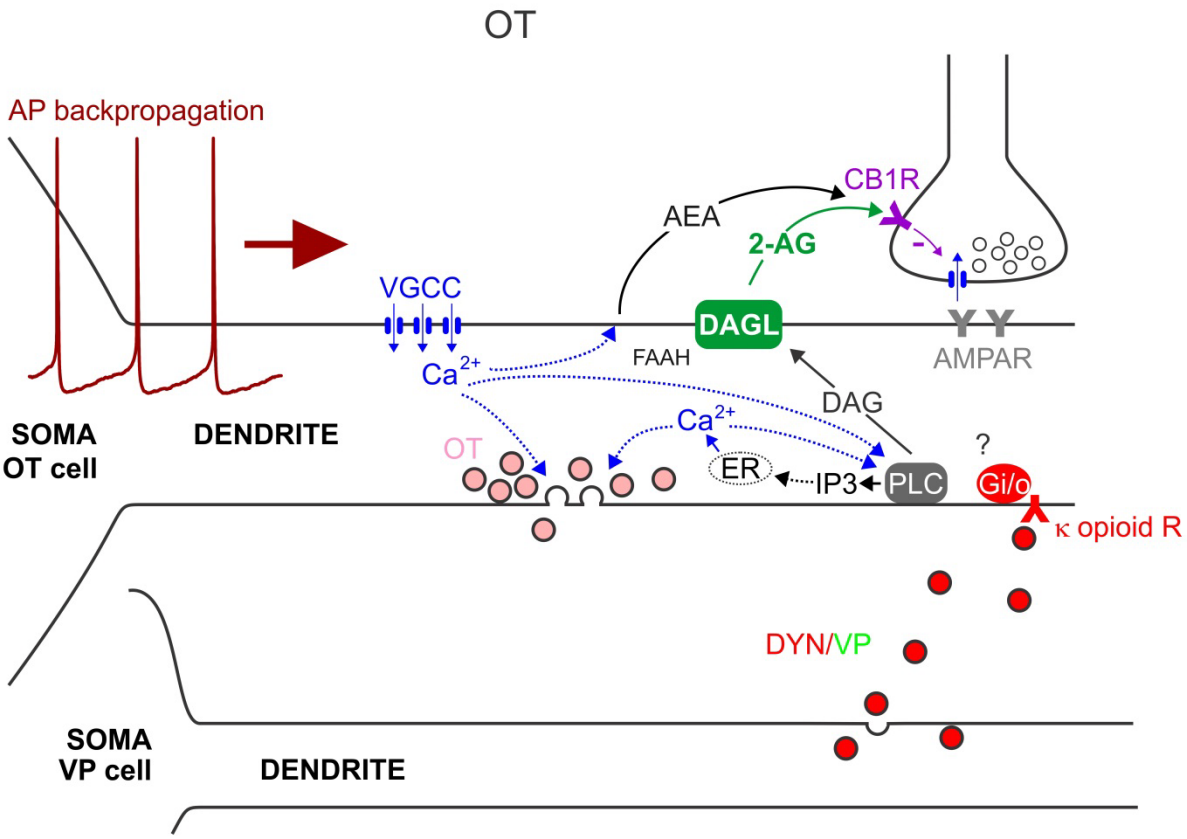

Figure 4.3.3. Model of activity-dependent retrograde inhibition of excitatory transmission in OT neurons

Action potentials (AP) backpropagate into dendrites during a mild postsynaptic protocol (10 Hz, 100 spikes) and cause the opening of VGCC. Ca^{2+} entry triggers the activation of PLCβ that generates DAG and IP3. The EC 2-AG, which is generated via the hydrolysis of DAG via DAGL activity, will passively diffuse across the plasma membrane and inhibit glutamatergic transmission by binding to presynaptic CB1 receptors. The EC AEA could also potentially participate in this inhibitory response following intracellular Ca^{2+} influx. The peptide OT is not involved in the suppression of glutamatergic transmission and κ-opioid receptors are involved in the suppression of excitatory transmission. This DYN-mediated presynaptic inhibition could rely on an endogenous DYN tone activating κ-opioid receptors located on the soma of OT neurons. Activation of somatic κ-opioid receptors, by activating the Gi/o subunit, could be involved in the release of an inhibitory retrograde messenger such as 2-AG/AEA.

VGCC; voltage gated calcium channels, PLCβ; phospholipase C beta, IP3; inositol triphosphate, DAG; diacylglycerol; DAGL; diacylglycerol lipase, EC; endocannabinoids, 2-AG; 2-Arachidonoylglycerol, AEA; anandamide, CB1 receptor; cannabinoid receptor type 1, OT; oxytoxin, DYN; dynorphin, κ-opioid receptors; kappa-opioid receptors, FAAH; fatty acid amide hydrolase

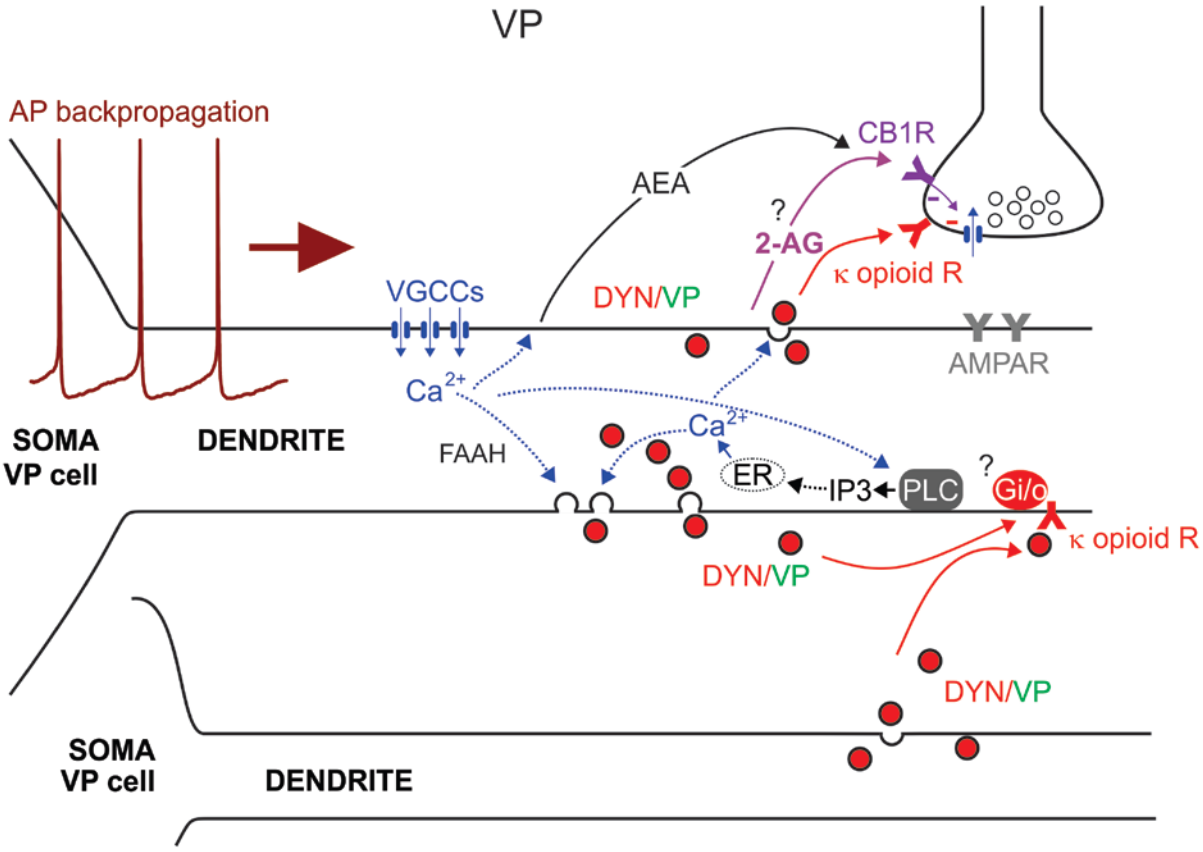

Figure 4.3.4. Model of activity-dependent retrograde inhibition of excitatory transmission in VP neurons

Action potentials (AP) backpropagate into dendrites during a mild postsynaptic protocol (10 Hz, 100 spikes) and cause the opening of VGCC. Ca^{2+} entry triggers the production and release of EC, presumably AEA, which will passively diffuse across the plasma membrane and inhibit glutamatergic transmission by binding to presynaptic CB1 receptors. The peptide VP is not involved in the suppression of glutamatergic transmission. κ-opioid receptors are involved in the suppression of excitatory transmission. This DYN-mediated presynaptic inhibition could also rely on an endogenous DYN tone activating κ-opioid receptors located on the soma of VP neurons. Activation of somatic κ-opioid receptors, by activating the Gi/o subunit, could be involved in the release of an inhibitory retrograde messenger such as AEA.

VGCC; voltage gated calcium channels, PLCβ; phospholipase C beta, IP3; inositol triphosphate, DAG; diacylglycerol; DAGL; diacylglycerol lipase, EC; endocannabinoids, 2-AG; 2-Arachidonoylglycerol, AEA; anandamide, CB1 receptor; cannabinoid receptor type 1, VP; vasopressin, DYN; dynorphin, κ-opioid receptors; kappa-opioid receptors, FAAH; fatty acid amide hydrolase

V: IMPACT OF CALCIUM AND SPIKE BROADENING IN SOMATO-DENDRITIC RELEASE

We saw in *Chapter IV* that administration of action potentials at higher frequencies of discharge in OT and VP neurons, as well as clustering activity in VP neurons, enhanced the inhibition of excitatory afferents via somato-dendritic release of retrograde messengers. The present chapter will therefore investigate the role of intra-dendritic calcium levels in this frequency-dependent inhibitory response, for both cell types (*Hypothesis five,* see section 1.6.6).

5.1. Overview

At the level of the neurohypophysis, calcium must enter the synaptic terminal via VGCC, following the arrival of an action potential, in order to trigger exocytosis of OT (see section 1.1.4.1) and VP (see section 1.1.5.1) into the bloodstream. Importantly, it appears that calcium influx within the somato-dendritic compartment also plays a significant role in regulating the release from this neuronal area. The release of EC, involved in the suppression of excitatory transmission as discussed in *Chapter IV*, also depends on postsynaptic calcium rise (Ohno-Shosaku and Kano, 2014). As elaborated in section 1.6.2, calcium currents recorded in MNC somata have indicated the presence of several subtypes of high voltage-activated VGCC (i.e. N-, L-, P/Q- and R-types). It was also demonstrated that blocking the N-type VGCC considerably reduced OT release from the somato-dendritic compartment (Tobin et al., 2011), indicating an important function of VGCC and calcium entry in the release process from the soma and dendrites.

A particular feature about MNC electrical activity is that the action potential width was shown to progressively increase at higher frequencies of discharge (see section 1.6.4). The frequency-dependent facilitation of secretion from the posterior pituitary can be explained by the presence of a spike frequency-dependent broadening mechanism that generates more calcium entry per spike at higher frequencies of stimulation within the axon terminal (Jackson et al., 1991). Analogously, a frequency-

dependent broadening mechanism has been observed in the soma of MNC and relies on a smaller outward K^+ current as well as an increase in calcium influx when reaching higher frequencies of discharge (see section 1.6.4). However, it is still unknown if the frequency-dependent broadening observed in the soma of OT and VP neurons also leads to a higher amount of calcium influx per action potential within the dendritic compartment. Therefore, the first aim of this chapter will be to investigate if higher frequencies of discharge result in a proportional increase in intra-dendritic calcium levels, per spike, in both cell types. The second aim of this chapter will be to investigate if rises in intra-dendritic calcium concentration are differentially regulated in both cell types when stimulating these cells at different frequencies of discharge.

5.2. Results

5.2.1. Presynaptic inhibition of glutamate release is dependent on postsynaptic calcium

To determine if intra-dendritic calcium rises in a frequency-dependent manner, we used two-photon calcium imaging to measure the relative increase in dendritic calcium levels following the induction of action potentials in OT and VP neurons at different frequencies of discharge (i.e. from 0.5-50 Hz). As illustrated in Figure 5.2.1.A, identified OT and VP neurons were filled with Alexa 594 (17 μM) to visualize the cell morphology and select areas where 1000 line scans per 1.12 s. were performed onto proximal dendrites (i.e. perpendicularly to their long axis). Cells were also filled with the calcium-sensitive dye Fluo-5F (180 μM) in order to assess changes in intracellular dendritic calcium level, measured as the change in the green Fluo-5F fluorescent signal (dG) normalized to the red Alexa 594 (R) fluorescent signal (dG/R). As illustrated in Figure 5.2.1.B and C, eliciting a train of action potentials in MNC, from 3 Hz to 50 Hz, led to a proportional increase in dendritic calcium level that was prevented when the cell was also filled with BAPTA (10 mM). These findings suggest that there is a frequency-

dependent increase in intra-dendritic calcium and this could be a key step in the retrograde activity-dependent inhibition of the eEPSC amplitude.

We therefore investigated the role of intracellular postsynaptic calcium on presynaptic glutamate release while performing our mild postsynaptic stimulation protocol (i.e. 10 Hz, 100 spikes). The results showed that filling OT neurons with BAPTA (10 mM) significantly decreased the suppression of glutamate release caused by a conditioning train (Control = 31.66 ± 10.61% $_{inhibition}$; n = 11; BAPTA = 1.76 ± 1.76% $_{inhibition}$; n = 11; *t* test; P = 0.012; Fig. 5.2.1.D and E). Similar findings were observed for VP neurons (Control = 27.33 ± 7.54% $_{inhibition}$; n = 13; BAPTA = 6.58 ± 3.59% $_{inhibition}$; n = 11; *t* test; P = 0.029; Fig. 5.2.1.F and G), indicating that a rise in intracellular calcium concentration is essential for the activity-dependent suppression of excitatory neurotransmission in both cell types.

We then examined if the activity-dependent rise in intra-dendritic calcium is differentially regulated in OT and VP neurons. As illustrated in Figure 5.2.2.B and C, both cell types expressed a significant frequency-dependent increase in intra-dendritic calcium when stimulated from 0.5 Hz to 50 Hz. Moreover, the increase in dG/R per action potential in VP cells was found to be significantly higher from 5 Hz to 50 Hz compared to OT neurons (two-way ANOVA with *post hoc* Holm–Sidak test; $P < 0.05$; Fig. 5.2.2.D). Together, these data suggest that both cell types show a frequency-dependent increase in intra-dendritic calcium, which appears to be higher for VP neurons, from 5 to 50 Hz.

5.2.2. Per spike intra-dendritic calcium influx is correlated to somatic action potential broadening

It was previously shown that the somatic action potential width in SON neurons broadens as a function of the firing frequency (Andrew and Dudek, 1985; Bourque and Renaud, 1985). Moreover, these studies have shown that the action potential duration progressively increases at the beginning of a spike train, reaching a stable (i.e. steady-state) duration after 25-30 spikes. As illustrated in Figure 5.2.3.A and B, stimulating OT and VP cells at 30 Hz elicited a progressive broadening within the first 25 action

potentials. We then investigated the impact of stimulating OT and VP neurons from 0.5 Hz to 50 Hz on the steady-state spike width. As shown in Figure 5.2.3.C, we also observed a positive relationship between the frequency of stimulation and the steady-state action potential duration in both cell types.

We then examined if there is a relationship between the action potential duration and the amount of intra-dendritic calcium per spike. To answer that question, we plotted the average values of dG/R per spike as a function of the average values of spike duration observed over the range of frequencies examined (0.5-50 Hz). Our results showed that there is a direct association between the action potential duration and the rise in intra-dendritic calcium concentration in both OT and VP neurons (Fig. 5.2.3.D). To summarize, our findings demonstrate that the frequency-dependent action potential broadening recorded in both cell types leads to a proportional increase in intracellular calcium within dendrites.

5.3. Discussion

5.3.1. Frequency-dependent rise in intra-dendritic calcium is differentially regulated in OT and VP neurons

It has been previously shown that a positive relationship is found between the frequency of discharge and calcium entry per spike in isolated neurohypophysial nerve terminals (Jackson et al., 1991). Our results are the first to shown that a frequency-dependent calcium rise is also present within proximal dendrites of OT and VP neurons (Fig. 5.2.2.B and C). Importantly, the increase in dG/R per action potential in VP cells was found to be significantly higher from 5 Hz to 50 Hz compared to OT neurons (Fig. 5.2.2.D). This difference between the cell types could be explained by the fact that OT neurons prominently express the calcium buffering proteins calbindin and calretinin in their soma, according to an immunofluorescence study (Arai et al., 1999), whereas a high proportion of VP neurons do not express these proteins. It is thus possible that lower frequencies of discharge (i.e. between 0.5

and 3 Hz) in OT neurons did not lead to a sufficient amount of calcium entry to saturate the high-affinity binding sites of calbindin (K_{d1} ~ 174 nM), whereas the second calcium kinetic displaying a low-affinity for calcium (K_{d2} ~ 513 nM) (Nagerl et al., 2000) could explain the difference observed at higher frequencies of discharge between both cell types. Electrophysiologically, it was previously demonstrated that introducing calbindin into VP neurons converted a phasic firing into a tonic discharge (Li et al., 1995), with a suppression of depolarizing after potentials (DAP). Additionally, including BAPTA in the recording electrode of phasic cells also led to the same results. Conversely, introduction of anti-calbindin into OT cells led to the emergence of a phasic firing and DAP (see *Introduction*, section 1.6.5), indicating that intracellular calcium concentration modulate the firing pattern of MNC.

Interestingly, calcium clearance mechanisms were examined in isolated SON neurons and appear to be differentially regulated than those localized in the synaptic terminal. More precisely, the plasmalemmal Na^+/Ca^{2+} exchanger, the ER and plasmalemmal Ca^{2+}-ATPase pumps and the uniporter-assisted mitochondrial Ca^{2+} uptake are complementary in actively clearing Ca^{2+} from the somato-dendritic compartment of SON neurons (Komori et al., 2010), whereas plasmalemmal Ca^{2+}-ATPase pumps and mitochondria were shown to significantly contribute to intracellular calcium relaxation at the level of the neurohypophysis (Sasaki et al., 2005). Additionally, the role of the calcium buffering proteins calbindin and calretinin in intracellular calcium clearance have not been investigated so far and therefore, understanding their role in the somato-dendritic compartment would be a key step.

Interestingly, preliminary results have shown the ER Ca^{2+}-ATPase pump differentially regulates basal intracellular calcium in OT and VP neurons. Indeed, application of cyclopiazonic acid (i.e. an inhibitor of Ca^{2+}-ATPase pumps on the ER) on VP neurons caused no increase in basal calcium, whereas a twofold increase was observed for OT cells (unpublished data (Komori et al., 2010)), suggesting a different calcium clearance mechanism for both cell types. To summarize, the higher intra-dendritic calcium rise found in VP neurons in our experiments could be attributable to differences in intracellular

calcium buffering properties in OT and VP neurons, but more work need to be done to elucidate the origin of this difference.

5.3.2. Role of calcium in the frequency-dependent inhibition of excitatory transmission

In *Chapter IV*, we saw that a relationship exists between the firing frequency of OT and VP neurons and the inhibition of presynaptic afferents. In other words, higher frequencies of discharge, in both cell types, were more effective at inhibiting glutamate release than lower firing frequencies (see section 4.2.1). This result could potentially be explained by the fact that a positive association was also found between the firing frequencies of MNC and the rise in intra-dendritic calcium concentration (Fig. 5.2.2.B and C). Importantly, the inhibition of presynaptic glutamate release following our mild depolarization protocol (10 Hz, 100 spikes) was prevented when the cells were filled with BAPTA (Fig. 5.2.1.D-G), indicating that postsynaptic intracellular calcium rises play an essential role in this presynaptic inhibition. Therefore, the progressive rise in intra-dendritic calcium, following the induction of action potentials at different firing frequencies, might have played a role in the release of retrograde messengers and in the subsequent suppression of excitatory transmission. More precisely, this frequency-dependent inhibition of excitatory afferents could be attributable to a frequency-dependent broadening mechanism generating more calcium entry in dendrites per spike, as described in the next section.

5.3.3. Frequency-dependent action potential broadening is correlated to a proportional rise in intra-dendritic calcium

Previous studies in SON neurons have shown the presence of a frequency-dependent spike broadening mechanism at the level of the soma, where higher frequencies of discharge elicited a longer action potential duration. This broadening mechanism can be explained by a reduction of K^+ current as well as a small increase in Ca^{2+} current (Kirkpatrick and Bourque, 1991; O'Regan and Cobbett, 1993). Our

results indicate that both OT and VP neurons display a spike frequency-dependent broadening mechanism (Fig. 5.2.3.C). Interestingly, our results are the first to provide a positive association between the somatic action potential duration and the rise in intra-dendritic calcium concentration generated by a single spike (Fig. 5.2.3.D). In other words, higher firing frequencies led to an increase in intracellular dendritic calcium concentration, per action potential. The correlation observed could potentially explain why depolarizing the postsynaptic cell at higher frequencies of stimulation elicited an enhanced inhibition of glutamatergic neurotransmission on a per-spike basis (see *Chapter IV*, section 4.2.1).

Using isolated SON neurons and calcium measurements with Fura-2 (Komori et al., 2010), it was shown that blocking calcium clearance mechanisms, such as the plasmalemmal Na^+/Ca^{2+} exchanger, the ER and plasmalemmal Ca^{2+}-ATPase pumps and the uniporter-assisted mitochondrial Ca^{2+} uptake delayed the recovery of intracellular calcium levels following a depolarizing K^+ stimulation. The findings mentioned above, combined to a frequency-dependent Ca^{2+} entry on a per-spike basis, could potentially explain why lower frequencies of stimulation elicited a smaller suppression of glutamate release in our conditions, while higher frequencies of discharge were found to enhance this presynaptic inhibition, considering that we kept the number of action potential constant across all frequencies tested. Indeed, the gradual action potential broadening observed at higher frequencies of stimulation resulted in an increase in intra-dendritic calcium per spike (Fig. 5.2.2.D), and because of the slow kinetics of calcium clearance, it is likely that intracellular calcium can accumulate to higher concentrations when elicited at higher frequencies, due to a smaller inter-spike interval. In other words, both mechanisms (i.e. frequency-dependent action potential broadening and slow kinetics of calcium clearance), could contribute to a frequency-dependent calcium build up and hence, result into a proportional level of release from the somato-dendritic compartment.

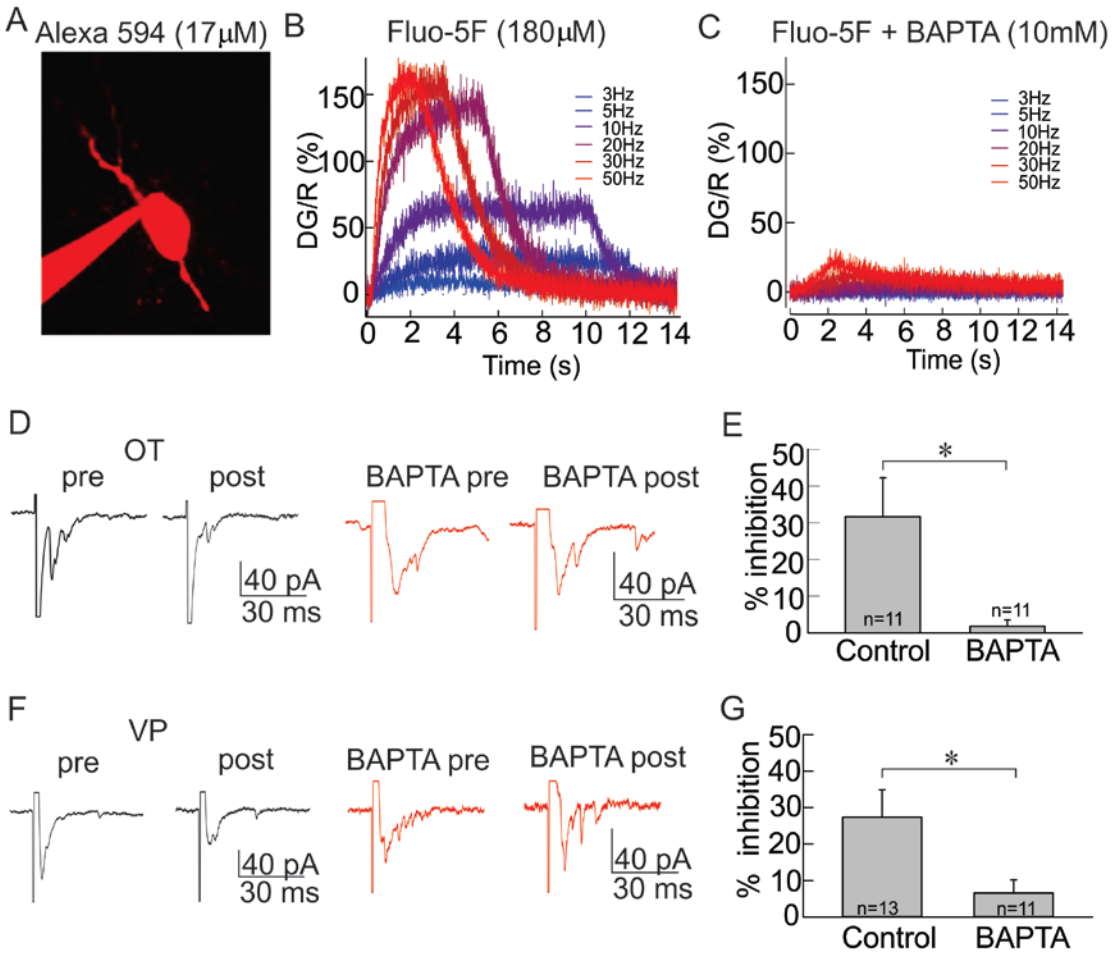

Figure 5.2.1. Presynaptic inhibition of glutamate release is dependent on postsynaptic calcium rises

A, A MNC was filled with the red dye Alexa 594 to visualize proximal dendrites where line scan were performed. **B**, Increase in intra-dendritic calcium levels measured in a MNC via the increase in fluorescence of the green calcium indicator Fluo-5F (dG) normalized over the red (R) dye Alexa (dG/R) where action potentials were delivered from 3 to 50 Hz. **C**, The relative calcium increase (dG/R) was prevented when recording electrodes were filled with the calcium chelator BAPTA (from 3-50 Hz). **D**, eliciting our mild stimulation protocol (10 Hz, 100 spikes) in OT neurons significantly reduced the eEPSC (post) and this effect was prevented in BAPTA-filled cells (**E**). **F**, The reduction of the eEPSC following our mild stimulation protocol in VP neurons (post) was also prevented in BAPTA-filled cells (**G**).

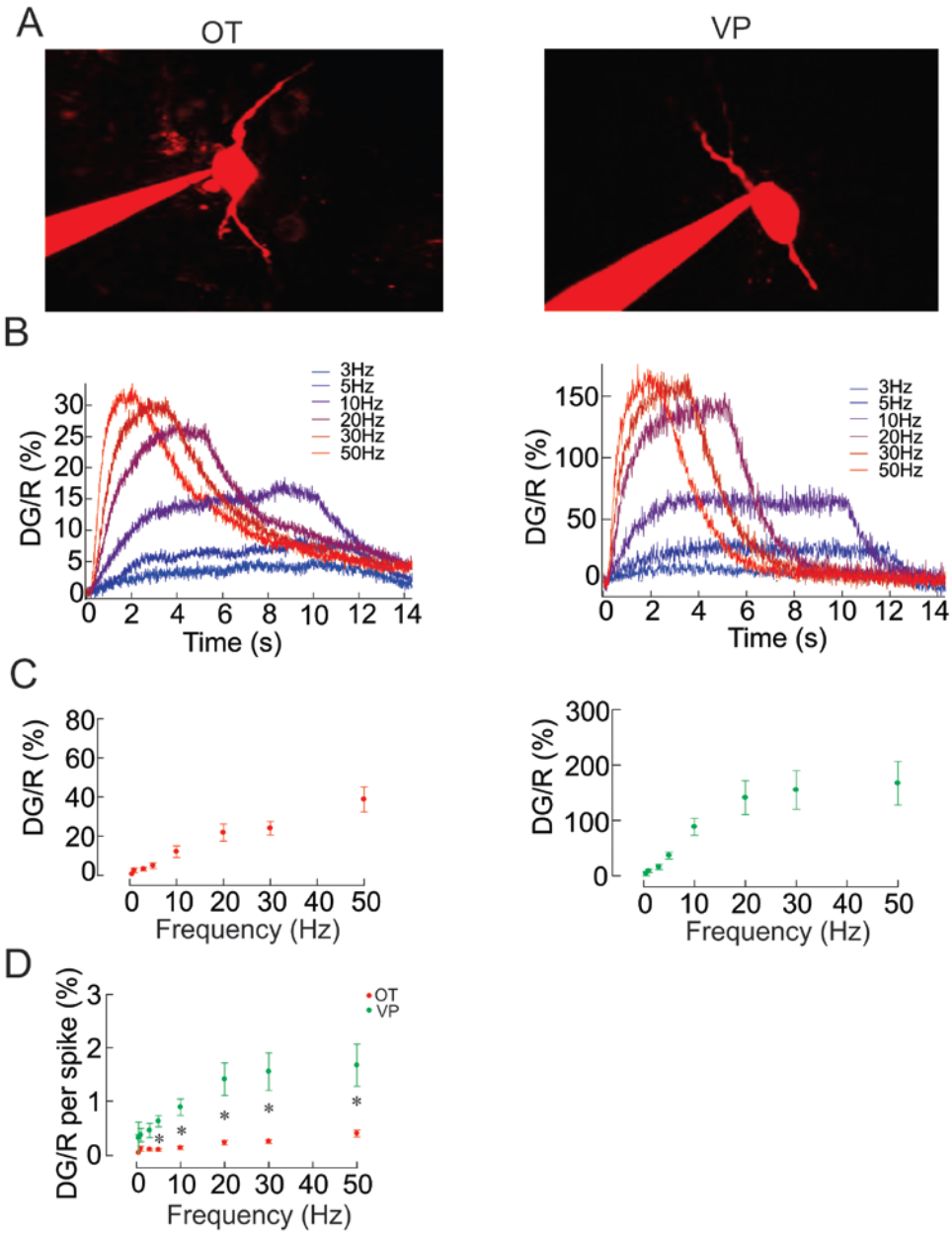

Figure 5.2.2. Frequency-dependent rise in intra-dendritic calcium is differentially regulated in OT and VP neurons

A, Identified OT neuron (left) and VP neuron (right) filled with Alexa 594 and Fluo-5F. **B**, Traces showing the increase in intra-dendritic calcium (% dG/R) in an OT neuron (left) and a VP neuron (right) when spikes are administered at a frequency between 3 and 50 Hz. **C**, A frequency-dependent increase in intra-dendritic calcium is found for both cell types when spikes are delivered from 0.5 to 50 Hz. **D**, The intra-dendritic calcium increase (% dG/R) per spike is significantly higher in VP cells compared to OT neurons, following the administration of postsynaptic action potentials, from 5 Hz to 50 Hz.

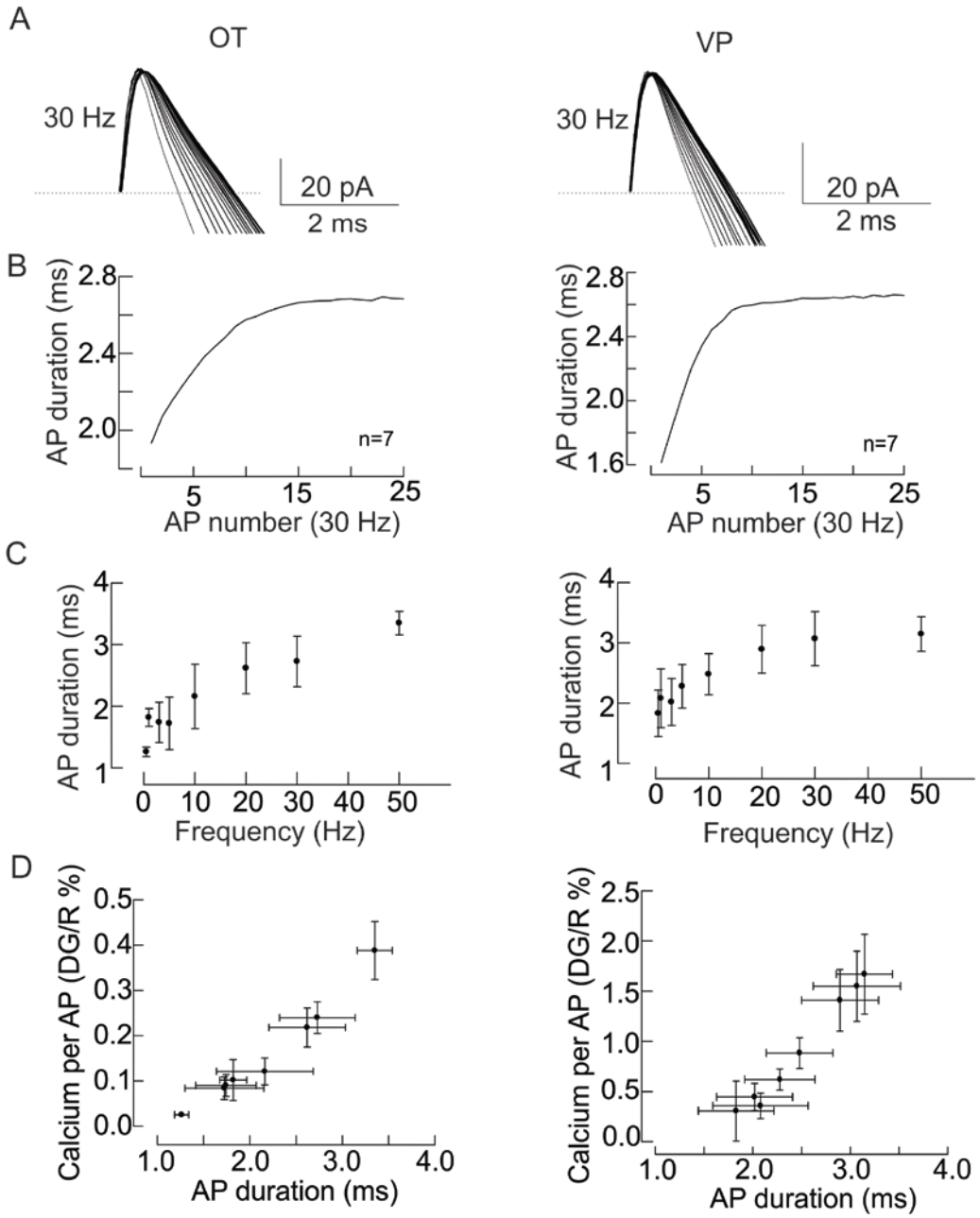

Figure 5.2.3. Per spike intra-dendritic calcium influx is correlated to somatic action potential broadening

A, Gradual action potential broadening over the 25 first spikes during a 30 Hz train in a OT neuron (left) and a VP neuron (right). **B**, Average action potential duration over the 25 first spikes during a 30 Hz train, in OT cells (left, n = 7) and VP cells (right, n = 7). **C**, Graph illustrating the presence of a frequency-dependent spike broadening in both cell types at steady-state values, from 0.1-50 Hz. **D**, A positive relationship was observed between the action potential duration and the increase in intra-dendritic calcium (dG/R%) per spike.

VI: GENERAL DISCUSSION

6.1. Overview

Throughout my doctoral studies, I was particularly interested in gaining an understanding of the mechanisms that regulate clustering activity, a rhythmic oscillation that was shown to emerge *in vivo* during dehydration in both OT and VP neurons, as elaborated in *Chapter I* (section 1.3.2). However, despite the fact that pharmacological activation of NMDA receptors triggers the onset of clustered firing, how this type of electrical activity is found to emerge from a network perspective has never been demonstrated. The data acquired from my research have shown that clustered firing can be effectively triggered *in situ*, via synaptic release of endogenous glutamate following the electrical stimulation of the OVLT (see *Chapter III*, section 3.2.1). Understanding how this rhythmic firing is regulated is of critical importance since this type of firing has been shown to maximize VP release from the neurohypophysis (Cazalis et al., 1985). In *Chapter III*, we have shown for the first time the expression of neurotensin (NT) receptors (NTS1 and NTS2) in isolated rat MNC and we demonstrated that the tridecapeptide NT potently modulates clustering activity by elongating the cluster duration (see section 3.2.4) and that inhibition of SK channels also causes an elongation of these short bursts (see section 3.2.3). Surprisingly, we also saw in *Chapter III* that NT does not inhibit the AHP studied by patch-clamp approaches (see section 3.2.5), despite the fact that this peptide was previously shown to inhibit the AHP amplitude in MNC studied with sharp electrodes (Kirkpatrick and Bourque, 1995).

Because I was strongly interested in understanding how the secretion from the somato-dendritic compartment inhibits glutamate release (see *Chapter I*, section 1.5.6 for the background literature), the second part of my PhD was conducted to investigate how the frequency as well as the pattern of postsynaptic stimulation both regulate the release of retrograde messengers and hence, inhibit

excitatory transmission. Importantly, the phenotype of the cell was assessed by using transgenic rats expressing either fluorescent OT or VP cells (see *Chapter II, Methods*). In *Chapter IV*, it was demonstrated for the first time that the frequency of stimulation of OT and VP neurons is correlated to the degree of inhibition of presynaptic glutamate release (see section 4.2.1) and that a clustering stimulation is more effective at suppressing excitatory neurotransmission, but only when this type of firing is elicited in VP neurons, at least when using the specific type of clustering described in section 4.2.2. Lastly, the aim of *chapter V* was to investigate the role of intra-dendritic calcium in the release of retrograde messengers considering that calcium influx, within the neurohypophysis, was shown to be a prerequisite in the release of peptides (Bicknell, 1988). Interestingly, our results showed that the progressive action potential broadening seen at higher frequencies of discharge is associated with a higher rise in intra-dendritic calcium per action potential. Therefore, this enhancement in intra-dendritic calcium influx observed at higher frequencies of discharge might explain why we observe a progressive increase in the degree of inhibition of glutamate release when reaching higher frequencies of electrical activity. Now that the most important findings from this thesis have been reported, the next sections will therefore discuss some aspects of my research that were not fully addressed within previous chapters and supplementary data will also be presented.

6.2. Differential short-term facilitation in OT and VP neurons at the onset of OVLT electrical stimulation

We observed in a subset of cells (i.e. for both OT and VP neurons) that initiating the stimulation of the OVLT at 0.2 Hz (i.e. every 5 seconds, as described in *Chapter IV*, section 4.2.1) elicited a gradual increase in the eEPSC amplitude. As illustrated in Figure 6.2.1.A and B, the increase of the eEPSC in both OT and VP neurons slowly appeared over the 60 pairs of stimulations performed on the OVLT (i.e. at the onset of the 5 minutes recording period). Interestingly, a difference in the kinetic of this response was observed between both cell types. When compared qualitatively, the progressive increase of the eEPSC

amplitude showed a slower time course for OT neurons (τ = 83.3 $\pm$ 39.6 s.; n = 7) compared to VP neurons (τ = 24 $\pm$ 7.8 s.; n = 8). As discussed below, presynaptic as well as postsynaptic mechanisms could be involved in this gradual response.

Previous studies have shown a short-term facilitation (STF) of mEPSC frequency in rat supraoptic neurons, following high frequency stimulation (HFS) of excitatory afferents, which relies on presynaptic calcium entry via VGCC (Quinlan et al., 2008; Quinlan and Hirasawa, 2013). Despite the fact that previous studies investigating the effect of stimulating presynaptic afferents with HFS used stimulation values $\geq$ 10 Hz (Kombian et al., 2000; Iremonger et al., 2011), our experiments suggest that a STF of the eEPSC amplitude was present when stimulating the OVLT at 0.2 Hz.

In our recording conditions, MNC were held at -70 mV, a membrane voltage at which AMPA receptors activation was shown to contribute to the inward conductance upon stimulation of glutamatergic inputs, with a small contribution of NMDA receptors, based on I-V relationship analysis (Panatier et al., 2006). The gradual increase of the eEPSC amplitude observed might therefore rely on a progressive increase in postsynaptic calcium influx via these receptors. Moreover, the slower time constant observed for OT neurons might be attributable to the fact that about 70% of these cells contain the buffering protein calretinin and calbindin, whereas the same proportion of VP neurons do not express those proteins (Arai et al., 1999), presumably leading to a faster calcium build up for the latter cell type. Lastly, as mentioned in the discussion from *Chapter V* (section 5.3.1), it is also possible that both cell types possess different calcium clearance mechanisms, which could explain the differential calcium build up found in our experiments. However, more work is needed to elucidate the locus of action of this response (i.e. presynaptic and/or postsynaptic).

During the induction of the postsynaptic cell conditioning train at different frequencies (i.e. from 0.1 Hz to 50 Hz) to elicit somato-dendritic release, the OVLT was not stimulated. Then, stimulation of

OVLT afferents was reintroduced within less than 2 seconds following the end of the postsynaptic cell conditioning. Because we used the same number of action potentials for all frequencies tested (i.e. 100 spikes), lower frequencies of stimulation resulted in a prolonged interval during which OVLT afferents were not stimulated electrically. For example, stimulating a MNC at 0.1 Hz to elicit 100 spikes took 1000 seconds (~16.6 minutes) with a proportional time for which the OVLT was not stimulated. Therefore, because not stimulating the OVLT for a prolonged period of time might also cause a reduction of the eEPSC amplitude upon reintroduction of the OVLT stimulation (such as what was seen in Fig. 6.2.1.A-C), we decided to investigate this effect. More precisely, we used the postsynaptic stimulation duration for all frequency tested (see Fig. 6.2.2.A) and applied this amount of time where no stimulation of the OVLT was performed and no postsynaptic spike conditioning was elicited, to investigate which impact the variable *time* would exert on the eEPSC amplitude upon reintroduction of the OVLT stimulation. As illustrated in Figure 6.2.2.B, longer periods of time without any stimulation resulted in a higher percent of inhibition of the eEPSC, measured as the eEPSC amplitude upon reintroduction of the OVLT stimulation. As mentioned earlier, the OVLT was always stimulated at a frequency of 0.2 Hz (i.e. every 5 seconds) to elicit an eEPSC in MNC. Importantly, not stimulating the OVLT nor the postsynaptic cell for such period of time (i.e. for 5 seconds, a *duration* equivalent to a 20 Hz postsynaptic conditioning) had no effect on the percent of inhibition of the eEPSC. This result suggests that the delay between frequencies of stimulation applied to the OVLT (i.e. 0.2 Hz; every 5 seconds) in all experiments conducted in *Chapter IV* was not too long to lead to an attenuation of the eEPSC amplitude.

The effect that the variable *time* (i.e. no stimulation) exerted on both cell types was averaged and subtracted from the frequency-dependent inhibition values observed following the postsynaptic spike train conditioning and appeared as their final form as presented in *Chapter IV* (section 4.2.1.D). In other words, the data presented in *Chapter IV* solely represent the effect that the variable *frequency-dependence* exerts on the inhibition of presynaptic glutamate release, rather than being contaminated

by the variable *time (or duration)* of the postsynaptic stimulation. Additional work will need to be done to investigate how this gradual increase in the eEPSC amplitude occurs at the onset of the OVLT stimulation as well as why long periods of time for which the OVLT is not stimulated also led to the same phenomenon when the stimulation was reintroduced. Finally, understanding why this response is slightly different in term of kinetic in both cell types and whether intracellular calcium buffering proteins play a role in this differential effect should also be address in the future.

6.3. Role of NMDA receptors in somato-dendritic release

Interestingly, a study has investigated the role of NMDA receptors in somato-dendritic release in lactating and virgin female rats (de Kock et al., 2004). Using nucleated outside-out patch, this group has shown that application of NMDA elicited an increase in capacitance measurement (C_m; a marker of exocytosis via membrane insertion) when the cell was held at −70 mV (i.e. below the threshold of action potential firing). Importantly, a histogram of the capacitance responses (i.e. endocytosis, failures or exocytosis) was drawn upon application of NMDA on SON neurons from lactating and virgin female rats. A higher incidence of exocytosis events was found for the first group, whereas a higher proportion of cells showed an increase in endocytosis events for virgin females, indicating that the reproductive status affected this capacitance response which appeared to be up-regulated towards exocytosis during lactation. Lastly, this study has shown using whole-cell patch clamp recordings that depolarizing OT neurons from -70 mV to -30 mV in the presence of CNQX, to block AMPA receptors, led to a significant decrease (~50%) in the frequency of IPSC. The idea was to relieve the Mg^{2+} block of NMDA receptors while staying below the threshold of action potential firing to show that the mechanism behind this presynaptic inhibition of GABAergic release relies on the activation of NMDA receptors. More precisely, application of APV prevented this effect (and other glutamate receptor blockers such as mGluR types II/III antagonists were used during this experiment to isolate the effect of NMDA receptors). Moreover, the retrograde messenger thought to mediate this inhibition of GABAergic neurotransmission appeared

to be the peptide OT, since blockade of OT receptors with dOVT also prevented the decrease in IPSC frequency.

Since NMDA receptor activation appears to play a role in the process of somato-dendritic release, we therefore decided to investigate if these receptors play a role in the release from the somato-dendritic compartment, measured via the inhibition of presynaptic glutamate release. These results appear as a preliminary form in Figure 6.3 where identified OT neurons were stimulated at either 10 Hz or 30 Hz in the absence and in the presence of the NMDA receptor channel blocker APV (100 μM). Interestingly, the results indicate that blocking NMDA receptors in OT neurons significantly decreased the percent of inhibition of presynaptic glutamate release (Control = 55.33 ± 10.3%; APV = 35.58 ± 8.27%; n = 9; paired *t*-test; P = 0.043).

The mechanism explaining how NMDA receptors are involved in the suppression of excitatory neurotransmission as seen in Figure 6.3 will need further investigation. Interestingly, it was shown that enhancing extracellular calcium concentration upon exogenous application of NMDA (from 2.4 to 5 mM Ca^{2+}) in lactating female rats led to an enhancement of exocytosis from the somato-dendritic compartment of OT neurons (de Kock et al., 2004), suggesting that calcium influx via NMDA receptors might help in the recruitment of retrograde messengers. Indeed, we have seen in *Chapter V* (Fig. 5.2.1.D-G) that OT and VP neurons filled with the calcium chelator BAPTA were ineffective at inhibiting presynaptic glutamate release following the induction of a postsynaptic spike train. Therefore, considering that NMDA receptors mediate the influx of calcium, these receptors might be a contributing factor in the rise of intracellular calcium, which could impact the release of retrograde messengers. Indeed, an important proportion of the eEPSC relies on NMDA current (Stern et al., 1999), which is largely attributable to the GluN2B subunit, since application of ifenprodil (a selective GluN2B antagonist) almost totally abolished the NMDA current, (Panatier et al., 2006), highlighting the importance NMDA receptors in the cationic conductance of MNC. Additionally, we saw in *Chapter IV* (Fig. 4.2.1.B) that the

decrease of the charge transfer following a postsynaptic 10 Hz spike train recovered after ~30 seconds for both cell types. It is thus possible that the slow decay offset of NMDA receptors participated in a prolonged release of retrograde messengers. Indeed, MNC express the GluN2D subunit (Monyer et al., 1994), which features the slowest time decay constant among all NMDA subunits. Lastly, how NMDA receptor activation regulates the release of retrograde messengers from VP neurons will also need to be addressed. It is important to mention that both males and virgin females were included in all experiments concerning somato-dendritic release in *Chapter IV*, and that eliciting action potentials in both genders was shown to effectively inhibit glutamate release. A study using juvenile male rats (P21-28) has shown that stimulating OT cells induced a decrease in the frequency of spontaneous IPSC, indicating that the release of retrograde messengers from the somato-dendritic compartment is also seen in male rats (de Kock et al., 2003). Now that we have seen which mechanisms regulate the inhibition of presynaptic neurotransmitter release, the next section will address in which physiological circumstances such inhibition is required.

6.4. What is the point of inhibiting presynaptic neurotransmitter release?

An important part of the work arising from this thesis was conducted to investigate the mechanisms regulating somato-dendritic secretion and hence, the inhibition of excitatory neurotransmitter release. Based on the findings from previous literature as well as my results, it is therefore relevant to understand in which context an inhibition of presynaptic neurotransmitter release would regulate presynaptic afferents to ensure an adequate amount of postsynaptic activity within a specific time frame.

The duration of presynaptic inhibition, following the release of postsynaptic messengers, was shown to vary among studies. Indeed, stimulating OT and VP cells in our conditions (10 Hz, 100 spikes) led to an inhibition of the eEPSC amplitude that recovered after ~30 seconds (*see Chapter IV*, section

4.2.1). Similarly, it was shown that stimulating VP cells at a mean frequency of 12 Hz (10 s. on, 10 s. off X 10) elicited a transient depression of the eEPSC that lasted less than ~1 minute and this response was completely blocked with the CB1 receptor blocker AM251 (Iremonger et al., 2011). However, the same study has demonstrated that pairing a presynaptic stimulation with a postsynaptic stimulation (10 s. on, 10 s. off X 10) led to a depression of the eEPSC that recovered only after 30 minutes. Lastly, this study has also shown that performing this double stimulation in the presence of AM251 led to a prolonged depression of the eEPSC amplitude (> 30 minutes) which is attributable to the activation of postsynaptic group I/II mGluR signaling and subsequent DYN release, which inhibited presynaptic glutamate release. Taken together, these results suggest that the type of stimulation performed as well as the nature of the messengers released differentially impact the amount of time for which presynaptic neurotransmission is suppressed.

MNC must regulate their synaptic input in a dynamic and reversible way, which seems to demonstrate the adaptability of these cells in different physiological contexts. For example, in the context of hypovolemia (i.e. a condition characterized by a decrease in water volume, notably via blood loss, see *Chapter I*, section 1.4.1), Ang II is released onto the SON where it triggers the release of EC from OT cells and thus, inhibit excitatory neurotransmission (Stachniak et al., 2014). On the contrary, application of Ang II onto VP neurons elicits the release of nitric oxide, which potentiates glutamatergic transmission onto these neurons. Therefore, these results indicate that both cell types have the ability to differentially regulate their synaptic inputs. During hypovolemia, VP release must be maximized to retain as much water as possible, while the plasma must remain isotonic, which is translated by the fact the OT release has no need to be potentiated, since this hormone was shown to promote natriuresis in rats (Verbalis et al., 1991).

Concerning the inhibition of presynaptic GABAergic release, it appears that the cell phenotype within the SON differentially regulates this response (Oliet et al., 2007). As a general rule, the Pr of GABA

onto OT cells displays PPF, whereas GABA transmission onto VP cells diplays paired-pulse depression (PPD). This study has shown that this low GABA Pr onto OT cells was due to the constitutive activation of OT receptors on these cells which subsequently release EC, leading to an inhibition GABAergic transmission. On the contrary, for VP neurons, neither the inhibition of CB1 receptors nor the blockade of VP receptors had an impact on the eIPSC amplitude, suggesting that the messengers EC and VP do not affect GABA Pr onto these cells. Why such difference is seen in the regulation of inhibitory inputs from both cell types remains to be determined. The fact that OT release is upregulated during lactation (Moos et al., 1989) might potentially explain why a decrease in inhibitory drive would be required from these cells, in order to maximize their hormone output.

We also have to keep in mind that no study so far has looked at the impact that somato-dendritic release exerts simultaneously onto the GABAergic and glutamateric neurotransmission. Since both types of fibers participate in the postsynaptic cell excitability (Yang et al., 1994), it would be relevant to consider how specific retrograde messengers regulate their synaptic input in a coordinated manner. Such question could be answered by analyzing the frequency of eIPSP and eIPSP following administration of action potentials in identified OT and VP neurons, and additionally, the use of different pharmacological blockers could help to elucidate which receptors are involved in this response. Lastly, a question emerges when looking at the literature concerning the inhibition of excitatory afferents via somato-dendritic release. More precisely, *why are excitatory afferents inhibited when MNC discharge action potentials?* Indeed, one might think that during dehydration (i.e. a state for which the release of OT and VP is maximized), this condition would also lead to an enhanced excitatory drive. Two hypothetical answers might be relevant in this case. First, since the OVLT increases its firing rate during dehydration (Sayer et al., 1984), MNC might release messengers to avoid exceeding a certain firing frequency, knowing that above ~35 Hz for OT cells (Dreifuss et al., 1971) and ~13 Hz for VP neurons (Bicknell, 1988), the hormone output is no longer optimized. Second, the excitatory drive plays a role in

the formation of phasic (Bourque et al., 1998) and clustering activity (see *Chapter III*) and the proportion of cells displaying these electrical firings increase during dehydration (Poulain et al., 1988). Therefore the release of retrograde messengers might help to maintain the excitatory drive in a range that favors the formation and the maintenance of these two types of electrical activity. Indeed, since postsynaptic depolarizations (induced via current injection) can greatly prolong phasic burst (Andrew and Dudek, 1983) and clustering activity (see *Chapter III*, section 3.2.1), an increase in excitatory drive could also elongate burst duration and lead to a *fatigue*, thus decreasing the hormone output from the nerve terminal, which should be optimized during dehydration. We have seen in *Chapter I* (*Introduction*, section 1.3.1) that DYN released via VP neurons promotes burst termination during phasic firing. Our results support a DYN-mediated presynaptic inhibition (see section 4.2.4) of excitatory transmission in VP neurons that could also participate in the maintenance of phasic firing, by preventing OVLT afferents from releasing excessive glutamate during dehydration.

Now that the role of different parameters regulating somato-dendritic release has been discussed, the next sections will briefly describe two models illustrating how the findings described in this thesis can be considered from a theoretical point of view. The first model is adapted from Hu and Bourque (1992) and will therefore integrate what has been previously found concerning clustering activity, with the addition of our new findings on how this rhythmic firing is modulated. The second model will illustrate which messengers are potentially released from OT and VP neurons to inhibit glutamate release.

6.5. Overview of the NMDA-induced clustering model

As illustrated in our *clustering activity model* (Fig. 6.5), synaptic endogenous glutamate release elicits clustered firing in MNC. Upon activation of NMDA receptors, the NMDA current (I_{NMDA}) increases the membrane voltage (Vm), which progressively relieves the Mg^{2+} block of these receptors. This

increase in membrane voltage, depending on the initial firing activity of the cell, will either trigger spiking activity or increase the rate of action potentials already observed, leading to the formation of a cluster in both cases. Importantly, we have shown in *Chapter III* (section 3.2.4) that exposing MNC to NT elongates the cluster duration. The subsequent increase in intracellular calcium concentration induces the activation of SK3 channels which have been shown to be crucial in the formation of pauses between cluster of activity and to regulate cluster length (see our findings in section 3.2.3). More precisely, activation of SK3 channels decreases the membrane voltage, which subsequently reduces I_{NMDA} via a block of NMDA receptors with Mg^{2+}. Finally, when the intracellular calcium concentration is lowered enough, a next rhythmic cycle can start where glutamate activates NMDA receptors.

6.6. Overview of the somato-dendritic release model for OT and VP neurons

The *somato-dendritic release model for OT neurons* (see *Chapter IV*, section 4.3.2) illustrates that back propagating action potentials invade the soma and dendrites of MNC. Importantly, we found a positive correlation between the action potential duration (which broadens at higher frequencies of discharge) and the amount of intra-dendritic calcium per spike (see *Chapter V*, section 5.2.2). In OT neurons, the amount of OT release might be too little to inhibit presynaptic glutamate release. Moreover, EC are thought to be released from the somato-dendritic compartment, presumably via an increase in intracellular calcium. The EC 2-AG is thought to contribute to the suppression of excitatory transmission by binding to presynaptic CB1 receptors, since DAGL activity, which hydrolyzes DAG in 2-AG, plays a role in this inhibitory response. It is also possible that OT neurons release the EC anandamide (AEA) via spiking-induced calcium entry (Ohno-Shosaku and Kano, 2014). Binding of EC to CB1 receptors suppress glutamate release via the activation of $G_{i/o}$ subunit, which was shown to inhibit VGCC, activate K^+ channels or inhibit the presynaptic release machinery (Ohno-Shosaku et al., 2005). Lastly, the opioid dynorphin (DYN), which is synthesized by VP cells, was shown to inhibit excitatory neurotransmission. It would therefore be possible that neighboring VP neurons constitutively release DYN on OT cells. Indeed,

activation of somatic κ-opioid receptors on OT neurons could in turn activate the $G_{i/o}$ subunit and trigger the release of retrograde messengers such as 2-AG via an increase in intracellular calcium, attributable to PLC activity (Inoue et al., 2003; Murthy et al., 2004). However, it is unlikely that an endogenous DYN tone constitutively activated presynaptic κ-opioid receptors and subsequently depressed glutamate release, since the charge transfer amplitude was not significantly different before and after bath application of nor-BNI (Control = 21.55 $\pm$ 3.21 pA, nor-BNI = 23.28 $\pm$ 3.83 pA; n = 8; paired *t*-test; P = 0.249).

The *somato-dendritic release model for VP neurons* is described in *Chapter IV*, section 4.3.3. As shown in *Chapter IV*, section 4.2.4, the peptide VP is probably not released in a sufficient amount to exert an impact on the spike-dependent retrograde inhibition of excitatory neurotransmission. However, the opioid DYN, which is co-package within VP-containing vesicles (Whitnall et al., 1983), inhibits excitatory neurotransmission by activating presynaptic κ-opioid receptors. The activation of presynaptic κ-opioid receptors, coupled to the $G_{i/o}$ subunit, was shown to depress glutamate release via a presynaptic inhibition of the vesicle fusion machinery (Iremonger and Bains, 2009). However, if postsynaptic κ-opioid receptor activation is involved in the depression of glutamate release remains to be elucidated, considering that the soma of MNC contains these receptors (Brown et al., 2000) and that DYN released from these cells might reach neighboring VP neurons. We can also rule out the possibility that a constitutive endogenous DYN tone activated presynaptic κ-opioid receptors, since no statistical difference in the charge transfer amplitude was found prior and following bath application of nor-BNI (Control = 22.32 $\pm$ 4.32 pA, nor-BNI = 25.04 $\pm$ 4.67 pA; n = 10; paired *t*-test; P = 0.264). Finally, we have shown that EC released from VP cells inhibit excitatory transmission, but interestingly, the DAGL pathway does not appear to be involved. It is also possible that the EC AEA is released from these cells following postsynaptic calcium rises, but this hypothesis remains to be confirmed.

6.7. Concluding remarks

At the beginning of my doctoral studies, I was first initiated to electrophysiology in order to investigate the mechanisms regulating clustering activity. During my research, I developed a strong interest in understanding how the release process is regulated from the somato-dendritic compartment of MNC and how messengers released from this area inhibit excitatory transmission. Despite the fact that the findings reported in this thesis are a small drop in the ocean of scientific literature, I am hoping that my contribution will bring at least a small advancement to the field of MNC.

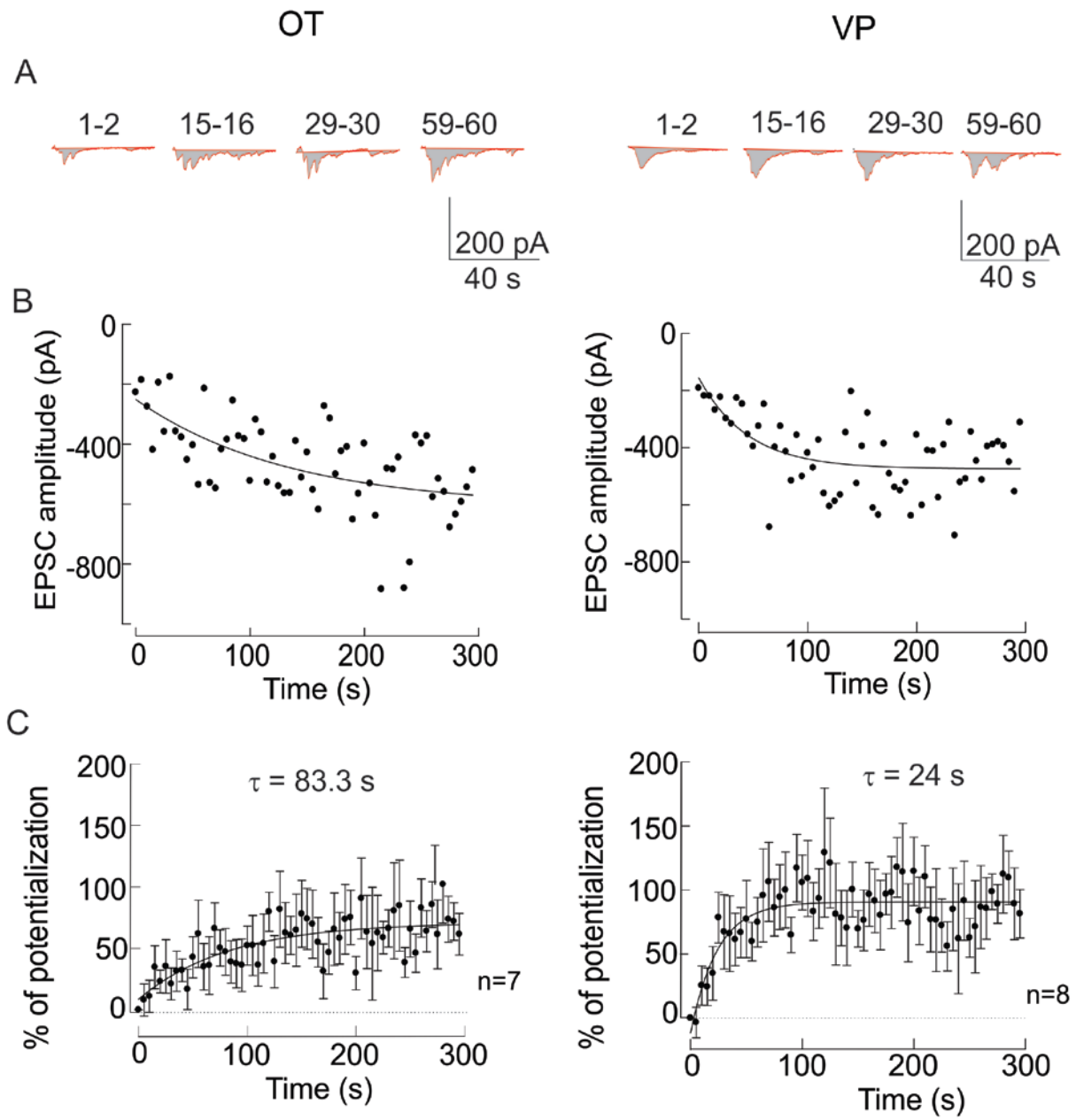

Figure 6.2.1. Differential short-term facilitation in OT and VP neurons at the onset of OVLT electrical stimulation

A, Gradual short-term facilitation (STF) of the eEPSC amplitude in an OT cell (left) and a VP cell (right) during the electrical stimulation of the OVLT at a frequency of 0.2 Hz, over a 5 minute recording period (the numbers on the top of traces represent the chronological sequence of the averaged eEPSC). **B**, Time course of the eEPSC STF in the same OT neuron (left) and VP neuron (right) during the electrical stimulation of the OVLT over 5 minutes (300 s.; every dot represents the acquisition of a single eEPSC). **C**, A slower time course of STF (expressed in % of potentialization) was found in OT neuron (left; τ = 83.3 s.; n = 7) compared to VP cells (right; τ = 24 s.; n = 8) when the OVLT was stimulated for 5 minutes.

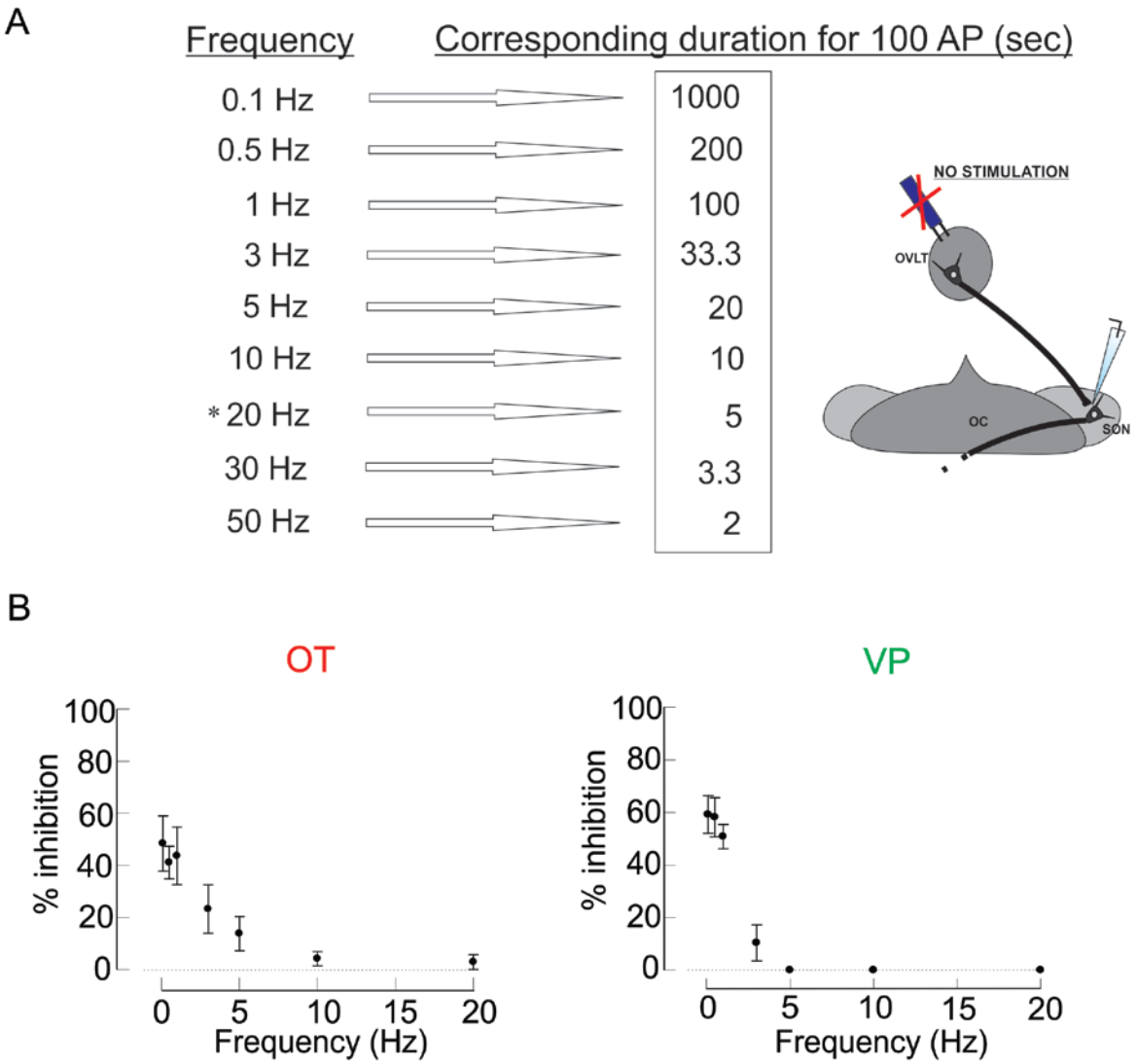

Figure 6.2.2. Time-dependent loss of short-term facilitation in OT and VP neurons

A, The time-dependent loss of short-term facilitation of the eEPSC was more pronounced when no electrical stimulation was applied to the OVLT for longer periods of time (measured upon reintroduction of the OVLT stimulation). The frequencies of stimulation used in *Chapter IV* to elicit spikes in OT and VP neurons (0.1-50 Hz) are associated with their corresponding duration (in seconds; inside the box) where no stimulation was performed on the OVLT for equivalent durations (*Note that eliciting 100 spikes in MNC at 20 Hz → for 5 sec, did not lead to a change in synaptic strength, considering that such interval was used to stimulate the OVLT for our experiments investigating the frequency-dependent inhibition of excitatory afferents). **B**, Relationship between the inhibition of the eEPSC and the time for which the OVLT was not stimulated (the frequencies on the X axis correspond to the amount of time for which the OVLT was not stimulated (see box in **A** for corresponding durations)).

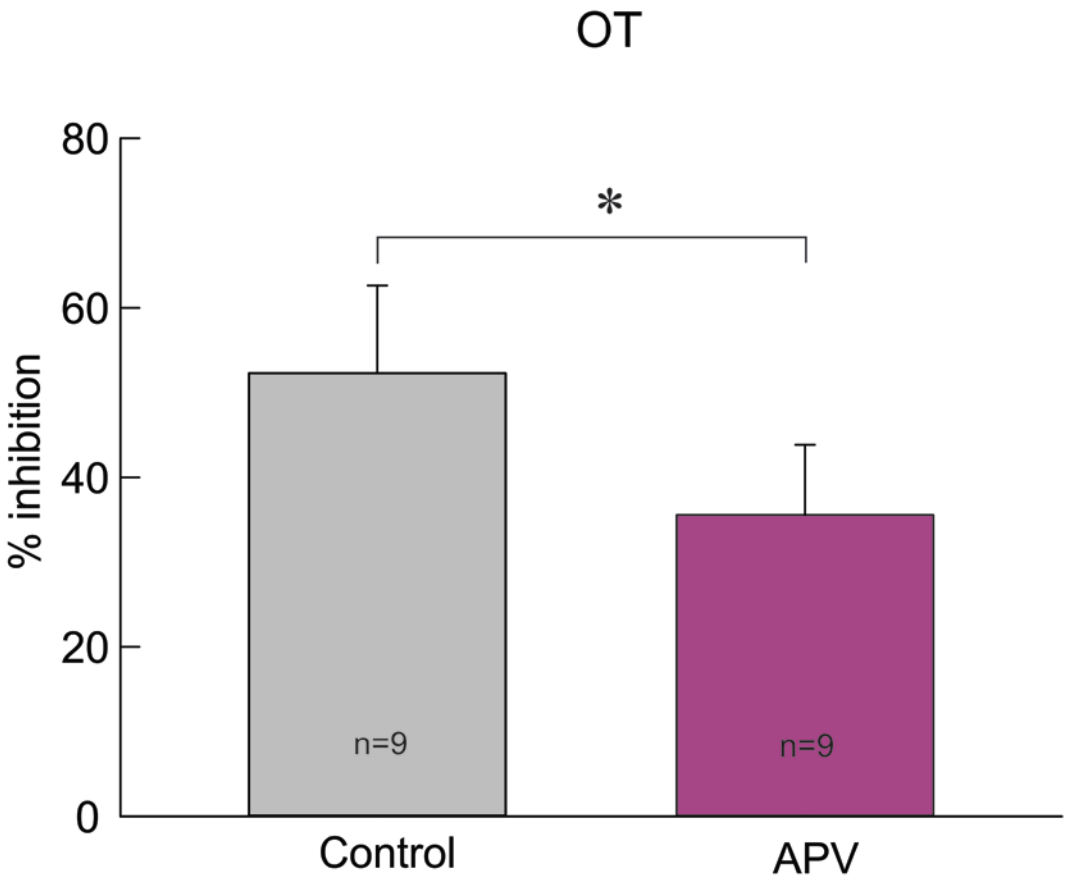

6.3. Contribution of NMDA receptors in spike-dependent somato-dendritic release from OT cells

Spike-dependent inhibition of excitatory transmission is significantly decreased in OT neurons following our mild stimulation protocol (10 Hz, 100 spikes) in the presence of the NMDA receptor blocker APV (100 μM). ∗P < 0.05

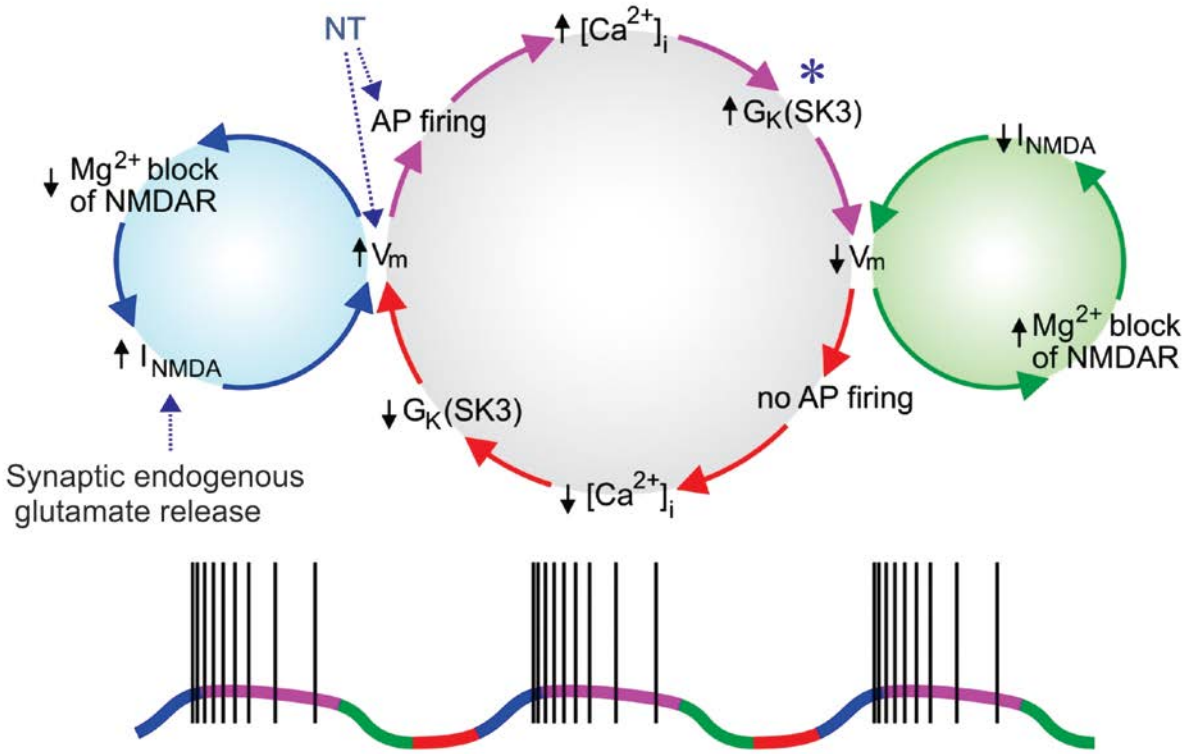

Figure 6.5. New clustering activity model

Stimulating the OVLT (10 Hz, 60 s.) elicits endogenous glutamate release, which induces clustering activity in MNC by increasing NMDA current. The subsequent increase in membrane voltage relieves the Mg^{2+} block of NMDA receptors and further enhances NMDA current, leading to a membrane depolarization and an increase in action potential firing. NT released onto MNC also depolarizes and excites SON neurons, leading to an increase in intracellular Ca^{2+} concentration, thus activating small conductance Ca^{2+}-activated K^{+} channels type 3 (SK3). Activation of SK3 channels repolarizes the cell and decreases action potential firing. Partially inhibiting these channels was shown to reduce the rate of clustering at positive voltages (see *chapter III*). Activation of SK3 channels, leading to a membrane repolarization, enables the Mg^{2+} block of NMDA receptors and promotes cluster termination (i.e. induction of the silent pause).

NT; neurotensin, V_m; membrane voltage, AP firing; action potential firing; I_{NMDA}; NMDA current

VII: REFERENCES

Acher R, Chauvet J (1988) Structure, processing and evolution of the neurohypophysial hormone-neurophysin precursors. Biochimie 70:1197-1207.

Acher R, Chauvet J (1995) The neurohypophysial endocrine regulatory cascade: precursors, mediators, receptors, and effectors. Frontiers in neuroendocrinology 16:237-289.

Adachi A, Niijima A, Jacobs HL (1976) An hepatic osmoreceptor mechanism in the rat: electrophysiological and behavioral studies. The American journal of physiology 231:1043-1049.

Adelman JP, Maylie J, Sah P (2012) Small-conductance Ca2+-activated K+ channels: form and function. Annual review of physiology 74:245-269.

Alonso G (1988) Effects of colchicine on the intraneuronal transport of secretory material prior to the axon: a morphofunctional study in hypothalamic neurosecretory neurons of the rat. Brain research 453:191-203.

Andersen LJ, Norsk P, Johansen LB, Christensen P, Engstrom T, Bie P (1998) Osmoregulatory control of renal sodium excretion after sodium loading in humans. The American journal of physiology 275:R1833-1842.

Andrew RD, Dudek FE (1983) Burst discharge in mammalian neuroendocrine cells involves an intrinsic regenerative mechanism. Science (New York, NY) 221:1050-1052.

Andrew RD, Dudek FE (1985) Spike broadening in magnocellular neuroendocrine cells of rat hypothalamic slices. Brain research 334:176-179.

Andrew RD, MacVicar BA, Dudek FE, Hatton GI (1981) Dye transfer through gap junctions between neuroendocrine cells of rat hypothalamus. Science (New York, NY) 211:1187-1189.

Antonijevic IA, Douglas AJ, Dye S, Bicknell RJ, Leng G, Russell JA (1995) Oxytocin antagonists delay the initiation of parturition and prolong its active phase in rats. The Journal of endocrinology 145:97-103.

Arai R, Jacobowitz DM, Deura S (1994) Heterogeneity in calbindin-D28k expression in oxytocin-containing magnocellular neurons of the rat hypothalamus. Histochemistry 101:9-12.

Arai R, Jacobowitz DM, Hida T (1999) Calbindin D28k and calretinin in oxytocin and vasopressin neurons of the rat supraoptic nucleus. A triple-labeling immunofluorescence study. Cell and tissue research 298:11-19.

Armstrong WE (1995) Morphological and electrophysiological classification of hypothalamic supraoptic neurons. Progress in neurobiology 47:291-339.

Armstrong WE, Tian M, Wong H (1996) Electron microscopic analysis of synaptic inputs from the median preoptic nucleus and adjacent regions to the supraoptic nucleus in the rat. The Journal of comparative neurology 373:228-239.

Arnauld E, du Pont J (1982) Vasopressin release and firing of supraoptic neurosecretory neurones during drinking in the dehydrated monkey. Pflugers Archiv : European journal of physiology 394:195-201.

Baylis PH, Thompson CJ (1988) Osmoregulation of vasopressin secretion and thirst in health and disease. Clinical endocrinology 29:549-576.

Belin V, Moos F, Richard P (1984) Synchronization of oxytocin cells in the hypothalamic paraventricular and supraoptic nuclei in suckled rats: direct proof with paired extracellular recordings. Experimental brain research Experimentelle Hirnforschung Experimentation cerebrale 57:201-203.

Bicknell RJ (1988) Optimizing release from peptide hormone secretory nerve terminals. The Journal of experimental biology 139:51-65.

Bicknell RJ, Leng G (1981) Relative efficiency of neural firing patterns for vasopressin release in vitro. Neuroendocrinology 33:295-299.
Bicknell RJ, Brown D, Chapman C, Hancock PD, Leng G (1984) Reversible fatigue of stimulus-secretion coupling in the rat neurohypophysis. The Journal of physiology 348:601-613.
Bjorklund A, Lindvall O (1975) Dopamine in dendrites of substantia nigra neurons: suggestions for a role in dendritic terminals. Brain research 83:531-537.
Black MP, Reavis RH, Grober MS (2004) Socially induced sex change regulates forebrain isotocin in Lythrypnus dalli. Neuroreport 15:185-189.
Boer K, Lincoln DW, Swaab DF (1975) Effects of electrical stimulation of the neurohypophysis on labour in the rat. The Journal of endocrinology 65:163-176.
Bolignano D, Cabassi A, Fiaccadori E, Ghigo E, Pasquali R, Peracino A, Peri A, Plebani M, Santoro A, Settanni F, Zoccali C (2014) Copeptin (CTproAVP), a new tool for understanding the role of vasopressin in pathophysiology. Clinical chemistry and laboratory medicine 52:1447-1456.
Bosch OJ, Neumann ID (2012) Both oxytocin and vasopressin are mediators of maternal care and aggression in rodents: from central release to sites of action. Hormones and behavior 61:293-303.
Bourque CW (1989) Ionic basis for the intrinsic activation of rat supraoptic neurones by hyperosmotic stimuli. The Journal of physiology 417:263-277.
Bourque CW (2008) Central mechanisms of osmosensation and systemic osmoregulation. Nature reviews Neuroscience 9:519-531.
Bourque CW, Renaud LP (1984) Activity patterns and osmosensitivity of rat supraoptic neurones in perfused hypothalamic explants. The Journal of physiology 349:631-642.
Bourque CW, Renaud LP (1985) Activity dependence of action potential duration in rat supraoptic neurosecretory neurones recorded in vitro. The Journal of physiology 363:429-439.
Bourque CW, Brown DA (1987) Apamin and d-tubocurarine block the afterhyperpolarization of rat supraoptic neurosecretory neurons. Neuroscience letters 82:185-190.
Bourque CW, Oliet SH (1997) Osmoreceptors in the central nervous system. Annual review of physiology 59:601-619.
Bourque CW, Randle JC, Renaud LP (1985) Calcium-dependent potassium conductance in rat supraoptic nucleus neurosecretory neurons. Journal of neurophysiology 54:1375-1382.
Bourque CW, Kirkpatrick K, Jarvis CR (1998) Extrinsic modulation of spike afterpotentials in rat hypothalamoneurohypophysial neurons. Cellular and molecular neurobiology 18:3-12.
Brimble MJ, Dyball RE (1977) Characterization of the responses of oxytocin- and vasopressin-secreting neurones in the supraoptic nucleus to osmotic stimulation. The Journal of physiology 271:253-271.
Brocard F, Verdier D, Arsenault I, Lund JP, Kolta A (2006) Emergence of intrinsic bursting in trigeminal sensory neurons parallels the acquisition of mastication in weanling rats. Journal of neurophysiology 96:2410-2424.
Brown CH, Bourque CW (2004) Autocrine feedback inhibition of plateau potentials terminates phasic bursts in magnocellular neurosecretory cells of the rat supraoptic nucleus. The Journal of physiology 557:949-960.
Brown CH, Ludwig M, Leng G (1998) kappa-opioid regulation of neuronal activity in the rat supraoptic nucleus in vivo. The Journal of neuroscience : the official journal of the Society for Neuroscience 18:9480-9488.
Brown CH, Russell JA, Leng G (2000) Opioid modulation of magnocellular neurosecretory cell activity. Neuroscience research 36:97-120.

Brown CH, Leng G, Ludwig M, Bourque CW (2006) Endogenous activation of supraoptic nucleus kappa-opioid receptors terminates spontaneous phasic bursts in rat magnocellular neurosecretory cells. Journal of neurophysiology 95:3235-3244.

Brown SP, Safo PK, Regehr WG (2004) Endocannabinoids inhibit transmission at granule cell to Purkinje cell synapses by modulating three types of presynaptic calcium channels. The Journal of neuroscience : the official journal of the Society for Neuroscience 24:5623-5631.

Carson DS, Garner JP, Hyde SA, Libove RA, Berquist SW, Hornbeak KB, Jackson LP, Sumiyoshi RD, Howerton CL, Hannah SL, Partap S, Phillips JM, Hardan AY, Parker KJ (2015) Arginine Vasopressin Is a Blood-Based Biomarker of Social Functioning in Children with Autism. PloS one 10:e0132224.

Cazalis M, Dayanithi G, Nordmann JJ (1985) The role of patterned burst and interburst interval on the excitation-coupling mechanism in the isolated rat neural lobe. The Journal of physiology 369:45-60.

Chakfe Y, Bourque CW (2000) Excitatory peptides and osmotic pressure modulate mechanosensitive cation channels in concert. Nature neuroscience 3:572-579.

Chakfe Y, Bourque CW (2001) Peptidergic excitation of supraoptic nucleus neurons: involvement of stretch-inactivated cation channels. Experimental neurology 171:210-218.

Chevaleyre V, Moos FC, Desarmenien MG (2001) Correlation between electrophysiological and morphological characteristics during maturation of rat supraoptic neurons. The European journal of neuroscience 13:1136-1146.

Chevaleyre V, Moos FC, Desarmenien MG (2002) Interplay between presynaptic and postsynaptic activities is required for dendritic plasticity and synaptogenesis in the supraoptic nucleus. The Journal of neuroscience : the official journal of the Society for Neuroscience 22:265-273.

Chevaleyre V, Dayanithi G, Moos FC, Desarmenien MG (2000) Developmental regulation of a local positive autocontrol of supraoptic neurons. The Journal of neuroscience : the official journal of the Society for Neuroscience 20:5813-5819.

Choi-Kwon S, Baertschi AJ (1991) Splanchnic osmosensation and vasopressin: mechanisms and neural pathways. The American journal of physiology 261:E18-25.

Ciura S, Bourque CW (2006) Transient receptor potential vanilloid 1 is required for intrinsic osmoreception in organum vasculosum lamina terminalis neurons and for normal thirst responses to systemic hyperosmolality. The Journal of neuroscience : the official journal of the Society for Neuroscience 26:9069-9075.

Coomarasamy A, Knox EM, Gee H, Khan KS (2002) Oxytocin antagonists for tocolysis in preterm labour -- a systematic review. Medical science monitor : international medical journal of experimental and clinical research 8:Ra268-273.

Csaki A, Kocsis K, Kiss J, Halasz B (2002) Localization of putative glutamatergic/aspartatergic neurons projecting to the supraoptic nucleus area of the rat hypothalamus. The European journal of neuroscience 16:55-68.

Cui LN, Saeb-Parsy K, Dyball RE (1997) Neurones in the supraoptic nucleus of the rat are regulated by a projection from the suprachiasmatic nucleus. The Journal of physiology 502 (Pt 1):149-159.

da Silva MP, Merino RM, Mecawi AS, Moraes DJ, Varanda WA (2015) In vitro differentiation between oxytocin- and vasopressin-secreting magnocellular neurons requires more than one experimental criterion. Molecular and cellular endocrinology 400:102-111.

Dayanithi G, Widmer H, Richard P (1996) Vasopressin-induced intracellular Ca2+ increase in isolated rat supraoptic cells. The Journal of physiology 490 (Pt 3):713-727.

de Kock CP, Burnashev N, Lodder JC, Mansvelder HD, Brussaard AB (2004) NMDA receptors induce somatodendritic secretion in hypothalamic neurones of lactating female rats. The Journal of physiology 561:53-64.

de Kock CP, Wierda KD, Bosman LW, Min R, Koksma JJ, Mansvelder HD, Verhage M, Brussaard AB (2003) Somatodendritic secretion in oxytocin neurons is upregulated during the female reproductive cycle. The Journal of neuroscience : the official journal of the Society for Neuroscience 23:2726-2734.

Deen PM, Weghuis DO, Sinke RJ, Geurts van Kessel A, Wieringa B, van Os CH (1994) Assignment of the human gene for the water channel of renal collecting duct Aquaporin 2 (AQP2) to chromosome 12 region q12-->q13. Cytogenetics and cell genetics 66:260-262.

Denk W, Strickler JH, Webb WW (1990) Two-photon laser scanning fluorescence microscopy. Science (New York, NY) 248:73-76.

Di Scala-Guenot D, Strosser MT, Richard P (1987) Electrical stimulations of perifused magnocellular nuclei in vitro elicit Ca2+-dependent, tetrodotoxin-insensitive release of oxytocin and vasopressin. Neuroscience letters 76:209-214.

Doherty FC, Sladek CD (2011) NMDA receptor subunit expression in the supraoptic nucleus of adult rats: dominance of NR2B and NR2D. Brain research 1388:89-99.

Domes G, Heinrichs M, Michel A, Berger C, Herpertz SC (2007) Oxytocin improves "mind-reading" in humans. Biological psychiatry 61:731-733.

Donaldson ZR, Spiegel L, Young LJ (2010) Central vasopressin V1a receptor activation is independently necessary for both partner preference formation and expression in socially monogamous male prairie voles. Behavioral neuroscience 124:159-163.

Dreifuss JJ, Kalnins I, Kelly JS, Ruf KB (1971) Action potentials and release of neurohypophysial hormones in vitro. The Journal of physiology 215:805-817.

Dyball RE, Kemplay SK (1982) Dendritic trees of neurones in the rat supraoptic nucleus. Neuroscience 7:223-230.

Erickson KR, Ronnekleiv OK, Kelly MJ (1993) Role of a T-type calcium current in supporting a depolarizing potential, damped oscillations, and phasic firing in vasopressinergic guinea pig supraoptic neurons. Neuroendocrinology 57:789-800.

Faber ES (2009) Functions and modulation of neuronal SK channels. Cell biochemistry and biophysics 55:127-139.

Faber ES, Sah P (2003) Ca2+-activated K+ (BK) channel inactivation contributes to spike broadening during repetitive firing in the rat lateral amygdala. The Journal of physiology 552:483-497.

Fisher TE, Bourque CW (1995) Voltage-gated calcium currents in the magnocellular neurosecretory cells of the rat supraoptic nucleus. The Journal of physiology 486 (Pt 3):571-580.

Foehring RC, Armstrong WE (1996) Pharmacological dissection of high-voltage-activated Ca2+ current types in acutely dissociated rat supraoptic magnocellular neurons. Journal of neurophysiology 76:977-983.

Fossier P, Tauc L, Baux G (1999) Calcium transients and neurotransmitter release at an identified synapse. Trends in neurosciences 22:161-166.

Freund-Mercier MJ, Richard P (1984) Electrophysiological evidence for facilitatory control of oxytocin neurones by oxytocin during suckling in the rat. The Journal of physiology 352:447-466.

Freund TF, Katona I, Piomelli D (2003) Role of endogenous cannabinoids in synaptic signaling. Physiological reviews 83:1017-1066.

Garcia ML, Knaus HG, Munujos P, Slaughter RS, Kaczorowski GJ (1995) Charybdotoxin and its effects on potassium channels. The American journal of physiology 269:C1-10.

Garlov PE (2005) Plasticity of nonapeptidergic neurosecretory cells in fish hypothalamus and neurohypophysis. International review of cytology 245:123-170.

Godin CM, Ferguson SS (2012) Biased agonism of the angiotensin II type 1 receptor. Mini reviews in medicinal chemistry 12:812-816.

Goodson JL, Bass AH (2000) Forebrain peptides modulate sexually polymorphic vocal circuitry. Nature 403:769-772.
Goodson JL, Evans AK, Bass AH (2003) Putative isotocin distributions in sonic fish: relation to vasotocin and vocal-acoustic circuitry. The Journal of comparative neurology 462:1-14.
Gordon I, Zagoory-Sharon O, Schneiderman I, Leckman JF, Weller A, Feldman R (2008) Oxytocin and cortisol in romantically unattached young adults: associations with bonding and psychological distress. Psychophysiology 45:349-352.
Gouzenes L, Desarmenien MG, Hussy N, Richard P, Moos FC (1998) Vasopressin regularizes the phasic firing pattern of rat hypothalamic magnocellular vasopressin neurons. The Journal of neuroscience : the official journal of the Society for Neuroscience 18:1879-1885.
Greffrath W, Magerl W, Disque-Kaiser U, Martin E, Reuss S, Boehmer G (2004) Contribution of Ca2+-activated K+ channels to hyperpolarizing after-potentials and discharge pattern in rat supraoptic neurones. Journal of neuroendocrinology 16:577-588.
Habermann E (1984) Apamin. Pharmacology & therapeutics 25:255-270.
Harikumar KG, Cawston EE, Lam PC, Patil A, Orry A, Henke BR, Abagyan R, Christopoulos A, Sexton PM, Miller LJ (2013) Molecular basis for benzodiazepine agonist action at the type 1 cholecystokinin receptor. The Journal of biological chemistry 288:21082-21095.
Hatton GI, Tweedle CD (1982) Magnocellular neuropeptidergic neurons in hypothalamus: increases in membrane apposition and number of specialized synapses from pregnancy to lactation. Brain research bulletin 8:197-204.
Higuchi T, Tadokoro Y, Honda K, Negoro H (1986) Detailed analysis of blood oxytocin levels during suckling and parturition in the rat. The Journal of endocrinology 110:251-256.
Hirasawa M, Schwab Y, Natah S, Hillard CJ, Mackie K, Sharkey KA, Pittman QJ (2004) Dendritically released transmitters cooperate via autocrine and retrograde actions to inhibit afferent excitation in rat brain. The Journal of physiology 559:611-624.
Honda K, Negoro H, Higuchi T, Tadokoro Y (1987) Activation of neurosecretory cells by osmotic stimulation of anteroventral third ventricle. The American journal of physiology 252:R1039-1045.
Hu B, Bourque CW (1992) NMDA receptor-mediated rhythmic bursting activity in rat supraoptic nucleus neurones in vitro. The Journal of physiology 458:667-687.
Hu SS, Ho YC, Chiou LC (2014) No more pain upon Gq-protein-coupled receptor activation: role of endocannabinoids. The European journal of neuroscience 39:467-484.
Huang W, Lee SL, Sjoquist M (1995) Natriuretic role of endogenous oxytocin in male rats infused with hypertonic NaCl. The American journal of physiology 268:R634-640.
Inenaga K, Honda E, Hirakawa T, Nakamura S, Yamashita H (1998) Glutamatergic synaptic inputs to mouse supraoptic neurons in calcium-free medium in vitro. Journal of neuroendocrinology 10:1-7.
Inoue M, Kawashima T, Allen RG, Ueda H (2003) Nocistatin and prepro-nociceptin/orphanin FQ 160-187 cause nociception through activation of Gi/o in capsaicin-sensitive and of Gs in capsaicin-insensitive nociceptors, respectively. The Journal of pharmacology and experimental therapeutics 306:141-146.
Insel TR, Shapiro LE (1992) Oxytocin receptor distribution reflects social organization in monogamous and polygamous voles. Proceedings of the National Academy of Sciences of the United States of America 89:5981-5985.
Iremonger KJ, Bains JS (2007) Integration of asynchronously released quanta prolongs the postsynaptic spike window. The Journal of neuroscience : the official journal of the Society for Neuroscience 27:6684-6691.

Iremonger KJ, Bains JS (2009) Retrograde opioid signaling regulates glutamatergic transmission in the hypothalamus. The Journal of neuroscience : the official journal of the Society for Neuroscience 29:7349-7358.
Iremonger KJ, Kuzmiski JB, Baimoukhametova DV, Bains JS (2011) Dual regulation of anterograde and retrograde transmission by endocannabinoids. The Journal of neuroscience : the official journal of the Society for Neuroscience 31:12011-12020.
Jackson MB, Konnerth A, Augustine GJ (1991) Action potential broadening and frequency-dependent facilitation of calcium signals in pituitary nerve terminals. Proceedings of the National Academy of Sciences of the United States of America 88:380-384.
Jacobsson G, Meister B (1996) Molecular components of the exocytotic machinery in the rat pituitary gland. Endocrinology 137:5344-5356.
Jhamandas JH, Lind RW, Renaud LP (1989) Angiotensin II may mediate excitatory neurotransmission from the subfornical organ to the hypothalamic supraoptic nucleus: an anatomical and electrophysiological study in the rat. Brain research 487:52-61.
Jobst A, Dehning S, Ruf S, Notz T, Buchheim A, Henning-Fast K, Meissner D, Meyer S, Bondy B, Muller N, Zill P (2014) Oxytocin and vasopressin levels are decreased in the plasma of male schizophrenia patients. Acta neuropsychiatrica 26:347-355.
Joe N, Scott V, Brown CH (2014) Glial regulation of extrasynaptic NMDA receptor-mediated excitation of supraoptic nucleus neurones during dehydration. Journal of neuroendocrinology 26:35-42.
Jones CW, Pickering BT (1972) Intra-axonal transport and turnover of neurohypophysial hormones in the rat. The Journal of physiology 227:553-564.
Joux N, Chevaleyre V, Alonso G, Boissin-Agasse L, Moos FC, Desarmenien MG, Hussy N (2001) High voltage-activated Ca2+ currents in rat supraoptic neurones: biophysical properties and expression of the various channel alpha1 subunits. Journal of neuroendocrinology 13:638-649.
Katoh A, Fujihara H, Ohbuchi T, Onaka T, Hashimoto T, Kawata M, Suzuki H, Ueta Y (2011) Highly visible expression of an oxytocin-monomeric red fluorescent protein 1 fusion gene in the hypothalamus and posterior pituitary of transgenic rats. Endocrinology 152:2768-2774.
Kelamangalath L, Dravid SM, George J, Aldrich JV, Murray TF (2011) kappa-Opioid receptor inhibition of calcium oscillations in spinal cord neurons. Molecular pharmacology 79:1061-1071.
Kirkpatrick K, Bourque CW (1991) Dual role for calcium in the control of spike duration in rat supraoptic neuroendocrine cells. Neuroscience letters 133:271-274.
Kirkpatrick K, Bourque CW (1995) Effects of neurotensin on rat supraoptic nucleus neurones in vitro. The Journal of physiology 482 (Pt 2):373-381.
Kirkpatrick K, Bourque CW (1996) Activity dependence and functional role of the apamin-sensitive K+ current in rat supraoptic neurones in vitro. The Journal of physiology 494 (Pt 2):389-398.
Kleiner SM (1999) Water: an essential but overlooked nutrient. Journal of the American Dietetic Association 99:200-206.
Knobloch HS, Grinevich V (2014) Evolution of oxytocin pathways in the brain of vertebrates. Frontiers in behavioral neuroscience 8:31.
Knobloch HS, Charlet A, Hoffmann LC, Eliava M, Khrulev S, Cetin AH, Osten P, Schwarz MK, Seeburg PH, Stoop R, Grinevich V (2012) Evoked axonal oxytocin release in the central amygdala attenuates fear response. Neuron 73:553-566.
Ko D, Wilson CJ, Lobb CJ, Paladini CA (2012) Detection of bursts and pauses in spike trains. Journal of neuroscience methods 211:145-158.
Kombian SB, Mouginot D, Pittman QJ (1997) Dendritically released peptides act as retrograde modulators of afferent excitation in the supraoptic nucleus in vitro. Neuron 19:903-912.

Kombian SB, Hirasawa M, Mouginot D, Chen X, Pittman QJ (2000) Short-term potentiation of miniature excitatory synaptic currents causes excitation of supraoptic neurons. Journal of neurophysiology 83:2542-2553.
Komori Y, Tanaka M, Kuba M, Ishii M, Abe M, Kitamura N, Verkhratsky A, Shibuya I, Dayanithi G (2010) Ca(2+) homeostasis, Ca(2+) signalling and somatodendritic vasopressin release in adult rat supraoptic nucleus neurones. Cell calcium 48:324-332.
Kosfeld M, Heinrichs M, Zak PJ, Fischbacher U, Fehr E (2005) Oxytocin increases trust in humans. Nature 435:673-676.
Kreitzer AC, Regehr WG (2001) Retrograde inhibition of presynaptic calcium influx by endogenous cannabinoids at excitatory synapses onto Purkinje cells. Neuron 29:717-727.
Kristal-Boneh E, Glusman JG, Chaemovitz C, Cassuto Y (1988) Improved thermoregulation caused by forced water intake in human desert dwellers. European journal of applied physiology and occupational physiology 57:220-224.
Lambert RC, Moos FC, Richard P (1993) Action of endogenous oxytocin within the paraventricular or supraoptic nuclei: a powerful link in the regulation of the bursting pattern of oxytocin neurons during the milk-ejection reflex in rats. Neuroscience 57:1027-1038.
Lambert RC, Dayanithi G, Moos FC, Richard P (1994) A rise in the intracellular Ca2+ concentration of isolated rat supraoptic cells in response to oxytocin. The Journal of physiology 478 (Pt 2):275-287.
Leathers VL, Linse S, Forsen S, Norman AW (1990) Calbindin-D28K, a 1 alpha,25-dihydroxyvitamin D3-induced calcium-binding protein, binds five or six Ca2+ ions with high affinity. The Journal of biological chemistry 265:9838-9841.
Leng G, Russell JA (1999) Coming to term with GABA. The Journal of physiology 516 (Pt 2):Vi.
Li Z, Hatton GI (1996) Oscillatory bursting of phasically firing rat supraoptic neurones in low-Ca2+ medium: Na+ influx, cytosolic Ca2+ and gap junctions. The Journal of physiology 496 (Pt 2):379-394.
Li Z, Decavel C, Hatton GI (1995) Calbindin-D28k: role in determining intrinsically generated firing patterns in rat supraoptic neurones. The Journal of physiology 488 (Pt 3):601-608.
Lim MM, Young LJ (2004) Vasopressin-dependent neural circuits underlying pair bond formation in the monogamous prairie vole. Neuroscience 125:35-45.
Lincoln DW (1974) Does a mechanism of negative feedback determine the intermittent release of oxytocin during suckling? The Journal of endocrinology 60:193-194.
Lincoln DW, Wakerley JB (1974) Electrophysiological evidence for the activation of supraoptic neurones during the release of oxytocin. The Journal of physiology 242:533-554.
Llano I, Leresche N, Marty A (1991) Calcium entry increases the sensitivity of cerebellar Purkinje cells to applied GABA and decreases inhibitory synaptic currents. Neuron 6:565-574.
Lovinger DM (2008) Presynaptic modulation by endocannabinoids. Handbook of experimental pharmacology:435-477.
Ludwig M, Leng G (1997) Autoinhibition of supraoptic nucleus vasopressin neurons in vivo: a combined retrodialysis/electrophysiological study in rats. The European journal of neuroscience 9:2532-2540.
Ludwig M, Stern J (2015) Multiple signalling modalities mediated by dendritic exocytosis of oxytocin and vasopressin. Philosophical transactions of the Royal Society of London Series B, Biological sciences 370.
Ludwig M, Callahan MF, Morris M (1995) Effects of tetrodotoxin on osmotically stimulated central and peripheral vasopressin and oxytocin release. Neuroendocrinology 62:619-627.

Ludwig M, Callahan MF, Neumann I, Landgraf R, Morris M (1994) Systemic osmotic stimulation increases vasopressin and oxytocin release within the supraoptic nucleus. Journal of neuroendocrinology 6:369-373.
Ludwig M, Sabatier N, Bull PM, Landgraf R, Dayanithi G, Leng G (2002) Intracellular calcium stores regulate activity-dependent neuropeptide release from dendrites. Nature 418:85-89.
Ludwig M, Bull PM, Tobin VA, Sabatier N, Landgraf R, Dayanithi G, Leng G (2005) Regulation of activity-dependent dendritic vasopressin release from rat supraoptic neurones. The Journal of physiology 564:515-522.
LuQui IJ, Fox CL (1976) The supraoptic nucleus and the supraopticohypophysial tract in the monkey (Macaca mulatta). The Journal of comparative neurology 168:7-39.
MacGregor DJ, Leng G (2012) Phasic firing in vasopressin cells: understanding its functional significance through computational models. PLoS computational biology 8:e1002740.
Maejima T, Hashimoto K, Yoshida T, Aiba A, Kano M (2001) Presynaptic inhibition caused by retrograde signal from metabotropic glutamate to cannabinoid receptors. Neuron 31:463-475.
McEwen BB (2004) General introduction to vasopressin and oxytocin: structure/metabolism, evolutionary aspects, neural pathway/receptor distribution, and functional aspects relevant to memory processing. Advances in pharmacology (San Diego, Calif) 50:1-50, 655-708.
McKinley MJ, Hards DK, Oldfield BJ (1994) Identification of neural pathways activated in dehydrated rats by means of Fos-immunohistochemistry and neural tracing. Brain research 653:305-314.
Montecucco C, Schiavo G, Pantano S (2005) SNARE complexes and neuroexocytosis: how many, how close? Trends in biochemical sciences 30:367-372.
Monyer H, Burnashev N, Laurie DJ, Sakmann B, Seeburg PH (1994) Developmental and regional expression in the rat brain and functional properties of four NMDA receptors. Neuron 12:529-540.
Moos F, Freund-Mercier MJ, Guerne Y, Guerne JM, Stoeckel ME, Richard P (1984) Release of oxytocin and vasopressin by magnocellular nuclei in vitro: specific facilitatory effect of oxytocin on its own release. The Journal of endocrinology 102:63-72.
Moos F, Poulain DA, Rodriguez F, Guerne Y, Vincent JD, Richard P (1989) Release of oxytocin within the supraoptic nucleus during the milk ejection reflex in rats. Experimental brain research Experimentelle Hirnforschung Experimentation cerebrale 76:593-602.
Morgan JI, Cohen DR, Hempstead JL, Curran T (1987) Mapping patterns of c-fos expression in the central nervous system after seizure. Science (New York, NY) 237:192-197.
Morquette P, Verdier D, Kadala A, Fethiere J, Philippe AG, Robitaille R, Kolta A (2015) An astrocyte-dependent mechanism for neuronal rhythmogenesis. 18:844-854.
Murthy KS, Zhou H, Huang J, Pentyala SN (2004) Activation of PLC-delta1 by Gi/o-coupled receptor agonists. American journal of physiology Cell physiology 287:C1679-1687.
Nagerl UV, Novo D, Mody I, Vergara JL (2000) Binding kinetics of calbindin-D(28k) determined by flash photolysis of caged Ca(2+). Biophysical journal 79:3009-3018.
Negoro H, Uchide K, Honda K, Higuchi T (1985) Facilitatory effect of antidromic stimulation on milk ejection-related activation of oxytocin neurons during suckling in the rat. Neuroscience letters 59:21-25.
O'Regan MH, Cobbett P (1993) Somatic currents contribute to frequency-dependent spike-broadening in supraoptic neuroendocrine cells. Neuroscience letters 161:169-173.
Ohno-Shosaku T, Kano M (2014) Endocannabinoid-mediated retrograde modulation of synaptic transmission. Current opinion in neurobiology 29:1-8.
Ohno-Shosaku T, Maejima T, Kano M (2001) Endogenous cannabinoids mediate retrograde signals from depolarized postsynaptic neurons to presynaptic terminals. Neuron 29:729-738.

Ohno-Shosaku T, Hashimotodani Y, Maejima T, Kano M (2005) Calcium signaling and synaptic modulation: regulation of endocannabinoid-mediated synaptic modulation by calcium. Cell calcium 38:369-374.
Okuya S, Inenaga K, Kaneko T, Yamashita H (1987) Angiotensin II sensitive neurons in the supraoptic nucleus, subfornical organ and anteroventral third ventricle of rats in vitro. Brain research 402:58-67.
Oliet SH, Bourque CW (1993) Mechanosensitive channels transduce osmosensitivity in supraoptic neurons. Nature 364:341-343.
Oliet SH, Baimoukhametova DV, Piet R, Bains JS (2007) Retrograde regulation of GABA transmission by the tonic release of oxytocin and endocannabinoids governs postsynaptic firing. The Journal of neuroscience : the official journal of the Society for Neuroscience 27:1325-1333.
Orloff J, Handler JS (1962) The similarity of effects of vasopressin, adenosine-3',5'-phosphate (cyclic AMP) and theophylline on the toad bladder. The Journal of clinical investigation 41:702-709.
Panatier A, Gentles SJ, Bourque CW, Oliet SH (2006) Activity-dependent synaptic plasticity in the supraoptic nucleus of the rat hypothalamus. The Journal of physiology 573:711-721.
Pearce D, Soundararajan R, Trimpert C, Kashlan OB, Deen PM, Kohan DE (2015) Collecting duct principal cell transport processes and their regulation. Clinical journal of the American Society of Nephrology : CJASN 10:135-146.
Pelaprat D (2006) Interactions between neurotensin receptors and G proteins. Peptides 27:2476-2487.
Penner R, Pusch M, Neher E (1987) Washout phenomena in dialyzed mast cells allow discrimination of different steps in stimulus-secretion coupling. Bioscience reports 7:313-321.
Perlmutter LS, Tweedle CD, Hatton GI (1984) Neuronal/glial plasticity in the supraoptic dendritic zone: dendritic bundling and double synapse formation at parturition. Neuroscience 13:769-779.
Perlmutter LS, Tweedle CD, Hatton GI (1985) Neuronal/glial plasticity in the supraoptic dendritic zone in response to acute and chronic dehydration. Brain research 361:225-232.
Persechini A, Moncrief ND, Kretsinger RH (1989) The EF-hand family of calcium-modulated proteins. Trends in neurosciences 12:462-467.
Pitler TA, Alger BE (1992) Postsynaptic spike firing reduces synaptic GABAA responses in hippocampal pyramidal cells. The Journal of neuroscience : the official journal of the Society for Neuroscience 12:4122-4132.
Pittman QJ, Hirasawa M, Mouginot D, Kombian SB (2000) Neurohypophysial peptides as retrograde transmitters in the supraoptic nucleus of the rat. Experimental physiology 85 Spec No:139s-143s.
Polenov AL, Chetverukhin VK (1993) Ultrastructural radioautographic analysis of neurogenesis in the hypothalamus of the adult frog, Rana temporaria, with special reference to physiological regeneration of the preoptic nucleus. II. Types of neuronal cells produced. Cell and tissue research 271:351-362.
Pologruto TA, Sabatini BL, Svoboda K (2003) ScanImage: flexible software for operating laser scanning microscopes. Biomedical engineering online 2:13.
Potts PD, Ludbrook J, Gillman-Gaspari TA, Horiuchi J, Dampney RA (2000) Activation of brain neurons following central hypervolaemia and hypovolaemia: contribution of baroreceptor and non-baroreceptor inputs. Neuroscience 95:499-511.
Poulain DA, Wakerley JB (1982) Electrophysiology of hypothalamic magnocellular neurones secreting oxytocin and vasopressin. Neuroscience 7:773-808.
Poulain DA, Brown D, Wakerley JB (1988) Statistical analysis of patterns of electrical activity in vasopressin- and oxytocin-secreting neurons. In Pulsatily in Neuroendocrine Systems, ed Leng, G:pp. 119-154. C.R.C Press, Boca Raton, FL, USA

Pow DV, Morris JF (1989) Dendrites of hypothalamic magnocellular neurons release neurohypophysial peptides by exocytosis. Neuroscience 32:435-439.
Prager-Khoutorsky M, Khoutorsky A, Bourque CW (2014) Unique interweaved microtubule scaffold mediates osmosensory transduction via physical interaction with TRPV1. Neuron 83:866-878.
Quinlan ME, Hirasawa M (2013) Multivesicular release underlies short term synaptic potentiation independent of release probability change in the supraoptic nucleus. PloS one 8:e77402.
Quinlan ME, Alberto CO, Hirasawa M (2008) Short-term potentiation of mEPSCs requires N-, P/Q- and L-type Ca2+ channels and mitochondria in the supraoptic nucleus. The Journal of physiology 586:3147-3161.
Rall W, Shepherd GM, Reese TS, Brightman MW (1966) Dendrodendritic synaptic pathway for inhibition in the olfactory bulb. Experimental neurology 14:44-56.
Randle JC, Bourque CW, Renaud LP (1984) Alpha-adrenergic activation of rat hypothalamic supraoptic neurons maintained in vitro. Brain research 307:374-378.
Randle JC, Bourque CW, Renaud LP (1986a) Alpha 1-adrenergic receptor activation depolarizes rat supraoptic neurosecretory neurons in vitro. The American journal of physiology 251:R569-574.
Randle JC, Bourque CW, Renaud LP (1986b) Serial reconstruction of Lucifer yellow-labeled supraoptic nucleus neurons in perfused rat hypothalamic explants. Neuroscience 17:453-467.
Rasmussen MS, Simonsen JA, Sandgaard NC, Hoilund-Carlsen PF, Bie P (2004) Effects of oxytocin in normal man during low and high sodium diets. Acta physiologica Scandinavica 181:247-257.
Rhodes CH, Morrell JI, Pfaff DW (1981) Immunohistochemical analysis of magnocellular elements in rat hypothalamus: distribution and numbers of cells containing neurophysin, oxytocin, and vasopressin. The Journal of comparative neurology 198:45-64.
Richard D, Bourque CW (1995) Synaptic control of rat supraoptic neurones during osmotic stimulation of the organum vasculosum lamina terminalis in vitro. The Journal of physiology 489 (Pt 2):567-577.
Roper P, Callaway J, Armstrong W (2004) Burst initiation and termination in phasic vasopressin cells of the rat supraoptic nucleus: a combined mathematical, electrical, and calcium fluorescence study. The Journal of neuroscience : the official journal of the Society for Neuroscience 24:4818-4831.
Russell JA, Leng G, Douglas AJ (2003) The magnocellular oxytocin system, the fount of maternity: adaptations in pregnancy. Frontiers in neuroendocrinology 24:27-61.
Sasaki N, Dayanithi G, Shibuya I (2005) Ca2+ clearance mechanisms in neurohypophysial terminals of the rat. Cell calcium 37:45-56.
Sayer RJ, Hubbard JI, Sirett NE (1984) Rat organum vasculosum laminae terminalis in vitro: responses to transmitters. The American journal of physiology 247:R374-379.
Schneiderman I, Zagoory-Sharon O, Leckman JF, Feldman R (2012) Oxytocin during the initial stages of romantic attachment: relations to couples' interactive reciprocity. Psychoneuroendocrinology 37:1277-1285.
Sharif Naeini R, Witty MF, Seguela P, Bourque CW (2006) An N-terminal variant of Trpv1 channel is required for osmosensory transduction. Nature neuroscience 9:93-98.
Shuster SJ, Riedl M, Li X, Vulchanova L, Elde R (1999) Stimulus-dependent translocation of kappa opioid receptors to the plasma membrane. The Journal of neuroscience : the official journal of the Society for Neuroscience 19:2658-2664.
Simmons ML, Chavkin C (1996) k-Opioid receptor activation of a dendrotoxin-sensitive potassium channel mediates presynaptic inhibition of mossy fiber neurotransmitter release. Molecular pharmacology 50:80-85.
Speidel D, Varoqueaux F, Enk C, Nojiri M, Grishanin RN, Martin TF, Hofmann K, Brose N, Reim K (2003) A family of Ca2+-dependent activator proteins for secretion: comparative analysis of structure, expression, localization, and function. The Journal of biological chemistry 278:52802-52809.

Stachniak TJ, Trudel E, Bourque CW (2014) Cell-specific retrograde signals mediate antiparallel effects of angiotensin II on osmoreceptor afferents to vasopressin and oxytocin neurons. Cell reports 8:355-362.
Stern JE, Armstrong WE (1998) Reorganization of the dendritic trees of oxytocin and vasopressin neurons of the rat supraoptic nucleus during lactation. The Journal of neuroscience : the official journal of the Society for Neuroscience 18:841-853.
Stern JE, Galarreta M, Foehring RC, Hestrin S, Armstrong WE (1999) Differences in the properties of ionotropic glutamate synaptic currents in oxytocin and vasopressin neuroendocrine neurons. The Journal of neuroscience : the official journal of the Society for Neuroscience 19:3367-3375.
Steward O (1997) Ultrastructural basis for gene expression at the synapse : Synapse associated polyribosome complexes. Neuron:9-12.
Stockand JD (2010) Vasopressin regulation of renal sodium excretion. Kidney international 78:849-856.
Stocker M, Pedarzani P (2000) Differential distribution of three Ca(2+)-activated K(+) channel subunits, SK1, SK2, and SK3, in the adult rat central nervous system. Molecular and cellular neurosciences 15:476-493.
Stricker EM (1981) Thirst and sodium appetite after colloid treatment in rats. Journal of comparative and physiological psychology 95:1-25.
Suh PG, Park JI, Manzoli L, Cocco L, Peak JC, Katan M, Fukami K, Kataoka T, Yun S, Ryu SH (2008) Multiple roles of phosphoinositide-specific phospholipase C isozymes. BMB reports 41:415-434.
Summerlee AJ (1981) Extracellular recordings from oxytocin neurones during the expulsive phase of birth in unanaesthetized rats. The Journal of physiology 321:1-9.
Taxi J, Sotelo C (1973) Cytological aspects of the axonal migration of catecholamines and of their storage material. Brain research 62:431-437.
Thrasher TN, Keil LC, Ramsay DJ (1982) Lesions of the organum vasculosum of the lamina terminalis (OVLT) attenuate osmotically-induced drinking and vasopressin secretion in the dog. Endocrinology 110:1837-1839.
Tobin V, Schwab Y, Lelos N, Onaka T, Pittman QJ, Ludwig M (2012) Expression of exocytosis proteins in rat supraoptic nucleus neurones. Journal of neuroendocrinology 24:629-641.
Tobin VA, Douglas AJ, Leng G, Ludwig M (2011) The involvement of voltage-operated calcium channels in somato-dendritic oxytocin release. PloS one 6:e25366.
Tobin VA, Hurst G, Norrie L, Dal Rio FP, Bull PM, Ludwig M (2004) Thapsigargin-induced mobilization of dendritic dense-cored vesicles in rat supraoptic neurons. The European journal of neuroscience 19:2909-2912.
Trudel E, Bourque CW (2003) A rat brain slice preserving synaptic connections between neurons of the suprachiasmatic nucleus, organum vasculosum lamina terminalis and supraoptic nucleus. Journal of neuroscience methods 128:67-77.
Trudel E, Bourque CW (2012) Circadian modulation of osmoregulated firing in rat supraoptic nucleus neurones. Journal of neuroendocrinology 24:577-586.
Tully K, Li Y, Bolshakov VY (2007) Keeping in check painful synapses in central amygdala. Neuron 56:757-759.
Tweedle CD, Hatton GI (1977) Ultrastructural changes in rat hypothalamic neurosecretory cells and their associated glia during minimal dehydration and rehydration. Cell and tissue research 181:59-72.
Ueta Y, Fujihara H, Serino R, Dayanithi G, Ozawa H, Matsuda K, Kawata M, Yamada J, Ueno S, Fukuda A, Murphy D (2005) Transgenic expression of enhanced green fluorescent protein enables direct visualization for physiological studies of vasopressin neurons and isolated nerve terminals of the rat. Endocrinology 146:406-413.
van Lieburg AF, Knoers NV, Deen PM (1995) Discovery of aquaporins: a breakthrough in research on renal water transport. Pediatric nephrology (Berlin, Germany) 9:228-234.

Verbalis JG, Mangione MP, Stricker EM (1991) Oxytocin produces natriuresis in rats at physiological plasma concentrations. Endocrinology 128:1317-1322.
Verkman AS, Lencer WI, Brown D, Ausiello DA (1988) Endosomes from kidney collecting tubule cells contain the vasopressin-sensitive water channel. Nature 333:268-269.
Verney EB (1947) The antidiuretic hormone and the factors which determine its release. Proceedings of the Royal Society of London Series B, Biological sciences 135:25-106.
Vincent JP, Mazella J, Kitabgi P (1999) Neurotensin and neurotensin receptors. Trends in pharmacological sciences 20:302-309.
Vivas L, Chiaraviglio E, Carrer HF (1990) Rat organum vasculosum laminae terminalis in vitro: responses to changes in sodium concentration. Brain research 519:294-300.
Voisin DL, Fenelon VS, Herbison AE (1996) Calbindin-D28k mRNA expression in magnocellular hypothalamic neurons of female rats during parturition, lactation and following dehydration. Brain research Molecular brain research 42:279-286.
Wakerley JB, Lincoln DW (1973) The milk-ejection reflex of the rat: a 20- to 40-fold acceleration in the firing of paraventricular neurones during oxytocin release. The Journal of endocrinology 57:477-493.
Wakerley JB, Poulain DA, Brown D (1978) Comparison of firing patterns in oxytocin- and vasopressin-releasing neurones during progressive dehydration. Brain research 148:425-440.
Wakerley JB, Poulain DA, Dyball RE, Cross BA (1975) Activity of phasic neurosecretory cells during haemorrhage. Nature 258:82-84.
Walum H, Westberg L, Henningsson S, Neiderhiser JM, Reiss D, Igl W, Ganiban JM, Spotts EL, Pedersen NL, Eriksson E, Lichtenstein P (2008) Genetic variation in the vasopressin receptor 1a gene (AVPR1A) associates with pair-bonding behavior in humans. Proceedings of the National Academy of Sciences of the United States of America 105:14153-14156.
Watts AG, Swanson LW (1987) Efferent projections of the suprachiasmatic nucleus: II. Studies using retrograde transport of fluorescent dyes and simultaneous peptide immunohistochemistry in the rat. The Journal of comparative neurology 258:230-252.
Westecker ME (1970) Excitatory and inhibitory interactions in the olfactory bulb involving dendrodendritic synapses between mitral cells and granular cells. Pflugers Archiv : European journal of physiology 317:173-186.
Whitnall MH, Gainer H, Cox BM, Molineaux CJ (1983) Dynorphin-A-(1-8) is contained within vasopressin neurosecretory vesicles in rat pituitary. Science (New York, NY) 222:1137-1139.
Wong MT (1970) Somato-dendritic and dendro-dendritic synapses in the squirrel monkey lateral geniculate nucleus. Brain research 20:135-139.
Wotjak CT, Ludwig M, Landgraf R (1994) Vasopressin facilitates its own release within the rat supraoptic nucleus in vivo. Neuroreport 5:1181-1184.
Yang CR, Phillips MI, Renaud LP (1992) Angiotensin II receptor activation depolarizes rat supraoptic neurons in vitro. The American journal of physiology 263:R1333-1338.
Yang CR, Senatorov VV, Renaud LP (1994) Organum vasculosum lamina terminalis-evoked postsynaptic responses in rat supraoptic neurones in vitro. The Journal of physiology 477 (Pt 1):59-74.
Yang H, Zhang G, Cui J (2015) BK channels: multiple sensors, one activation gate. Frontiers in physiology 6:29.
Yao ST, Antunes VR, Bradley PM, Kasparov S, Ueta Y, Paton JF, Murphy D (2011) Temporal profile of arginine vasopressin release from the neurohypophysis in response to hypertonic saline and hypotension measured using a fluorescent fusion protein. Journal of neuroscience methods 201:191-195.
Young LJ, Wang Z (2004) The neurobiology of pair bonding. Nature neuroscience 7:1048-1054.

Zaelzer C, Hua P, Prager-Khoutorsky M, Ciura S, Voisin DL, Liedtke W, Bourque CW (2015) DeltaN-TRPV1: A Molecular Co-detector of Body Temperature and Osmotic Stress. Cell reports 13:23-30.
Zaidi SM, Heller H (1974) Can neurohypophysial hormones cross the blood-cerebrospinal fluid barrier? The Journal of endocrinology 60:195-196.
Zhang Z, Bourque CW (2003) Osmometry in osmosensory neurons. Nature neuroscience 6:1021-1022.
Zhang Z, Kindrat AN, Sharif-Naeini R, Bourque CW (2007) Actin filaments mediate mechanical gating during osmosensory transduction in rat supraoptic nucleus neurons. The Journal of neuroscience : the official journal of the Society for Neuroscience 27:4008-4013.
Zhang Z, Bhalla A, Dean C, Chapman ER, Jackson MB (2009) Synaptotagmin IV: a multifunctional regulator of peptidergic nerve terminals. Nature neuroscience 12:163-171.
Zucker RS (1999) Calcium- and activity-dependent synaptic plasticity. Current opinion in neurobiology 9:305-313.

VIII: APPENDICES